FEDERAL UNIVERSITY OF ITAJUBÁ

POST GRADUATE PROGRAM IN

ELECTRICAL ENGINEERING

Flávio Eduardo Spressola

LIFE SPAN ESTIMATION OF OIL-IMPREGNATED PAPER HIGH VOLTAGE CURRENT TRANSFORMERS BASED ON LONG DURATION TESTS UNDER SIMULTANEOUS THERMAL AND ELECTRICAL STRESSES

Itajubá, February 2024

FEDERAL UNIVERSITY OF ITAJUBÁ
POST GRADUATE PROGRAM IN
ELECTRICAL ENGINEERING

Flávio Eduardo Spressola

LIFE SPAN ESTIMATION OF OIL-IMPREGNATED PAPER HIGH VOLTAGE CURRENT TRANSFORMERS BASED ON LONG DURATION TESTS UNDER SIMULTANEOUS THERMAL AND ELECTRICAL STRESSES

Thesis submitted to the Post Graduate Program in Electrical Engineering as part of requirements to obtaining Doctor Degree in Electrical Engineering Science.

Concentration field:
Electrical Power Systems
Supervisor:
Prof. Estácio Tavares Wanderley Neto, DSc

Itajubá, February 2024

SPRESSOLA, Flávio Eduardo

Life span estimation of oil-impregnated paper high voltage current transformers based on long duration tests under simultaneous thermal and electrical stresses / Flávio Eduardo Spressola. – Itajubá: UNIFEI, 2024.

145p.

Tese (doutorado) – Universidade Federal de Itajubá, 2024.

Orientador: Estácio Tavares Wanderley Neto

1. Aging of Oil-impregnated Paper Insulation. 2. High Voltage Current Transformers.

I. Wanderley Neto, Estácio Tavares. II. Universidade Federal de Itajubá. III. Life span estimation of oil-impregnated paper high voltage current transformers based on long duration tests under simultaneous thermal and electrical stresses.

FEDERAL UNIVERSITY OF ITAJUBÁ
POST GRADUATE PROGRAM IN
ELECTRICAL ENGINEERING

Flávio Eduardo Spressola

LIFE SPAN ESTIMATION OF OIL-IMPREGNATED PAPER HIGH VOLTAGE CURRENT TRANSFORMERS BASED ON LONG DURATION TESTS UNDER SIMULTANEOUS THERMAL AND ELECTRICAL STRESSES

Thesis submitted to the Post Graduate Program in Electrical Engineering as part of requirements to obtaining Doctor Degree in Electrical Engineering Science.

Examination Board:
Prof. Estácio Tavares Wanderley Neto, DSc (Supervisor)
Prof. Edson Guedes da Costa, DSc
Prof. Gustavo Paiva Lopes, DSc
Prof. Ivan José da Silva Lopes, DSc
Prof. Ivan Paulo de Faria, DSc

Approval Date: February 7th, 2024.

Dedication

This work is dedicated to those who are willing, with humility and reverence, to seek answers to the questions that are asked of them.

ACKNOWLEDGEMENT

First of all, I thank God for sustaining me in all challenges, strengthening me in the face of difficulties and allowing me to rejoice in the fruits reaped by the efforts sown. He is the one who gives meaning to everything I set out to do.

I especially thank my wife, Raquel and my children, Isabela and Lucas, for their support, loving encouragement in the most difficult moments and for their understanding in times of absence. I thank my mother, Darlene, whose prays always find me during all my challenges.

I would like to thank my supervisor, Professor Estácio Wandeley Neto, for his friendship, patience, attentive reading, guidance, and suggestions throughout this work. I also thank professors Edson Guedes da Costa, Gustavo Paiva Lopes, Ivan José da Silva Lopes, and Ivan Paulo de Faria, for their generous and valuable contributions to this work after the presentation.

I also record my thanks to GE Grid Solutions for the support and for all the resources made available through Renato Sarlas and Thiago Bueno so that this investigation could be carried out and concluded. I thank my manager, Rodrigo Gomes Oliveira, for his support and understanding, and together with Fernando Lagos and Zoltan Roman, for their contributions and technical discussions that enriched the content of this thesis and the conduct of the investigations.

I especially thank my colleagues from the test laboratory and industrial maintenance teams who actively participated in the preparation, assembly and monitoring activities over the years in which the tests for this investigation were carried out: Ronivaldo Vasconcelos, André Correa, Vagner Lucio, Ronaldo Silva, Juliano de Souza, Gustavo Batista, Edson Silva, and César Cortez.

Finally, I express my gratitude to Professor Manuel Luiz Barreira Martinez (in memorian). I still reap the fruits of the seeds that he generously sowed in my life.

ABSTRACT

A large number of power system apparatus around the world are over 30 years old in operation. Replacement of power system assets involves high investments. On the other hand, the failure of such equipment causes a high economic impact. The lifespan estimation of high voltage apparatus is an important information to determine the best moment for the replacement. Although the current transformer is an essential component in the electrical power system and its failure may result in serious consequences, there are no accelerated aging tests for this equipment prescribed by technical standards. Life estimation for this equipment is generally made based on field experience, something that cannot be done for new models and/or new manufacturers. In this work, experimental results of life tests performed on reduced models, representing high voltage current transformers with oil-impregnated paper insulation, are presented and discussed. The analysis is based on the application of a multi-stress model, which combines the Montsinger rule and Inverse Power Law. The proposed approach considers the existence of threshold values for electrical and thermal stresses, below them, electrical and thermal degradation are negligible. An order of magnitude for the electrical stress threshold value (E_0) and for the electrical aging exponent (n) is obtained from the application of the test results to the model used in this investigation. The scope of the investigation includes several diagnostic tests which are performed after interruptions of the long-duration test. The diagnostic tests include some classical high voltage power frequency measurements, tests on oil samples and finally, dielectric frequency response (*DFR*), one of the most recent insulation diagnostic techniques. The application of the thermoelectrical multi-stress model to the results indicates that the estimated lifespan for the test samples is about 50 years, that the exponent related to electrical stress n is in the range of 1.3-3 and that the electrical stress threshold E_0 is in the range of 1.17 to 1.21 p.u. The results of diagnostic tests carried out as part of this investigation revealed the relevant variation of several parameters along the aging test and, combined with the findings obtained in the autopsy of the failed test samples indicated a dielectric failure caused by the combined action of electrical and thermal stresses. The variations of these parameters are of great value for evaluating the degradation conditions of the insulation over its service life. The cross-analysis of several different diagnostic tests is recommended for decision-making regarding the replacement of equipment in service.

Keywords: 1. Accelerated aging test, 2. current transformer, 3. life estimation, 4. oil-paper insulation

LIST OF FIGURES

LIST OF TABLES

LIST OF ABBREVIATIONS AND ACRONYMS

ABNT	Brazilian Association of Technical Standards
AC	Alternating current
AIS	Air-insulated switchgear
ANEEL	National Electric Energy Agency
CIGRE	International Council on Large Electric Systems
CT	Current transformers
DC	Direct current
DDF	Dielectric dissipation factor
DEV	Discharge extinction voltage
DFR	Dielectric frequency response
DGA	Dissolved gas analysis
DIV	Discharge inception voltage
DP	Degree of polymerization
EPRI	Electric Power Research Institute
FDS	Frequency Domain Spectroscopy
FEA	Finite element analysis
GE	General Electric
HPGH	High pressure gas filled
HPLC	High performance liquid chromatography
HV	High voltage
IEC	International Electrotechnical Committee
IEEE	Institute of Electrical and Electronic Engineers
LIWV	Lightning impulse withstand voltage
LV	Low voltage
MME	Ministry of Mines and Energy
ONS	National System Operator
PD	Partial discharges
PDC	Polarization and depolarization current
PFWV	Power frequency withstand voltage
SEM-EDS	Scanning Electron Microscopy with an Energy Dispersive X-ray Spectroscopy

SIWV	Switching impulse withstand voltage
TUP	Thermally upgraded paper
VT	Voltage transformer
WG	Working group

TABLE OF CONTENTS

1 INTRODUCTION

Most power systems around the world have a large number of transformers over 30 years old in operation [1]. Since the common expected design life for transformers corresponds to 30 years, equipment owners and system operation players are concerned about their replacement and on the risks of keeping them in operation [2]. Replacement of power system assets involves huge investments. On the other hand, the failure of such a type of apparatus causes high economic losses. The lifespan estimation of such equipment is an important information to determine the best moment for the replacement, balancing investments, and operational risks.

Oil-impregnated paper is the most used insulation system for transformers [2], either power transformers or instrument transformers. The life span of a transformer is mainly determined by the life span of its insulation system [3]. Many publications are available related to the aging of the paper-oil insulation system in power transformers, describing the aging mechanisms, methods of age evaluation, remaining lifetime prediction and aging tests based on transformer loading and operation temperature [2]. The focus on the power transformer is justifiable since this is the most expensive power system equipment. Although the cost of a current transformer is much lower than a power transformer one, current transformer failures can cause a hugh impact considering personnel injury, outage, and damage to adjacent switchgear equipment, i.e., circuit breakers, disconnectors, or even other instrument transformers.

During operation, the insulation system of a high voltage apparatus is subjected to multiple simultaneous stresses such as thermal, electrical, mechanical, environmental, or chemical. For high voltage current transformers, simultaneous thermal and electrical stresses can be considered the most relevant in terms of aging acceleration [4]. Thermal stress is considered as the most important aging acceleration factor for power transformers and its impact on the insulation degradation can be described using the Arrhenius equation [2]. Montsinger has studied the influence of thermal stress on oil-impregnated paper insulation and defined an empirical rule, based on Arrhenius relation, which is the basis for the IEC loading power transformer guide [5]. The aging acceleration due to electrical stress can be represented by inverse power law model or by the exponential model [6]. These models relate continuous electrical stress applied to the insulation system with the time to breakdown. Both the inverse power law model and the exponential model are based on empiricism.

Simoni [7] has proposed a general equation based on the Arrhenius relation and the inverse power law to describe aging under simultaneous thermal and electrical stresses. This model also considers the existence of threshold values for electrical and thermal stresses, below them, electrical and thermal degradation can be considered as negligible [8].

Following the same approach used by Simoni, Occhini et al [9] applied an equation based on Montsinger and on the inverse power law for simultaneous thermal and electrical stresses applied on long duration aging tests performed on oil-impregnated paper insulated power cables. However, there is no mention of the definition of a minimum electrical stress to be considered as the threshold value to trigger the degradation due to electrical stress.

There are many similarities between oil impregnated paper insulation systems applied to high voltage power cable insulation and to high voltage current transformers. Both are built with thin kraft paper wrapped on a metallic electrode with circular or elliptical cross section. Kraft paper is carefully wound to obtain a good compaction and suitable overlap of the paper layers. For both cases, capacitive grading with semiconductive layers is used to distribute the electrical field across the insulation. The main heat dissipation mechanism for the insulation of current transformers and for power cables is the thermal conduction once convection is considered as negligible due to the limited oil volume. For both cases, the insulation is simultaneously a thermal conductor for the ohmic losses and a heat source due to the dielectric losses. These similarities justify a resembling behavior under thermal and electrical stresses and may result in similar empirical parameters for the aging equations.

The accuracy of the thermal-electrical aging model to fit experimental results depends on the empirically determined voltage aging exponent n and on the threshold value for electrical stress (E_0) from which acceleration of aging by an electrical field can no longer be considered as negligible.

According to the inverse power law, the inverse of the electrical stress is raised to the n^{th} power [6]. This exponent has been considered in the range from 10 to 12 by Occhini et al [9] and Allam et al [10] for oil-impregnated paper power cables. Recently, Zhou et al [11] proposed that this exponent has a value in the range from 4 to 6 for oil-impregnated paper current transformers. However, none of these references considers a threshold electrical stress E_0. The application of thermal-electrical aging models to oil-impregnated paper current transformers remains an open matter. Given this scenario, an investigation carrying out accelerated aging tests on samples of current transformer insulation systems contributes to the

determination of more appropriate empirical values so that an aging model can be applied to estimate the lifespan of this equipment.

1.1 MOTIVATION

The large number of power system apparatus over 30 years old is also a concern in Brazil. A report published by the MME (Ministry of Mines and Energy), under the coordination of the ONS (National System Operator), indicated that 96 740 equipment installed in the national transmission power system would have their regulatory life[1] exceeded until 2022. Transformers correspond to 25 043 units: 1 776 power transformers and 23 267 instrument transformers (voltage transformers and current transformers). Current transformers correspond to 14 230 units, resulting in an equivalent investment cost exceeding 2 billion reais [12] .

The current transformer is considered a critical component of the electrical power systems once it plays an essential role in protection and measurement. The failure of a current transformer can result in catastrophic consequences besides the power interruption, such as damage to nearby apparatus and/or fatal accidents with personnel. However, in general, it does not have any local or remote protection [13].

The figures indicated by the ONS motivated a public consultation by ANEEL (National Electric Energy Agency) regarding the regulatory life of the power system apparatus [14]. Although no regulatory changes were introduced from the results of the public consultation [15], it led to an intense debate related to the life expectancy of the equipment. In addition to the economic impacts that the massive replacement of apparatus with an expired regulatory life would generate, aspects such as the possibility of extending the lifespan of the equipment and mechanisms for diagnosing the aging conditions of the equipment were also discussed as ways to balance the technical and economic aspects which are involved in this topic.

For power transformers, lifespan estimation is more consolidated knowledge. The existence of criteria established in technical standards is evidence of this fact. The IEC Power Transformer Loading Guide [5] defines aging acceleration rates depending on the hot-spot

[1] The regulatory life of an apparatus is the period defined to deduct the cost of the apparatus over its useful life. Ideally, the regulatory lifetime should correspond to the physical lifetime of the equipment [14].

temperature and provides fundamentals for estimation of remaining life at a defined load condition based on the Montsinger model.

For instrument transformers, technical standards define tests and criteria to evaluate if the new equipment is designed and manufactured for a long life under the typical operation conditions. But there is nothing defined about criteria for assessment of aging conditions and/or lifespan estimation. The IEC insulation co-ordination standard [16] states that the prescription of a long-duration power frequency test intended to demonstrate the response of the equipment with respect to aging of internal insulation is left to the equipment relevant technical committee. Nowadays, instrument transformer standards do not define any long-duration power frequency aging tests.

The study of the aging of current transformers with oil-impregnated insulation systems contributes to the development of knowledge on insulation degradation under combined thermal and electrical stresses. If diagnostic measurements are performed during a long duration accelerated aging test, the results of such measurements may contribute to establishing useful relations to the evaluation of some aging indicators.

1.2 OBJECTIVES

The present study discusses the aging of the oil-impregnated paper insulation of high voltage current transformers, intending to contribute to this topic by performing long-term tests at power-frequency and analyzing the results based on a thermal-electrical multi-stress model.

This investigation has been done based on a long-duration power frequency test at controlled voltage and temperature conditions on current transformer insulation samples built for this purpose. The main objective is to investigate the accelerated aging of paper-oil insulation under the simultaneous action of thermal and electrical stresses by applying an empirical equation found in the literature on power cables [9], extending its use to the case of current transformers. This equation includes an empirical exponent which is related with the aging acceleration under continuous power frequency electric stress. The determination of this empirical exponent is essential for the accuracy of the lifespan estimation.

However, it is also necessary to consider the existence of the threshold electrical stress value as proposed by Simoni [7, 8]. A specific objective of this work is the investigation of this empirical exponent and of the threshold electrical stress for the high voltage oil-impregnated paper current transformer case based on the analysis of the results obtained in this investigation.

The scope of the investigation includes several diagnostic tests which are performed after interruptions of the long-duration test. The diagnostic tests include some classical high voltage power frequency measurements (partial discharge and dielectric dissipation factor measurements), tests on oil samples (dissolved gas analysis, content of furanic compounds, moisture content, acidity, dissipation factor and other tests) and finally, dielectric frequency response (*DFR*), one of the most recent insulation diagnostic techniques. The joint and comparative analysis of all test results could allow the establishment of correlations between the measured quantities and the insulation degradation conditions. An additional contribution of the present research work is to demonstrate the use of a cross-analysis of the results of these tests obtaining the diagnostic of the failure cause.

1.3 THESIS OUTLINE

This thesis is organized into six chapters, including this one. A summary of the topics covered by each one is given below.

Chapter 2 provides the theoretical background for the present investigation. It provides relevant information regarding the technology of high voltage current transformers with oil-impregnated paper insulation including design and manufacture aspects, as well as the relevant tests for the insulation performance and condition assessment. Oil-impregnated paper insulation degradation and the main aging models existing in literature are presented.

A summary of the relevant existing literature is given in Chapter 3.

Chapter 4 focuses on the investigation methodology. It provides a description of the test samples, procedure, and test facilities.

Chapter 5 provides the presentation and analysis of the testing results.

Chapter 6 concludes the thesis and presents opportunities for future work.

2 THEORETICAL BACKGROUND

This chapter presents a theoretical background related to the oil-impregnated insulation of high voltage current transformers and on the aging process of this insulation system.

2.1 HIGH VOLTAGE CURRENT TRANSFORMERS - CONSTRUCTIONS, DESIGN, MANUFACTURE AND TESTS

Instrument transformers are apparatus intended to transmit an information signal to measuring instruments, meters and protective or control devices. In the case of magnetic instrument transformers, this information signal corresponds to a voltage or current waveform supplied by a secondary winding of this transformer which is proportional to the corresponding voltage or current waveform in its primary winding.

Current transformer (CT) is defined as *"an instrument transformer in which the secondary current, in normal conditions of use, is substantially proportional to the primary current and differs in phase from it by an angle which is approximately zero for an appropriate direction of the connections"* [17].

In addition to providing a current signal to measurement and protection devices, high voltage current transformers are also intended to provide electrical insulation between high voltage circuits (power circuits) and the measurement and control circuits connected to their secondary windings. These two functions, current sensing and insulation, are completely separated.

2.1.1 Main constructions for oil-impregnated paper high voltage current transformers

There are two main construction solutions currently used for oil-impregnated paper high voltage current transformers: top core (or live tank) and hairpin (bottom core or dead tank). For the top core type of construction, the secondary windings wound on toroidal magnetic cores

(ring type windings) are accommodated inside a metallic toroidal housing connected to a metal tube through which the cables connected to the secondary windings descend to be connected to the respective terminals. The set formed by the metallic housing and metallic tube is connected to the ground potential, providing an electrostatic shield around the secondary circuits. The oil-impregnated paper insulation is built by wrapping layers of insulating paper over this metallic grounded set. A generic cross section view of this type of construction is showed in Figure 1(a). For the hairpin construction, the secondary cores/windings are mounted around the insulated primary conductor, accommodated inside the tank at grounded potential as showed in Figure 1 (b). The present work is focused on the top core type, once the specimens built for the investigation are based on this type.

Figure 1 − Top core (a) and Hairpin (b) CT constructions.

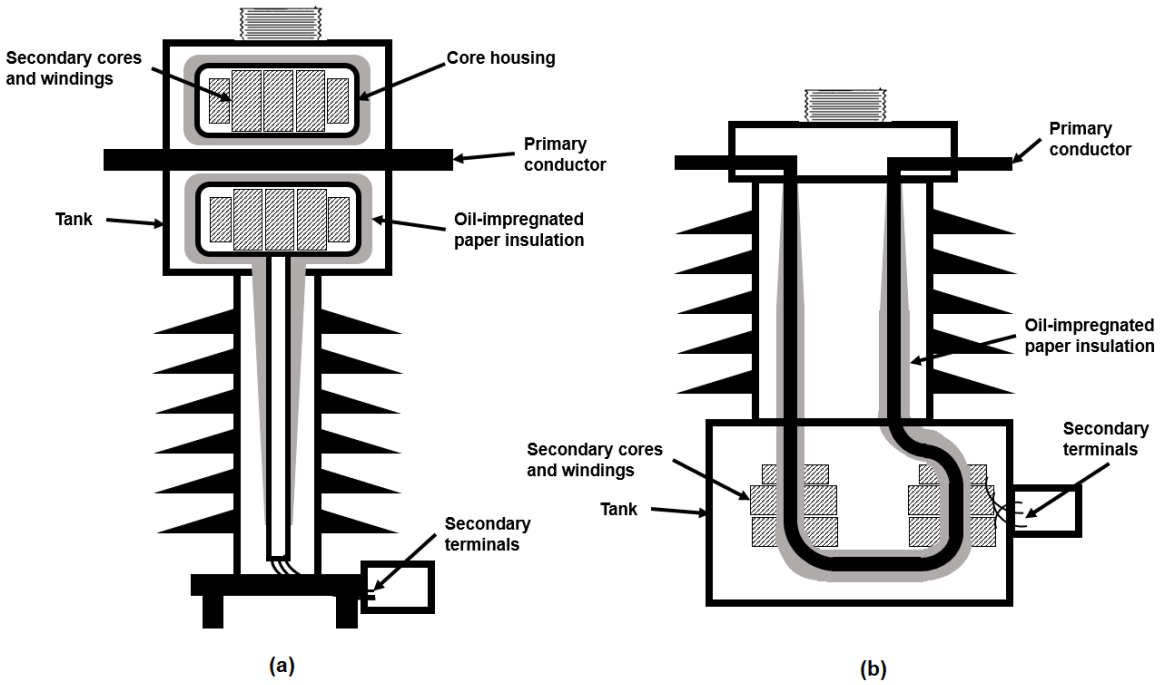

Source: own authorship

2.1.2 Insulation design and manufacture aspects

In the scope of the present work, the focus is on the main insulation, built with oil−impregnated paper. This insulation system consists of layers of insulating kraft paper, elastic crepe paper and/or a combination of both. Even when the insulation is based on plain kraft paper, the elastic crepe paper is usually used to get proper accommodation in some

sections of the insulation, achieving the designed geometry, i.e., targeted insulation thickness, smooth shape and suitable paper compaction. The insulation manufacture consists of applying the insulating paper on the grounded shielding (metallic core box and stem tube), drying this paper and impregnating it with treated insulating oil. A global view of insulation manufacturing is presented in Figure 2.

Figure 2 − Global view of the manufacture process of the insulation system of a top core oil-impregnated paper CT.

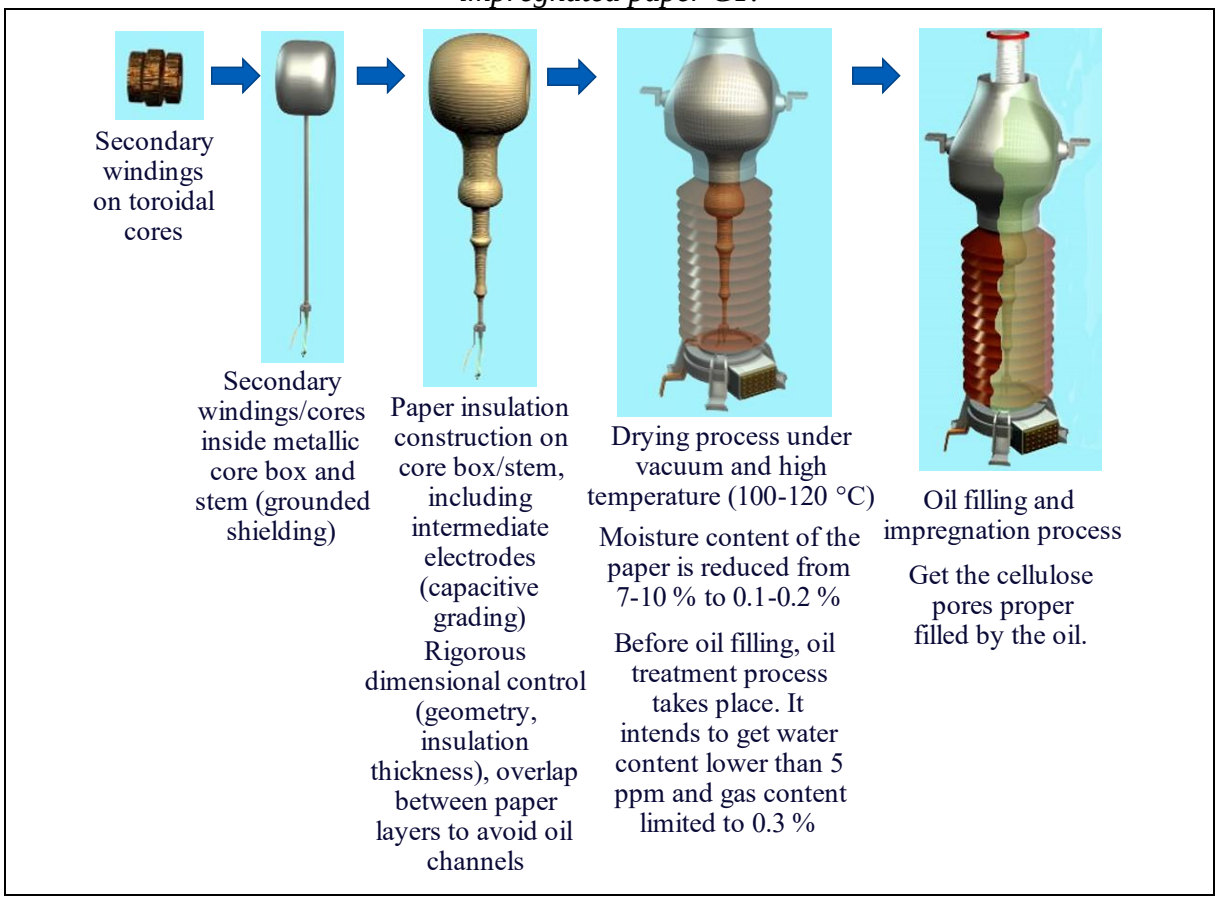

Source: own authorship

Before starting the paper taping process, a layer of semi−conductive carbon paper is applied on the core box and on the stem to compensate irregularities on their surface as showed in Figure 3. The assembly formed by the metallic core box and stem corresponds to the grounded electrode of the insulation. The insulating paper layers are then applied over this initial layer of semi-conductive carbon paper.

The process applying the paper is a critical step for which rigorous dimensional control is mandatory to guarantee the electrical field distribution defined for each specific design. This process is made, where possible, by winding machines, but it is usually predominantly

handmade work. Figure 4 shows an example of the taping process on the metallic core box of a current transformer.

Figure 3 − Semi-conductive carbon paper applied on grounded electrode (metallic core box and stem).

Source: own authorship

Figure 4 − Taping process on the metallic core box a current transformer.

Source: [18]

The paper is applied in the form of strips and/or sheets. The dimensional control is done by regular measurements during the taping process aiming to guarantee the conformity of the thickness of the layers and the suitable smooth geometry. It is also necessary to ensure adequate compaction of the paper. To this end, manufacturers control the tension in the paper during the taping process. If the insulation structure becomes excessively dense, it will be difficult for the oil to penetrate, impairing the subsequent impregnation process. On the other hand, if the compaction is insufficient, the insulation structure will become loose during the drying process due to the mass reduction caused by the removal of moisture from the pores of the paper. The mass reduction of solid insulation during the drying process is around 7 – 10 % [19].

It is also mandatory to guarantee a suitable overlap between paper layers to minimize oil-filled channels longitudinal to the paper. The construction of the insulation with paper layers immersed and impregnated by oil leads to a high withstand voltage capability in the plane perpendicular to the paper layers [19]. The paper layers act as barriers between the very thin oil channels between them. On the other hand, the dielectric withstand along the paper is not so high. When the overlapping of paper layers is not properly done, longitudinal oil channels to the paper will form, resulting in the occurrence of partial discharges or even flashovers [19].

This fact is explained by Hou et al: "*The insulation system of these transformers consists of oil-impregnated cellulose insulation and mineral oil. The structure of cellulose insulation causes it to be strongly polar, resulting in the permittivity of cellulose insulation ($\varepsilon_{cellulose} \approx 4.1–4.8$) to be almost twice that of oil ($\varepsilon_{oil} \approx 2.2$). Therefore, the electric field strength in the oil duct is almost twice of that in the cellulose insulation when an AC voltage is applied. However, the breakdown voltage of mineral oil is much lower than that of the paper, causing small oil ducts to become the weakest parts of the whole insulation system"* [20].

Figure 5 shows some examples of geometrical irregularities in the insulation system associated with the occurrence of partial discharges detected during routine tests.

Figure 5 − Examples of geometrical insulation system defects associated with partial discharges detected during routine tests.

Source: own authorship

After wounding all the necessary layers to the insulation system, the paper is dried under special temperature and pressure (vacuum) conditions and later it is fully impregnated with insulating mineral oil. In the assembly of the current transformer, the active part is fully oil immersed.

More information on the materials, paper and oil, is given in 2.4.1 and 2.4.2. The drying process relevance and objectives are described in 2.5.3.1. As discussed in [19], to guarantee a suitable service performance, the following aspects are considered by the manufacturers for the design of CT insulation:

- Suitable voltage distribution from power frequency to 2-3 MHz conditions to avoid undesirable high electric field at both temporary and transient overvoltage conditions;
- Capacity of shields to withstand high peak value currents originated by steep-front high voltage transient surges, e.g., overvoltages caused by switching disconnector activities;
- Thermal stability at rated voltage, frequency, and temperature, at maximum current (maximum steady state insulation temperature condition).

The suitable and homogenous voltage distribution of the insulation system is achieved by the application of capacitance grading technology which consists of inserting screen electrodes between insulating paper layers, at regular thickness intervals, resulting in an equal voltage difference between adjacent screens. These electrode screens may be made up of layers of metal foil sheets or carbonized semi-conductive paper together with copper wire mesh.

As showed in [19], for the bushing of the CT (insulation on the metallic tube), two different design solutions are used to get a suitable and homogenous voltage distribution:

- Grading with toroidal electrodes: use a few capacitive grading screens and add grading toroidal rings at the end of each screen;
- Fine grading: use a large number of screens, avoiding the need of grading toroidal rings.

The use of toroidal electrodes is necessary to limit electric field stress due to the high concentration of equipotential lines. For the fine grading solution, the number of screens limits electric field stress due to the low difference of potential between screens. Figure 6 shows an illustrative diagram showing the concepts of toroidal electrodes and fine grading solutions.

In addition to the suitable voltage distribution at low frequency, which is reached by applying the technology solutions showed in Figure 6, special care is taken to the high voltage screens. These screens play important roles, as follows:

- guarantee the same potential along all its surface and, consequently, the same difference of potential between adjacent screens;

– provide a low and suitable surge impedance to avoid undesirable electrical field stress between adjacent screens, i.e., when a fast front impulse is applied to the CT primary, this impulse is transferred to the intermediate screens without any delay;
– provide a suitable capability to conduct high frequency currents when a fast front transient is applied to the insulation system.

Figure 6 – CT bushing with capacitive grading solutions: (a) with toroidal electrodes and (b) fine grading.

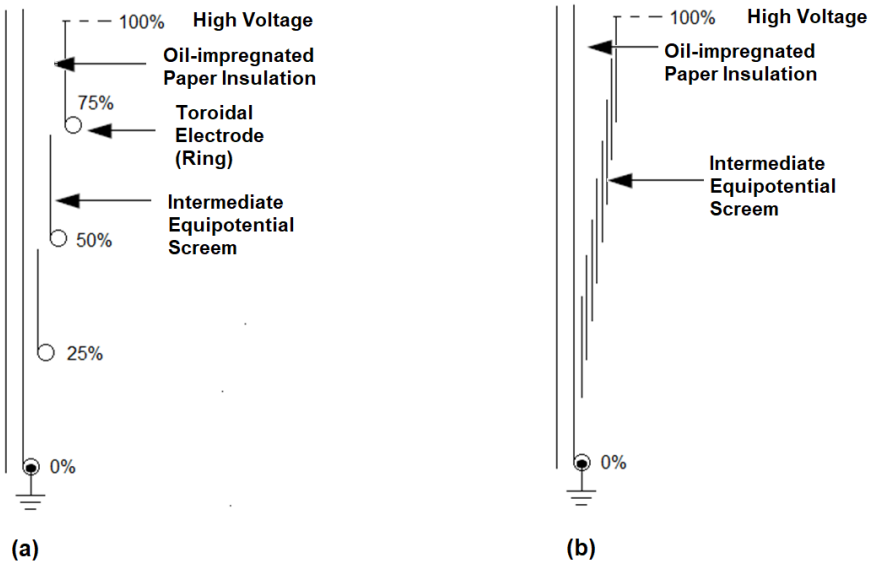

Source: adapted from [19]

As discussed in [19], the oil-impregnated paper system of a top core CT can be modeled by the equivalent circuit showed in Figure 7. The resistors and inductors correspond to the equivalent resistances and inductances of the screens and the capacitors correspond to the equivalent capacitances of the impregnated paper insulation between the screens.

The voltage distribution is particularly examined for the temporary and transient overvoltage conditions as defined by [16]: short-duration power frequency overvoltages, slow-front and fast-front transient overvoltages. For this purpose, the design of the insulation system is analyzed under the representative standard withstand voltages: short-duration power-frequency withstand test voltage, switching impulse test voltage and lightning impulse test voltage. This analysis corresponds to the insulation coordination of the equipment, and it is explained in 2.1.3.

Figure 7 − Example of equivalent electrical circuit of CT insulation with high voltage screens.

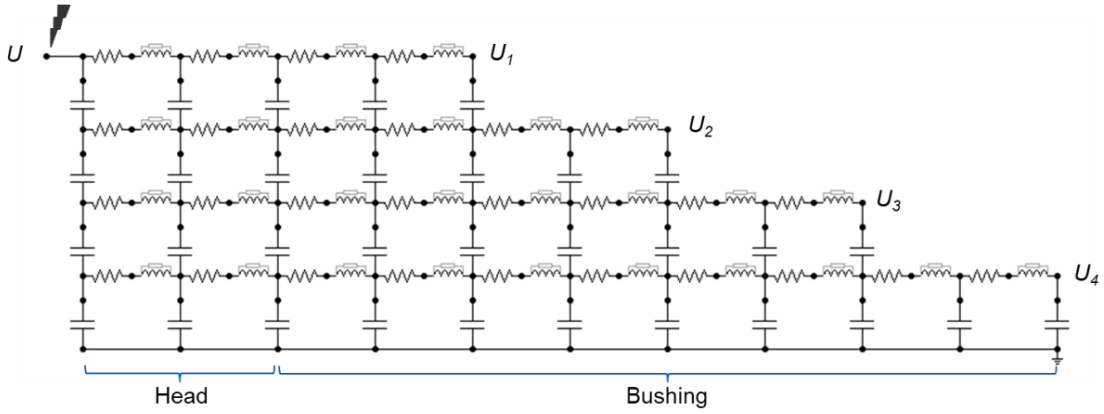

Source: adapted from [19]

An illustrative example of voltage distribution for a CT with capacitance grading technology is showed in Figure 8. This example shows the output of the electrical field calculation related to the design of the bushing of a CT active part. Each equipotential line corresponds to a screen. The outermost screen is connected to the metallic headhousing tank at the high voltage potential. The innermost screen is wound immediately on the metallic core box assembled together with the metallic stem connected to the ground potential. The potential of the other intermediate screens depends on the distribution of the capacitances between the screen electrodes according to the capacitor grading solution employed by the manufacturer (see Figure 6).

Figure 8 − Example of voltage distribution for a CT with capacitance grading.

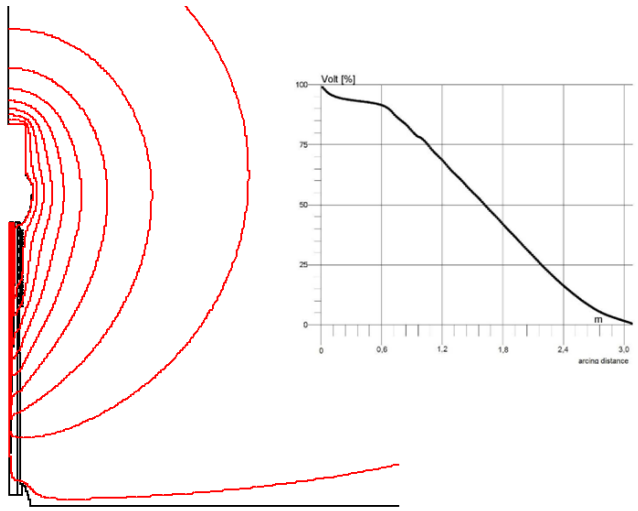

Source: [21]

Another key aspect in the design of a high voltage (or extra high-voltage) oil-impregnated paper CT insulation is thermal stability. There are three main heating sources in this type of apparatus:

- ohmic losses due to current flowing through the primary winding;
- the sum of ohmic losses due to current flowing through the secondary windings;
- dielectric losses.

In general, iron losses (magnetic losses from the cores) are considered as negligible for current transformers. The CIGRE A3 Study Committee [19] states the insulation thermal stability condition *"is reached when the quantity of the heat produced by dielectric losses and Joule effect in the active part is less than the heat that can be dissipated by conduction through the solid HV insulation."*

The losses in the primary and secondary windings are directly related to the dimensioning of the conductors that constitute these windings, since these losses are the result of the product of the ohmic resistance of the winding by the respective current to the square.

The dielectric losses are originated from conduction, polarization, and ionization processes. Polar losses are mainly a consequence of the presence of moisture and aging products. For the study of the insulation system at power frequency, the CT insulation can be represented by a capacitor in parallel with an equivalent resistance. By using this model, the active component of the electric current obtained when a sinusoidal voltage is applied to the CT insulation is the current through the equivalent resistance in parallel with the capacitance. The value of the dielectric dissipation factor (*DDF*) is the tangent of the angle δ between the reactive and active components of the total current as showed in Figure 9.

Dielectric losses are proportional to the *DDF* value and to the square of the voltage applied to the insulation. These proportionality relationships are verified in the equation (1). Therefore, the higher is the operating voltage of the *CT* the more critical and significant is the influence of dielectric losses on the steady state temperature of the *CT*.

$$P = \varpi C \tan \delta_\theta U^2 [W] \quad (1)$$

Where:

P is the dielectric losses.

ω is the angular velocity (2πf, f: frequency in Hz).

C is the capacitance in F.

U is the rms voltage in V.

Figure 9 − Equivalent RC circuit and dielectric dissipation factor.

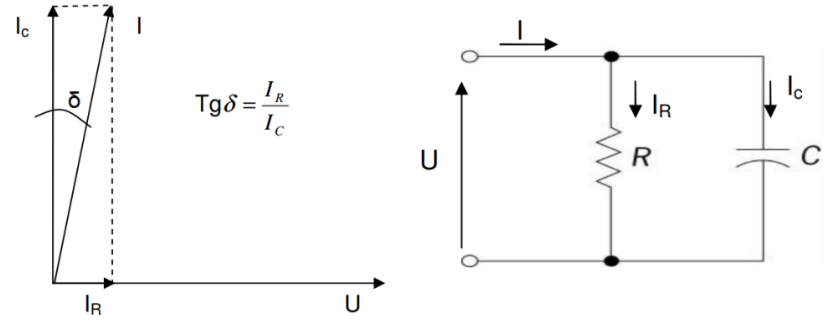

Source: adapted from [22]

The additional temperature rise due to dielectric losses is discussed in [23]. A thermal stability test (i.e., maximum continuous current applied to the windings with simultaneous maximum voltage applied to the insulation) has been performed on 145 kV, 245 kV and 800 kV top core oil-impregnated paper current transformers. Each test has been performed with current application in the first stage until the temperature of windings reached steady state condition and with simultaneous current and voltage application in the second stage. The additional temperature rise has been obtained as the difference in temperature at the end of each test stage. A summary of the test results obtained in [23] is showed in Table 1.

Table 1 − Relevance of dielectric losses on temperature rise of top core oil-impregnated paper current transformers.

	Sample 01 800 kV CT	**Sample 02 800 kV CT**	**Sample 03 245 kV CT**	**Sample 04 145 kV CT**
Maximum temperature rise with current only (°C)	26.0	36.2	23.8	20.6
Maximum temperature rise with simultaneous voltage and current (°C)	36.0	43.1	26.7	21.9
Additional temperature rise due to dielectric losses (°C)	10.0	6.9	2.9	1.3
Total losses in secondary windings at the end of the test (W)	29.2	51.9	39.7	45.5
Total losses in primary winding at the end of the test (W)	106.4	189.2	8.0	7.0
Dielectric losses at the end of the test (W)	145.8	145.0	14.8	5.0
Ratio between dielectric losses and winding losses	1.07	0.59	0.29	0.10

Source: [23]

It is evident the high relevance of the dielectric losses in the final temperature rise for extra high voltage current transformers. To manage thermal stability of the CT, manufacturers limit the ohmic losses from primary and secondary windings, taking into account the dielectric losses to obtain a suitable thermal balance and to prevent excessive temperature that can accelerate the aging of the materials. The dielectric losses are managed by a suitable drying process of the insulating paper and proper oil treatment (removal of moisture and gases) before the oil filling/paper impregnation process, as discussed in 2.5.3.1. From a design perspective, the CIGRE A3 Study Committee [19] recommends control of the specific dielectric losses of the insulation at an alternating electric field, which is the dielectric loss per unit of volume p_0, at a reference temperature and at an electrical stress corresponding to 1 kV/cm, as defined by equation (2).

$$p_0 = \varpi \varepsilon_0 \varepsilon_r \tan \delta_\theta \, 10^6 \left[\frac{W}{cm^3} / \left(\frac{kV}{cm}\right)\right] \quad (2)$$

Where:

$\varepsilon_0 = 1 / (3.6\pi)\ 10^{-12}\ F/cm$ and $\varepsilon_r \approx 3$ for oil-impregnated paper insulation.

Once $tan\ \delta$ is temperature (θ) and electrical stress (E) dependent, from equation (2) the dielectric losses per unit of volume $p\ (\theta, E)$ at nominal frequency is expressed by Equation (3)(3)(3) [19]:

$$p\ (\theta, E) = p_0 e^{\alpha_c (\theta_2 - \theta_1)} E^2 \left[\frac{W}{cm^3}\right] \quad (3)$$

Where α_c is the dielectric losses temperature coefficient:

$$\alpha_c = \frac{ln(tan\ \delta_{\theta 2}) - ln(tan\ \delta_{\theta 1})}{\theta_2 - \theta_1} \quad (4)$$

θ_1 and θ_2 are two values of insulation temperature in the operating range.

As discussed in 2.3.4, the value of the temperature coefficient of dielectric losses α_c became a useful parameter for the evaluation of degradation conditions of oil-impregnated paper current transformers [24].

After the paper application process is finished, the active part is placed under a controlled temperature/pressure (vacuum) process to remove moisture and gases from cellulose pores. During this process, the moisture content of the paper is reduced from 7 - 10 % to 0.1 - 0.2 % [19]. In a first stage, the temperature is increased to at least 100 °C at atmospheric

pressure for a time enough to guarantee a suitable temperature equalization. After this, the vacuum is applied, keeping the high temperature for a suitable time to dry the paper properly. The temperature cannot exceed 120 °C to avoid paper thermal degradation [19]. The conformity of the drying process is essential to guarantee the lifespan of the insulation system once the water and oxygen increases the degradation acceleration. An explanation of the influence of moisture and oxygen on paper and oil degradation is given in 2.5.3.

After the drying process, the active part is assembled inside the CT housing (tank + insulator) which will be filled with treated oil, i.e., the oil after the drying/degassing process. During the oil filling, temperature, vacuum, and time are carefully controlled to obtain a good impregnation, i.e., get the cellulose pores properly filled by the oil. Bad impregnation will result in partial discharges when the electrical stress is applied to the insulation, once the dielectric strength of paper pores filled by air and/or moisture is lower than that of the oil-filled pores.

2.1.3 Tests on current transformers concerning to the dielectric performance

Technical standards are documents prepared by consensus among involved stakeholders to standardize solutions that meet the requirements of the application. The objective of product technical standards is to establish minimum standardized performance requirements, as well as methods of verification of compliance with these requirements, in general, through tests.

According to their function, tests are classified as [25]:

- Type Tests: Tests performed on an equipment to demonstrate that all equipment manufactured to the same specification meets the requirements not covered by routine tests. Type tests are intended to validate an equipment design.
- Routine tests: Tests that are performed individually on all manufactured equipment, whose purpose is to reveal manufacturing defects. They do not impair the properties and reliability of the test object.
- Special test: A test other than type or routine tests agreed on by manufacturer and purchaser. These tests may be intended to cover special operating conditions not covered by the type tests. The special test classification is also used for some type of test whose approval criteria or procedures are not yet

fully determined, but for which it is to be encouraged to carry out it so that a level of experience is sufficient for it to become a type test.

- Sample test: a selected test, type or special, carried out on one or more complete equipment of a specified production batch.

The insulation system of a current transformer is intended to meet the specified dielectric requirements, i.e., the insulation co-ordination of the equipment. For a high voltage current transformer, the insulation coordination is defined by the following specified voltage values:

- Highest voltage for equipment (U_m) which corresponds to the maximum r.m.s. value of phase-to-phase voltage for which the equipment is designed in respect of its insulation [25].
- Temporary overvoltage withstanding:
  - Short-duration power frequency withstand voltage (*PFWV*), based on a sinusoidal waveform with frequency between 48-62 Hz and duration of 60 s [16];
- Transient overvoltage withstanding:
  - Switching impulse withstand voltage (*SIWV*), based on voltage impulse 250 x 2 500 μs, representative of slow-front transient overvoltages [16];
  - Lightning impulse withstand voltage (*LIWV*), based on voltage impulse 1.2 x 50 μs, representative of fast-front transient overvoltages [16].

Rated withstand overvoltage values are defined following the insulation co-ordination procedure. The dielectric withstand of the equipment insulation is evaluated based on representative overvoltages, as defined by insulation co-coordination standard [16]. The representative overvoltages classification is summarized in [16] as showed in Table 2. This table clarifies how each type of overvoltage is classified and how it is represented by a standard test waveform voltage. To determine the dielectric ratings of an instrument transformer, users should determine the maximum expected overvoltage conditions by simulations and calculations; classify each overvoltage considering duration, frequency, and front-time; apply the suitable safety factor (to consider differences in assembly, dispersion of product quality, insulation aging etc) and finally, choose the suitable standard value.

Table 2 − Representation of Table 1 of IEC 60071-1:2019 [16] with the classes and standard representative overvoltage waveforms.

Class	Low frequency		Transient		
	Continuous	Temporary	Slow-front	Fast-front	Very-fast-front
Voltage or over-voltage shapes	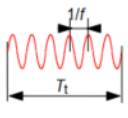	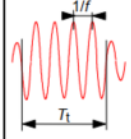	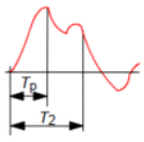	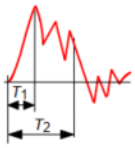	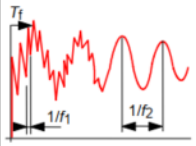
Range of voltage or over-voltage shapes	f = 50 Hz or 60 Hz $T_t \geq$ 3 600s	10 Hz < f < 500 Hz 0,02 s ≤ T_t ≤ 3 600 s	20 µs < T_p ≤ 5 000 µs $T_2 \leq$ 20 ms	0,1 µs < T_1 ≤ 20 µs $T_2 \leq$ 300 µs	$T_f \leq$ 100 ns 0,3 MHz < f_1 < 100 MHz 30 kHz < f_2 < 300 kHz
Standard voltage shapes	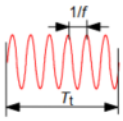 f = 50 Hz or 60 Hz T_t [a]	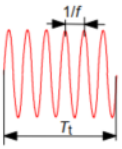 48 Hz ≤ f ≤ 62 Hz T_t = 60 s	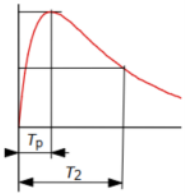 T_p = 250 µs T_2 = 2 500 µs	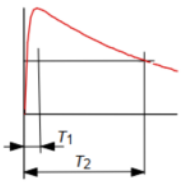 T_1 = 1,2 µs T_2 = 50 µs	[a]
Standard withstand voltage test	[a]	Short-duration power frequency test	Switching impulse test	Lightning impulse test	[a]

[a] To be specified by the relevant apparatus committees.

Source: [16]

During service, the instrument transformer is not expected to be subjected to overvoltages that reach the withstand voltage values, since the adoption of the insulation co-ordination procedure supposes the consideration of a suitable margin between the values obtained in calculations and simulations and the rated withstand voltage values defined for the equipment. For instance, to determine the rated power frequency withstand voltage of a current transformer, the user shall consider the maximum temporary overvoltage determined by calculations and simulations (insulation coordination studies) and add a suitable safety factor due to the following combined effects: the differences in the equipment assembly, dispersion in the product quality, quality of installation, the aging of the insulation during the expected lifetime and other unknow influences [16].

Lightning and switching impulse tests are classified by the relevant standards as type tests. In general, switching impulse is more severe to the external insulation. For current transformers, switching impulse is only applicable to equipment with $U_m \geq 300$ kV and under wet conditions (focus on external insulation). External insulation of equipment below 300 kV

is verified by a wet power frequency test. The assessment of the proper manufacture of the insulation is verified on each manufactured unit by performing the following routine tests:

- Power frequency withstand voltage test, usually performed at rated frequency for one minute;
- Partial discharge measurement, which is usually performed combined with power frequency withstand voltage test;
- Capacitance and dielectric dissipation factor measurement.

From a manufacturing quality perspective, partial discharge performance depends on the dimensional control of the active part and on the quality of the processes for drying the paper, drying/degassing the oil, and on the impregnation of paper by oil. Dielectric dissipation factor is strongly associated with drying and oil treatment processes.

Besides the dielectric withstanding, other tests are related to the insulation assessment. The requirements and tests related to the aging of the insulation of oil-impregnated paper current transformers are presented in 2.3.

2.2 THERMAL AND ELECTRIC STRESSES ON CURRENT TRANSFORMERS

As discussed in 2.1.2, a high voltage current transformer operates with three main heating sources: ohmic losses due to current flowing through the primary winding, ohmic losses due to current flowing through the secondary windings and dielectric losses. The manufacturers design and produce the CT by managing these heating sources to get a suitable thermal balance at steady state conditions without exceeding the maximum allowable temperatures defined by equipment standards.

The maximum temperature is the sum of the maximum operating ambient temperature (in general this temperature is 40 °C) plus the maximum temperature rise. IEC [16] defines 65 °C as the maximum temperature rise for the windings (during the test, it is determined based on winding resistance variation for secondary windings and on direct measurement for primary winding) and for other metallic parts and 55 °C measured on the top of oil. The compliance with this requirement is confirmed by the temperature rise test which is presented in 2.3.3.

Based on these limits, it is not expected that the temperature of any part of the CT exceeds 105 °C. In real operation, CT usually does not operate long periods at the rated maximum continuous operating current and at the maximum prescribed ambient temperature. In general, manufacturers define some standardization for the product ranges in terms of primary winding solutions, insulation design, core housing dimensions etc, leading to solutions which normally do not reach the temperature limits even considering the rated maximum continuous operating current. The range from 70 °C to 90 °C can be considered as an acceptable reference for insulation operating temperature. This is a remarkable difference in the approach between the application of oil-impregnated paper insulation system for current transformers and power transformers. Temperature operation for power transformers is usually higher and temperature is considered as the main aging factor for them.

Electrical stresses applied on CT insulation include continuous operating voltage, as well temporary and transient overvoltages, as discussed in 2.1.3. In the scope of the present work, the focus is on the maximum continuous operating voltage which corresponds to the maximum voltage U_m, defined by the standards as a phase-to-phase value, divided by $\sqrt{3}$ once the insulation system of the CT is connected to the grid between phase and ground.

For the internal insulation design, manufacturers in general analyze the voltage stress at rated power frequency withstand voltage and at partial discharge test voltage corresponding to 1.2 U_m / $\sqrt{3}$. The voltage stress at rated lightning impulse voltage is also considered. As demonstrated in Figure 10, the higher is the system rated voltage the lower is the standard rated power frequency withstand voltage in p.u. Thus, voltage stress at continuous operating voltage becomes more relevant to the insulation design definition for higher system voltages.

As discussed in 2.1.2, dielectric losses at U_m / $\sqrt{3}$ are more relevant for higher system voltage cases, once losses are directly proportional to the voltage to the square. This is the reason because IEC and IEEE standards prescribe that the temperature rise test is performed with simultaneous application of voltage to the insulation and current to the windings for current transformers with maximum voltage $U_m \geq 550$ kV.

Figure 10 − Power frequency withstand voltage standard values in comparison with rated maximum operating voltage.

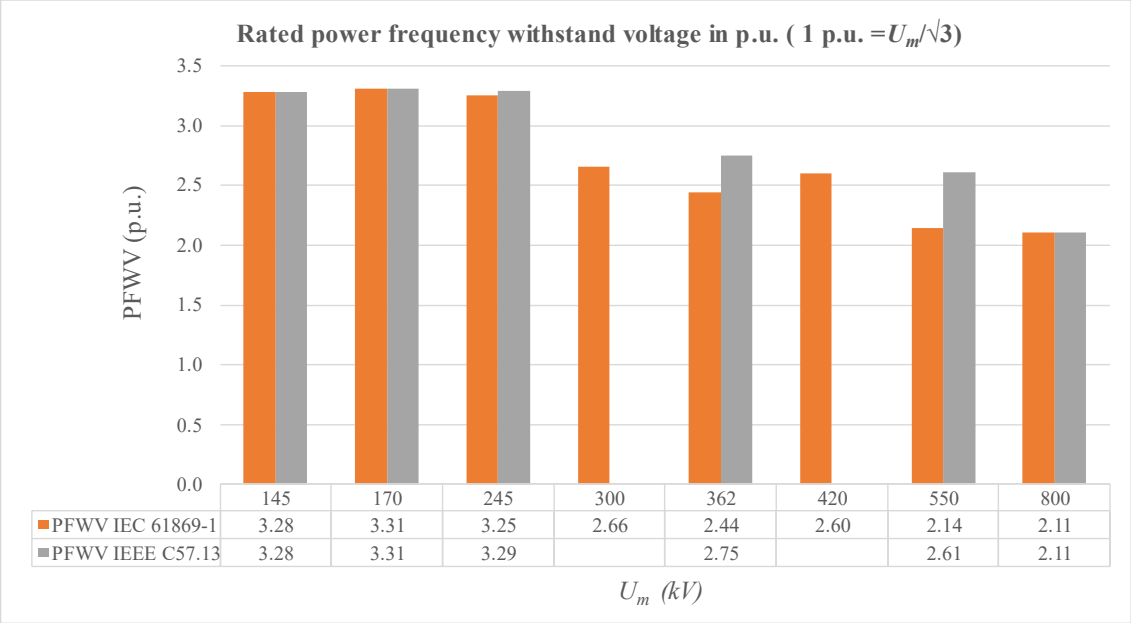

	145	170	245	300	362	420	550	800
PFWV IEC 61869-1	3.28	3.31	3.25	2.66	2.44	2.60	2.14	2.11
PFWV IEEE C57.13	3.28	3.31	3.29		2.75		2.61	2.11

Source: own authorship

2.3 REQUIREMENTS AND TESTS RELATED TO THE ASSESSMENT OF DIELECTRIC PERFORMANCE OF OIL-IMPREGNATED PAPER INSULATED CURRENT TRANSFORMERS

The withstand requirements that the insulation system of a high voltage apparatus shall comply with are defined by the relevant insulation co-ordination standards. As discussed in 2.1.3, based on an insulation co-ordination study, the user defines the following rated withstand voltage values, based on which the apparatus manufacturer will define the design of the insulation system:

- Rated power frequency withstand voltage;
- Rated lightning impulse withstand voltage;
- Rated switching impulse withstand voltage.

As discussed in 2.1.3, these values correspond to prescribed test voltages to be performed on a new equipment. In general, the power frequency withstand test is prescribed as a routine test and lightning and switching impulse are prescribed as type tests. The

determination of such values is based on overvoltage simulations and calculations and takes into account suitable margins to consider relevant factors, including the aging of the insulation system. Besides these withstand overvoltage values, the apparatus is specified for a maximum operation voltage condition. The IEC insulation co-ordination standard [16] defines the highest voltage for equipment (U_m) as the maximum r.m.s. value of phase-to-phase voltage for which the equipment is designed in respect of its insulation. The main insulation of a high voltage current transformer is connected phase-to-ground to the power grid. Thus, the highest r.m.s. voltage can be applied continuously to its insulation under normal service conditions corresponds to $U_m / \sqrt{3}$.

The IEC insulation co-ordination standard [16] *"leaves it to the relevant technical committee to prescribe a long-duration power frequency test intended to demonstrate the response of the equipment with respect to aging of internal insulation or to external pollution"*.

However, there is no long-duration power frequency test prescribed to be performed on instrument transformers for an aging assessment. Nevertheless, some tests are very relevant for the continuous operation voltage condition. Partial discharge and dielectric dissipation factor measurements are prescribed to be performed as routine tests, i.e., on every single manufactured unit. These measurements are the most relevant measurements to assess the quality of the insulation manufacture process. Additionally, the temperature rise test, prescribed as a type test, is intended to ensure critical temperatures will not be exceeded at the limiting rated operating conditions.

The tests related to slow-front and fast-front transients are not discussed in the present thesis because they are not part of the scope of this investigation.

2.3.1 Partial discharge measurement

Partial discharge is a localized *"electric discharge that only partially bridges the insulation between conductors"* [17]. In an oil-impregnated paper insulation system, partial discharges are a consequence of local electrical stress concentration that can exceed the local dielectric strength. In general, they occur in weak points of the insulation system caused by e.g., gas bubbles, voids, contaminants (e.g., moisture), and/or points at higher electrical fields. High electrical stress concentration can be caused by geometric imperfections of the insulation system. For the current transformer insulation system, partial discharge can also occur when

the overlap of paper layers is not properly done, resulting in oil-filled channels (refer to 2.1.2). Partial discharges cause local heating and result in gas generation which can increase partial discharge levels. Thus, partial discharges are a cause and a consequence of insulation aging.

IEC 61869-1:2007 [25] prescribes limiting values for partial discharge levels to be met during the routine test. In general, partial discharge measurement consists in applying the power frequency withstand voltage value for 1 minute, decreasing the test voltage to the partial discharge voltage values. Maximum prescribed partial discharge levels are 10 pC at U_m (or 1.2 U_m depending on the ground system where the equipment is intended to operate) and 5 pC at 1.2 U_m / $\sqrt{3}$. The control of partial discharge in the new apparatus is essential for a suitable insulation lifespan. Ideally, partial discharge inception and extinction voltages should be higher than the maximum continuous operating voltage since it is well known that the partial discharge inception voltage tends to decrease as a consequence of insulation aging.

2.3.2 Dielectric dissipation factor measurement

Dielectric dissipation factor (or *tan δ*) corresponds to the ratio between resistive and capacitive components of the current measured through a real capacitor, e.g., an insulation system. As discussed in 2.1.2, the value of the dielectric losses value is directly proportional to the dielectric dissipation factor. The IEC instrument transformers standard [25] prescribes 0.005 as the maximum value for tan δ for oil-impregnated paper equipment, measured at U_m / $\sqrt{3}$ at ambient temperature. However, typical values for *tan δ* for top core CT with oil-impregnated paper insulation are in the range of 0.002 to 0.003.

The dielectric losses are minimized by a suitable drying process of the insulating paper and proper oil treatment (removal of moisture and gases) before the oil filling/paper impregnation process, as discussed in 2.1.2. Moisture is one by-product of oil-impregnated paper insulation degradation, which increases *tan δ* value, i.e., it increases dielectric losses and the temperature of the insulation system. Chmura et al [26], in agreement with several authors, has demonstrated the increase of *tan δ* value as a consequence of degradation processes. In 2.5.3.1, the impact of the moisture in insulation degradation is explained.

2.3.3 Temperature rise test

The temperature rise test consists of submitting the CT to the maximum conditions of ohmic and dielectric losses according to the maximum heating conditions. The test is always performed at the rated continuous thermal current (i.e., the maximum current for continuous operation) with rated burdens connected to the secondary windings. As demonstrated in Table 1, dielectric losses are more relevant at higher operating voltages. Thus, for CT with $U_m \geq 550$ kV, IEC [27] and IEEE [28] prescribe that the temperature rise test shall be performed with simultaneous application of the rated continuous thermal current the primary winding and the voltage $U_m/\sqrt{3}$ to the CT insulation (between primary terminals and earth). The CT remains energized until the steady state temperature rise (thermal equilibrium condition) is reached. Both IEC [27] and IEEE [28] standards prescribe thermal equilibrium condition achieved after three times the thermal time constant of the transformer.

2.3.4 Thermal stability test and *tan δ* measurements at high temperature

Some electrical utility companies prescribe in their technical specifications the thermal stability test which corresponds to the temperature rise test with voltage and current simultaneous application but with the addition of tan δ measurements during the test. In general, a thermal stability test is prescribed to be performed at a controlled 40 °C ambient temperature. However, practically, it is not easy to find test facilities that can apply high voltage and high current simultaneously at controlled 40 °C ambient temperature.

As discussed in [19] and [24] another test related to the thermal stability assessment is the measurement of tan δ at a high temperature. This measurement is usually performed with CT insulation at 85 ± 5 °C. Based on measurements at high and normal ambient temperature, the dielectric loss temperature coefficient α_c is calculated using equation (4) as demonstrated in 2.1.2 . Based on investigations mentioned in [19] and [24], CT is considered as thermally stable when α_c is ≤ 0.01 and thermally unstable if α_c is ≥ 0.02. When $0.01 < \alpha_c < 0.02$, it is recommended to perform the thermal stability test.

2.3.5 Dielectric frequency response (*DFR*) and polarization and depolarization current (*PDC*) measurements

Dielectric frequency response (*DFR*) and polarization and depolarization current (*PDC*) are recent non-invasive techniques for oil-impregnated paper insulation assessment

based on the measurement of dielectric response functions. *PDC* is a time-domain technique and *DFR* (which is also called Frequency Domain Spectroscopy – *FDS*) is a frequency-domain technique. Both are based on polarization processes of insulation and are intended to evaluate moisture content of solid insulation and conductivity of impregnating oil, quantities impacted by thermal aging of oil-impregnated paper insulation. Morsalin et al [29] published a review on dielectric loss assessment which is used as the basis for the explanation of *PDC* and *DFR* measurements as follows.

2.3.5.1 PDC measurement

When a DC electrical field is applied on an oil-impregnated paper insulation system, three different currents (and respective losses) are observed (see *Figure 11*):

- Resistive (or leakage) current (in phase with electrical field): related to solid contaminants on the surface or inside the insulation;
- Capacitive charging current (in quadrature with electrical field): originated by charge displacement in the electrodes;
- Dielectric absorption current (in quadrature with electrical field); related to polarization of molecules in the insulating medium.

Figure 11 − Current components related to a DC electrical field applied on an insulation system.

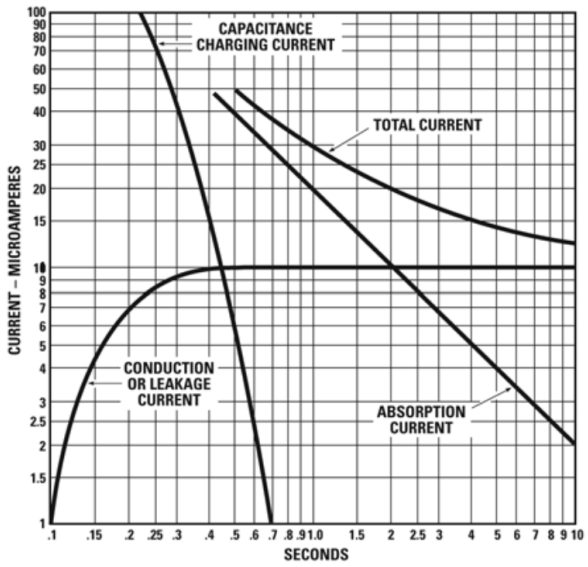

Source: [30]

As presented by Morsalin et al [29], when an electrical field *E(t)* is applied on an insulation system, the total current density *J(t)* can be expressed as the sum of a conduction current and a displacement current as described by equation (5):

$$J(t) = \sigma_0 . E(t) + \frac{\partial D(t)}{\partial t} \tag{5}$$

Where σ_0 is the DC conductivity of the insulation and the electrical displacement D*(t)* is:

$$D(t) = \varepsilon_0 . \varepsilon_\infty E(t) + \Delta P(t) \tag{6}$$

Where:

ε_0 is the vacuum permittivity.

ε_∞ is the relative permittivity of the insulation.

ΔP(t) is the polarization function described by equation (7), φ(t) is the dielectric response function.

$$\Delta P(t) = \varepsilon_0 \int_0^t \varphi(t-\tau) E(\tau) d\tau \tag{7}$$

Where τ is the relaxation time.

Following Morsalin et al [29] demonstration, from equations (5), (6) and (7), the expression of dielectric current is rewritten as follows:

$$J(t) = \sigma_0 . E(t) + \varepsilon_0 . \varepsilon_\infty \frac{dE(t)}{dt} E(t) + \varepsilon_0 \frac{d}{dt} \int_0^t \varphi(t-\tau) E(\tau) d\tau \tag{8}$$

The *PDC* method consists of the measurement of polarization and depolarization current by the excitation of insulation with a *DC* electrical field, aiming to obtain the polarizing information of the material in the time domain. Kumar and Mahajan [31] define dielectric polarization as the "*relative shift of positive and negative charges under the influence of applied electrical field (...) produced due to different polarization processes namely induced polarization of individual atoms and/or ions, orientation polarization of permanent dipoles, interfacial polarization and hopping of charges at localized sites.*" According to them, the

interfacial polarization is dominant in composite insulation system as the oil-impregnated paper insulation.

As presented by Morsalin et al [29], a simplified test circuit and the basic principle is clarified in

Figure 12. The polarization and later, the depolarization of the test object is provided by closing the switches S_1 and S_3 respectively. T_p and T_d are the periods of polarization and depolarization. The switch S_2 is intended to provide a short-circuit between the terminals of the meter to avoid any damage before the periods T_p and T_d. The measured polarized current $i_p(t)$ contains absorption and conduction components. The depolarization current $i_d(t)$ contains the absorption component only. Equations (9) and (10) give the expressions for $i_p(t)$ and $i_d(t)$.

$$i_p(t) = C_0 U_0 \left[\frac{\sigma_0}{\varepsilon_0} + \varepsilon_\infty \delta(t) + \varphi(t)\right] \tag{9}$$

Where:

C_0 is the geometrical capacitance.

U_0 is the excitation DC voltage.

σ_0 is the DC conductivity of the insulation.

$\delta(t)$ is the loss angle.

$\varphi(t)$ is the dielectric response function.

$$i_d(t) = -C_0 U_0 \left[\varphi(t) - \varphi\left(t + T_p\right)\right] \tag{10}$$

According to Morsalin et al [29], $\varphi(t+T_p) \approx 0$ and the *DC* conductivity is obtained from the combination of equations (9) and (10) resulting in equation (11).

$$\sigma_0 \approx \frac{\varepsilon_0}{C_0 U_0}\left[i_p(t) - i_d(t)\right] \tag{11}$$

Figure 12 − PDC simplified circuit and basic principle.

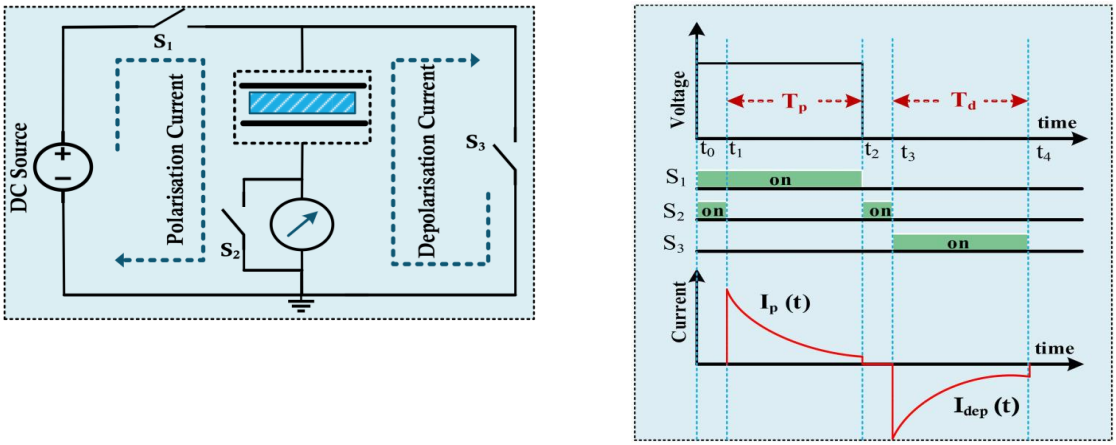

(a) PDC measurement circuit *(b) PDC basic principle*

Source: [29]

According to Morsalin et al [29], for oil-paper insulation, the dielectric response function *φ(t)* is given by:

$$\varphi(t) = \frac{A}{\left(\frac{1}{T_0}\right)^x + \left(\frac{1}{T_0}\right)^y}; 0 < x < y \; and \; T_0 > 0 \tag{12}$$

Where A, x and y are constants dependent on the materials and construction of the insulation system. Morsalin et al [29] states "*After measuring the polarization/depolarization current, all the unknown parameters of the equations can be obtained mathematically using a non-linear fitting process*."

2.3.5.2 DFR measurement

As explained by Chunming et al [32], when a sinusoidal voltage *U*(*t*) is applied on an insulating medium, the respective current is done by equation (13) .

$$I(\omega) = \left[\frac{\gamma_0}{\varepsilon_0} + j\omega\left(\varepsilon_\infty + F(\omega)\right)\right] C_0 U(\omega) \tag{13}$$

The repolarization rate is given by equation (14)

$$X(\omega) = F(\omega) = X'^{(\omega)} - jX''^{(\omega)} = \int_0^\infty f(t)\, e^{-j\omega t} dt \tag{14}$$

The full current in the frequency domain is given by equation (15)

$$I(\omega) = j\omega C_0 \varepsilon^*(\omega) U(\omega) \tag{15}$$

And finally, the dielectric dissipation factor is given by equation (16). The real part is related to the complex capacitance of the measured insulating medium, and the imaginary part is related to its losses, and both are frequency dependent.

$$tan\delta(\omega) = \frac{\varepsilon"(\omega)}{\varepsilon'(\omega)} = \frac{\frac{\gamma_0}{\varepsilon_0} + X"(\omega)}{\varepsilon_\infty + X'(\omega)} \tag{16}$$

In DFR measurements, "*a sinusoidal voltage of variable frequency (typically 1 mHz to 1 kHz) is used to get the frequency domain spectra of the permittivity, dissipation factor and complex capacitance of the insulation system*" [33] . The losses in an insulation system under a sinusoidal *AC* electrical field are caused by the following main polarization mechanism:

- Electronic polarization (displacement of electron orbits);
- Ionic polarization (ionic molecules moving along the electrical field);
- Orientation (Dipolar) polarization (rotation of polar molecules, e.g., water);
- Interfacial polarization (space charge accumulation at the interface of oil and paper, predominant mechanism at frequencies lower than 10 Hz).

Each one of these processes has a different time constant. Thus, depending on the time constant, each process is predominant for a defined excitation frequency range. *Figure 13* shows the frequency range linked to each type of polarization mechanism. By exciting the insulation system with an electrical field at different frequencies and measuring losses at each excitation frequency, it is possible to identify the presence of polarization mechanisms in the insulation system.

Chunming et al [32] gives a typical *FDS* chart for oil-impregnated paper insulation which is presented in *Figure 14*. The curve line presented in this chart is a combination of the *DDF* values of solid and liquid insulation. Three frequency bands are identified by the color of the line: low frequencies in blue, medium frequencies in red and high frequencies in yellow. The aging degree and moisture content of oil-impregnated paper affect the *DDF* values mainly at very low frequencies (blue line), but there is an impact on the yellow line too. The higher is the moisture content in solid insulation the higher are the *DDF* values at these frequencies. The red line is mainly affected by the insulating oil conductivity. The greater the oil conductivity,

the red line will move to the right, the smaller the oil conductivity, this line will move to the left [32].

Figure 13 − Frequency range of polarization mechanisms.

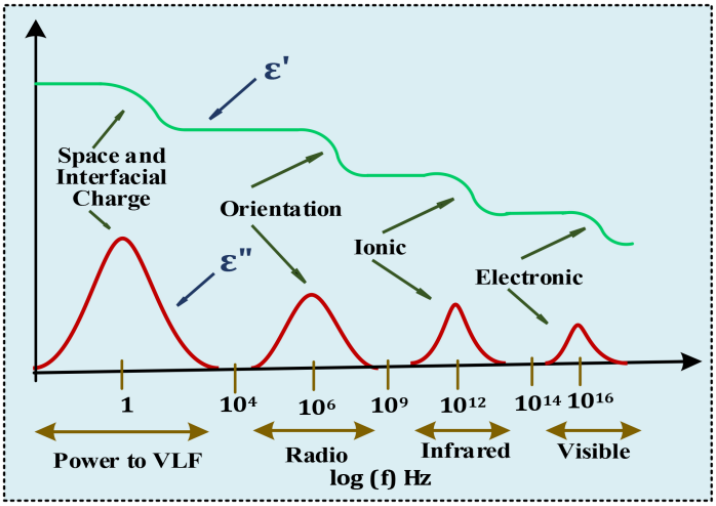

Source: [29]

Figure 14 − Typical oil-impregnated paper FDS chart.

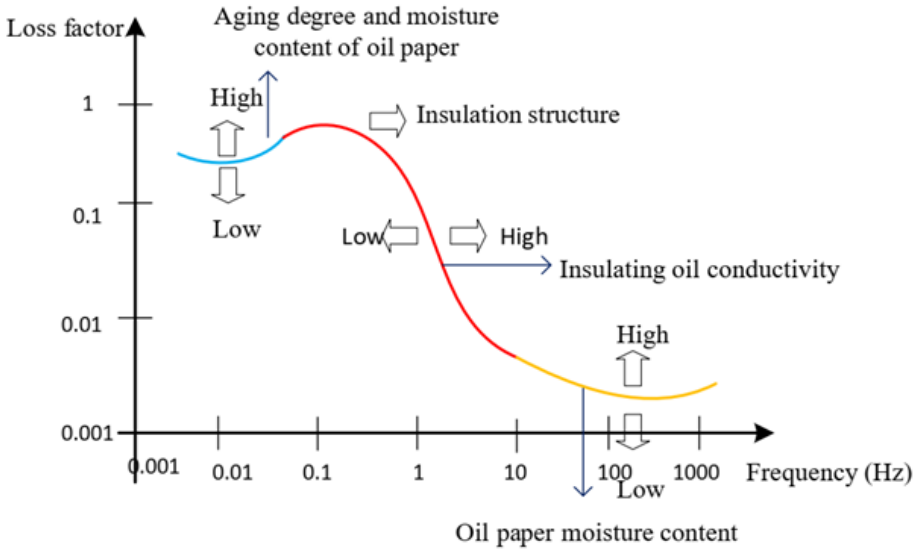

Source: [32]

FDS measurement is also affected by the temperature of insulating media [33]. However, the temperature effect can be compensated by suitable algorithms [34] . According

to Zhang et al [35] this compensation is done using an *FDS*-curve frequency translation method based on equation (17).

$$f_T = f_0 e^{\left[-\frac{E_A}{k_B}\left(\frac{1}{\theta_T}-\frac{1}{\theta_0}\right)\right]} \quad (17)$$

Where:

f_T is the frequency of the translation temperature, in Hz.

f_0 is the base frequency, in Hz.

E_A is the activation energy, in eV.

k_B is the Boltzmann's constant, which is equal to 1.38 x 10^{-23} J/K.

θ_T is the required translation temperature, in K.

θ_0 is the base temperature, in K.

The estimation of moisture based on the *FDS* technique was initially developed for the power transformers case and it is based on the representation of the insulation system using the XY model [34, 35]. The moisture content in solid insulation is done based on a comparison between the measured and modeled curves. Raetzke, Koch and Anglhuber [36] gives a representation of the XY model showing the parameters X and Y for a cylindrical multi-layer insulation as used for power transformers (See *Figure 15*). The parameter X represents the ratio of the total thickness of the solid barriers to the total insulation thickness between HV and LV windings. The parameter Y represents the ratio of the total width of solid spacers to the average circumference of the main insulation between HV and LV windings.

Figure 15 − Representation of a cylindrical multi-layer-insulation by the XY model as used for power transformers.

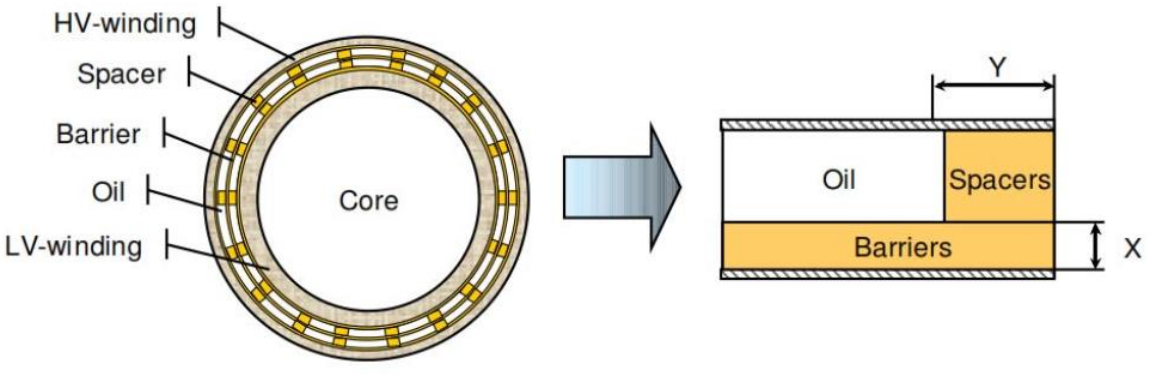

Source: [36]

Raetzke, Koch and Anglhuber [36] mentioned that it is possible to use the XY model to represent the insulation of instrument transformers as well. According to them, the solid insulation (70 % - 90 %) that consists of paper enwrapping the inner conductor (which is the set formed by the core box and the stem tube for a top core CT) has a similar behavior as barriers. There are also oil gaps between the layers of paper.

In other work, Anglhuber and Kock [37] mentioned the use of this technique for instrument transformers depends on knowledge about the insulation construction and influence of specific effects. According to them, its use for voltage transformers is of almost no benefit due to the specific construction insulation design. However, for current transformers, a similar model applied to power transformers can be applied for estimation of aging conditions. Robalino and Güner [38] related an experience based on the approach of measuring "sister units" under similar conditions and evaluating the dissipation factor variation. According to them, the relevant frequency range for instrument transformers is from 1 kHz down to 10 mHz. Anglhuber and Kock [37] consider measurements from 1 kHz to 1 mHz for current transformers. According to them, the measurements at lower frequencies are not needed due to the absence of large oil gaps.

2.3.6 Tests on oil samples

As mentioned in 2.4.2, one additional function of the insulation liquids in power equipment is to become an information carrier on the solid insulation condition. In 2.5.3.4, the main degradation products related to the oil-impregnated paper insulation are presented. Most of them will remain in the insulating oil. Thus, tests on oil samples removed from the current transformer are useful, in combination with the other tests discussed in 2.3, for the assessment of dielectric performance and insulation system condition. These tests are presented in 5.2.1.

The most common tests performed on new equipment by manufacturers in combination with routine tests are:

- Dissolved gas analysis, DGA (usually performed on samples taken before and after power frequency withstand voltage test);
- Dielectric strength;
- Dissipation factor;

- Moisture content;
- Interfacial tension.

For the assessment of insulation during service life, the most common test is *DGA*. During preventive maintenance activities, many utilities also carry out the other tests listed above and oil acidity content. Other tests that are indicated in special investigations are: *HPLC* (High Performance Liquid Chromatography), intended to determine the content of furanic compounds, and the content of alcohol.

2.4 OIL IMPREGNATED PAPER INSULATION – MATERIALS

Oil-impregnated cellulose is the most commonly used insulation system for transformers, either power transformers or instrument transformers. According to Prevost and Oommen [39] "*the 1920s and 1930s were periods of much experimentation on how to improve the dielectric performance of the paper-oil system*" and "*by the late 1920s and early 1930s, kraft paper insulation began to be used in combination with insulation oil in transformers*."

Life span of a transformer is mainly determined by the life span of its insulation system, which corresponds to solid insulation life for paper-oil transformers, since cellulose aging is not reversible. Most transformers use mineral oil as the impregnation liquid, but synthetical and natural ester liquids are also used. Solid insulation is based on impregnated cellulose. Electrical cellulose includes single or multiply papers and moldable, calendered, or hot press dried pressboard [2].

The use of cellulose and mineral oil to form a hybrid system results in a medium whose dielectric strength reaches values higher than the values obtained for the cellulose and oil components separately [40] . The main roles of solid insulation are to provide electrical insulation between electrodes at different potentials and support conductors mechanically. The impregnation liquid improves dielectric properties of solid insulation, acts as a coolant and as an information carrier that assesses solid insulation condition.

Krause [41] differentiates between two main uses of cellulose and mineral oil insulation: the full solid insulation technique, i.e., oil-impregnated soft paper insulation and

oil/barrier insulation with predominant application of cellulose as pressboard parts. Krause [41] also mentions that "*the first one is predominantly used in current and voltage transformers and bushings; the latter constitutes the current power transformer insulation technique worldwide*."

2.4.1 Cellulose materials for electrical insulation

Cellulose is a complex carbohydrate which is the most important constituent of most plants. For electrical insulation purposes, cellulose is refined from trees (mainly pine or spruce wood from Scandinavia, Canada and Chile) by the suphate of kraft process [2], to obtain unbleached softwood kraft pulp whose typical composition is:

- 75 % - 85 % Cellulose;
- 10 % - 20 % Hemicelluloses;
- 2 % - 6 % Lignin;
- < 0.5 % Inorganics.

Cellulose is a linear polymer consisting of anhydroglucose joined together by glycosidic bonds. The average number of glycosidic rings in a cellulose macromolecule is called degree of polymerization and it is the most used parameter to assess the aging condition of cellulose insulation. For unbleached softwood kraft pulp, the degree of polymerization (*DP*) is usually in the order of 1 200 and it is considered at the end of life when the DP value reaches about 200 [41]. Hemicelluloses are complex polysaccharides with lower degree of polymerization (50-250) which form the matrix in which cellulose fibers are embedded [2]. They play an important role in the mechanical strength of the kraft pulp. Lignins are amorphous polymers which give firmness and solidity to the cellulose fibers, but they have high reactivity with oxidizing agents [2]. When the thickness is smaller than 0.8 mm, it is referred to as paper, otherwise it is referred to as pressboard. An overview of the types of cellulose materials used for electrical insulation is given in Figure 16.

Once temperature is a key aging factor of cellulose insulation, the use of thermally upgraded paper (*TUP*) in power transformers has become very common. This is a cellulose-based paper chemically modified to reduce the rate at which the paper decomposes due to temperature. Chemical modification is based on the use of additives for water formation inhibition (stabilizing agents) and or partial neutralization of water forming agents [2].

Figure 16 − Overview of cellulose materials used for electrical insulation.

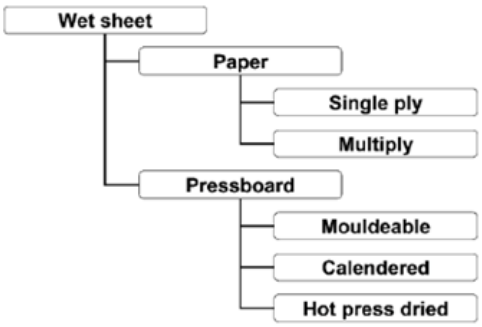

Source: [2]

As defined in [42], thermally upgraded paper is a cellulose-based paper that meets the life criteria defined in [43], i.e., 50 % retention in tensile strength after 65 000 hours in a sealed tube at 110 °C or any other time/temperature combination given by the equation (18), where θ is the aging temperature in °C and *L(h)* is the life in hours. This equation is a particular case of the Arrhenius model which will be discussed in 2.5.7.

$$L(h) = e^{\frac{15000}{(\theta+273)}-28.028} \tag{18}$$

TUP is not used for instrument transformers in general since the maximum hottest spot temperature is limited to 105 °C. Insulating paper used for instrument transformers is unbleached, not calendered with sulphate cellulose content in the dry mass of 90 % minimum. Plain kraft paper and/or crepe paper are used. The typical thickness ranges from tens to a few hundred micrometers and the apparent density from 0.60 to 0.75 g/cm^3.

2.4.2 Electrical insulating oil

Electrical insulation liquids in power equipment perform different functions as follows:

- electrical insulation between electrodes at different potentials;
- impregnation of solid insulation improving dielectric strength of composite insulation systems (e.g., oil impregnated paper insulation);
- act as cooler by convection;
- be an information carrier that assesses solid insulation condition.

Mineral oils are the most used insulating liquids for impregnated-paper oil insulation in transformers. They are refined mixtures of different hydrocarbons obtained by fractional

distillation of natural petroleum [40]. Petroleum oils are mixtures of 3 main different types of compounds: paraffinic, naphthenic, and aromatic compounds. Depending on the predominant component of the mixture, mineral oils are classified as paraffinic or naphthenic base oils. Naphthenic oils are more frequently used as dielectrics due to their better fluidity at lower temperatures. Oils with aromatic content equal or higher than 5 % are classified as aromatic oils, or highly aromatic if this content exceeds 10 %. Mixtures to be used as transformer oils are refined to meet suitable electrical insulation and heat transfer characteristics. According to Prevost and Oommen [39], the use of transformer oil was introduced by General Electric (GE) in 1892, but its use in combination with cellulose dates back to 1920s, as well the improvement from paraffinic to naphthenic.

Since high voltage current transformers are usually hermetic sealed equipment and considering a suitable control of manufacturing process conditions which leads to an initial condition of the inner environment with very low moisture and gas content, the most relevant stresses are electrical and thermal.

2.5 OIL IMPREGNATED PAPER INSULATION – DEGRADATION PROCESSES, AGING MODELS AND ASSESSMENT OF AGING CONDITIONS

The aging of the oil-impregnated cellulosic insulation systems is the most determinant factor that limits the life expectance of an oil-impregnated transformer [2]. Since the solid insulation degradation is not reversible, the life spam of the transformer is currently linked to the aging of the cellulosic insulation. The insulation is affected by different types of stresses like thermal, electrical, mechanical and environmental. For a current transformer, these stresses can be as follows:

- Electrical stresses: electrical gradients in the insulation need to be considered for different conditions, i.e., gradients at long duration/continuous operating voltage, at short duration overvoltages and at fast or very fast transient conditions;
- Thermal stresses: thermal stability of the transformer shall be determined considering the heating sources at continuous operating conditions: power

losses from the windings (RI^2), core losses and insulation losses (dielectric dissipation factor);

- Mechanical stresses: vibrations, mechanical forces in short time current conditions, etc.;
- Environmental stresses: physical-chemical conditions of the environment of the insulation, i.e., presence of moisture, oxidation, gases, etc.

High voltage current transformers are usually hermetic sealed equipment. Thus, external environmental stresses are not very important for the degradation of the internal insulation. They are static equipment, and mechanical loads are not relevant stresses for the internal insulation. Considering a suitable control of the manufacturing process which leads to an initial condition of the inner environment with very low moisture and gas content (i.e., moisture content in paper 0.1-0.2 %, with moisture content in oil ≤ 5 ppm and gas content ≤ 0.3 %), the most relevant stresses concerned to the degradation of the internal insulation are electrical and thermal stresses.

2.5.1 Aging effect on cellulose properties

The aging condition of cellulose is assessed by the variation of some key properties of the material which are related to the mechanical and insulation functions. The following properties of cellulose can be considered for aging condition assessment: tensile strength, degree of polymerization and elongation.

The tensile strength of the cellulosic insulation is a key property for evaluating aging conditions and life assessment. This is important mainly for power transformers, considering the mechanical function of solid insulation in supporting transformer windings. Dielectric strength is less affected, even a significant reduction of the tensile strength. For power transformers, the end of life of cellulosic insulation is considered when its tensile strength is 50 % less than the initial value. The tensile strength is linked to the degree of polymerization and the relationship between these two properties has been determined experimentally [2].

The degree of polymerization (*DP*) is a measure of the average number of glucose units of the cellulose molecules. This quantity is the most widely used parameter to assess the aging condition of cellulosic insulation. As presented in [2], typical values of *DP* for new paper supplied to transformer manufacturers are between 1 100 and 1 200. After the drying process, this value is reduced to 900 - 1 000. The DP value at end of life is defined by the users,

considering some margin. A typical value is 200 [44]. Although it is feasible that a physical-chemical parameter such as *DP* can be used to determine the insulation end of life, monitoring *DP* value during operation is an issue, since it is generally not possible to take samples from the hottest points of the insulation. Many works have been proposed to relate the *DP* value of the cellulosic insulation with the concentration in oil of cellulose decomposition products such as furans or alcohols.

For high voltage current transformers, it is impossible to take samples of the insulation paper without damaging and losing it. Paper samples of instrument transformers at end-of-life condition many times do not show relatively low DP value, which is an indicative, for these cases, that the thermal aging was not the predominant degradation mechanism that has led the insulation to the end of life. The maximum admissible temperatures for oil-impregnated paper current transformers are 65 °C of temperature rise for maximum ambient temperature at 40 °C, resulting in 105 °C. Typically, the average insulation temperature does not exceed 85 °C.

At the end of life, elongation becomes very small. As the tensile strength, elongation is linked to the degree of polymerization. As an illustration, *Figure 17* shows an example of the loss of properties for crepe kraft paper.

Figure 17 − Aging and loss of properties for crepe kraft paper.

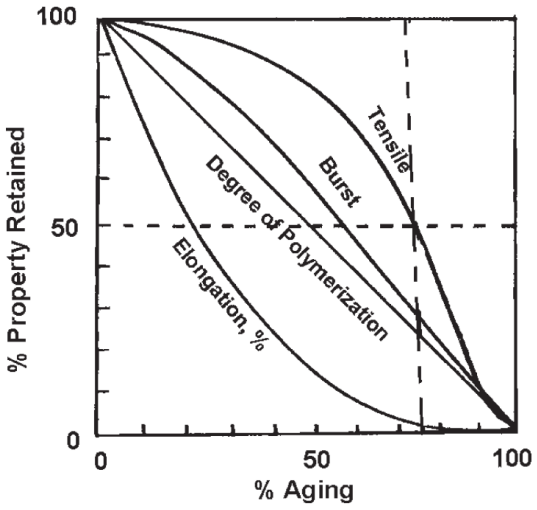

Source: [45]

2.5.2 Aging effect on insulating oil

Mineral insulating oils are refined mixtures of different hydrocarbons obtained by fractional distillation of natural petroleum [40]. Oxidation is the primary mechanism of mineral insulating oil aging [46]. This process is explained in 2.5.3.2. As explained in [46], in this process, oxygen is involved in the extraction of a hydrogen atom from a hydrocarbon molecule, forming radicals that then undergo propagation, branching and termination stages of oil oxidation. These reactions produce acids, moisture, and polar compounds such as alcohols and hydroperoxides. Thus, the total concentration of oxidation inhibitors is one of the parameters used to assess oil aging conditions. Other parameters frequently employed to assess the degree of aging of insulating oil are interfacial tension and acidity. The interfacial tension is an indirect measure of the concentration of polar substances which impact oil dielectric performance. Many different acids can be formed when oil is oxidized. As acid values increase, oil quality decreases. In general, acidic by-products increase dielectric loss, corrosivity and sludge formation.

2.5.3 Oil-impregnated paper aging kinetics

Most of the literature on oil-impregnated paper aging is focused on power transformers, for which the thermal degradation is the predominant aging process, and the mechanical properties of the solid insulation are essential to determine end-of-life criteria. Thus, the degree of polymerization (*DP*) is the most important parameter used to assess cellulose degradation. Heat, the presence of water, water-soluble organic acids and oxygen accelerate the degradation of cellulosic insulation. During the aging process, *DP* is reduced due to scission of cellulose chains. The initial degree of polymerization DP_0 and DP_t, i.e., value of *DP* after an aging period t [47], can be combined with the Arrhenius equation as follows [2]:

$$\frac{1}{DP_t} - \frac{1}{DP_0} = A.e^{-\frac{E_A}{R.\theta}}.t \tag{19}$$

where *A* is a constant depending on the chemical environment, E_A is the activation energy (kJ/mol), *R* is the molar gas constant (8.314 J/(mol.K)) and *T* is the absolute temperature in K. Since a value for the degree of polymerization is set as an end-of-life criteria, the equation

(19) can be reorganized to express the expected lifespan *L(h)* as a function of temperature θ and the parameters *A* and E_A, as follows:

$$L(h) = \frac{\frac{1}{DP_t} - \frac{1}{DP_0}}{A} . e^{-\frac{E_A}{R.\theta}} \quad (20)$$

Degradation of oil-impregnated paper insulation in transformers is governed by three simultaneous processes: hydrolysis, oxidation and pyrolysis. Each one of these processes will be the predominant one depending on the temperature. These degradation processes are explained in 2.5.3.1, 2.5.3.2 and 2.5.3.3, and they are summarized in Figure 18. As presented in [2], total degradation can be expressed as a sum of degradation caused by each process:

$$\eta_{tot} = \left(A_{oxi} . e^{-\frac{E_{oxi}}{R.\theta}} + A_{hyd} . e^{-\frac{E_{hyd}}{R.\theta}} + A_{pyr} . e^{-\frac{E_{py}}{R.\theta}} \right) . t \quad (21)$$

Where:

η_{tot} is total degradation.

A_{oxi}, A_{hyd} and A_{pyr} are the chemical environment constants related to oxidation, hydrolysis and pyrolysis, respectively.

E_{oxi}, E_{hyd} and E_{pyr} are the activation energy related to oxidation, hydrolysis and pyrolysis, respectively.

Figure 18 – Cellulose aging mechanisms.

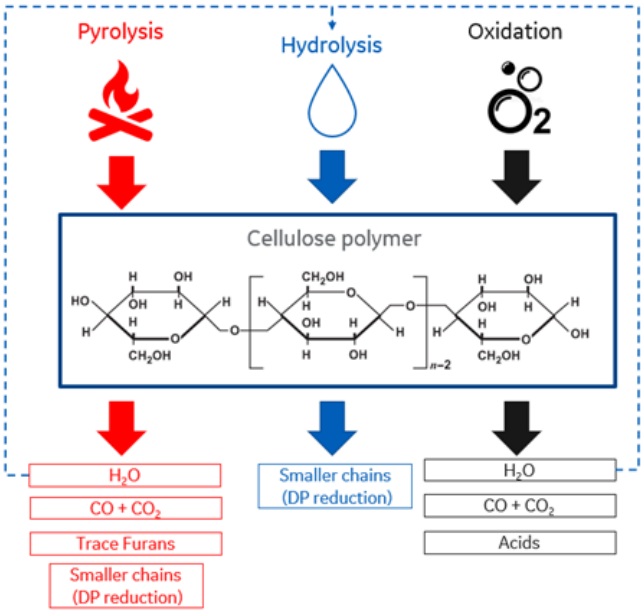

Source: Adapted from [48] *and* [45]

Figure 19 illustrates the aging rates dependence on temperature varying depending on the predominant process of each region.

Figure 19 - Sketch of aging rates due to different aging mechanisms documented in mineral oil. The arrow shows the effect of increased water content increasing the A-factor for hydrolysis.

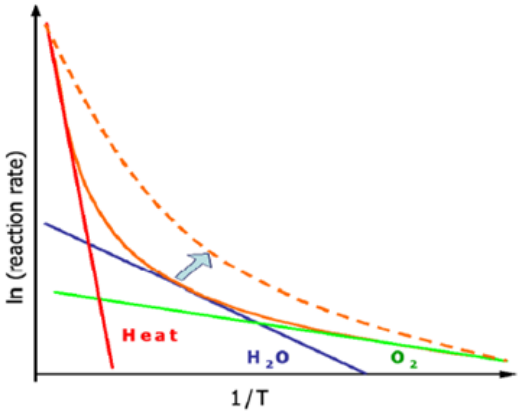

Source: [2]

Thus, considering a real-life oil-impregnated paper insulation system, it is not a simple task to determine the specific constants related to the chemical environment for each degradation process, as well as the specific activation energy related to each one of these processes. Many authors found values of activation energy related to oil-impregnated paper insulation (based on standard kraft paper), as summarized in Table 3.

Table 3 − Activation energy E_A for standard kraft paper.

Author	**Activation Energy (E_A) kJ/mol**	**Year**
Emsley et al **[49]**	105 - 117	1997
Lundgaard **[50]**	96 - 125	2004
Gilbert et al mentioned by **[2]**	96 -107	2009

2.5.3.1 Hydrolysis

Hydrolysis is a degradation process of cellulose related to the presence of moisture and liquid acids. Martins [51] explains the hydrolysis process in the following terms: *"The water molecule reacts directly with the bridge oxygen formed between two glucose monomers in the cellulose chain to form two hydroxyl groups (OH), each linked to its monomer, at the*

same time as the opening of the glucose ring, with breakage of the cellulose polymer chain, into two shorter segments, (which causes the degree of polymerization of the cellulose to be reduced). This process is autocatalytic, being for each cell division of the cellulose chain, consumed and produced water."

According to Lundgaard et al [52] hydrolysis of cellulose is a catalytic process governed by H+ ions from dissociated carboxylic acids whose aging rate is proportional to the number of H+ ions. The presence of water affects the H+ concentration by causing the dissociation of carboxylic acids, enhancing the aging process. According to Martins [51], there is a direct relationship between the speed of aging of the paper by hydrolysis and the moisture content in the paper, so that if the moisture content in the paper doubles, the speed of aging of the paper also doubles. Likewise, a reduction of 1 % in moisture content on paper roughly doubles the lifetime of the solid insulation.

Before the impregnation with insulating oil, the cellulosic insulation is submitted to a drying process to reduce the water content from 6-10 % to a value lower than 0.5 % [45]. For hermetically sealed apparatus (i.e., most instrument transformers), the purpose of the drying is to reach a water content between 0.1 % and 0.2 % [19]. Even the impregnation oil should be dried and degassed before the impregnation process. This oil treatment process intends to get water content lower than 5 ppm and gas content limited to 0.3 % [19]. The drying process is a key part of the insulation manufacture process once the presence of water increases the degradation rate of cellulose.

As demonstrated by Fallou, mentioned in [2], the degradation rate of paper starting from an initial water content value of 4 % is 20 times more than that at 0.5 %. Oommen and Prevost [45] state: "*Wet insulation is a dielectric hazard in several ways: 1) PD inception becomes significant above 3% moisture level and may result in gas bubbles and release of hydrogen, 2) insulation power factor would be above acceptance limits, 3) paper degradation and aging would be excessive"*.

The pre-exponent constant *A* (environment factor), from the Arrhenius relation, depends on the chemical environment where the insulation is. Thus, a higher moisture content value results in a higher constant *A* and, consequently, in a higher degradation acceleration. Research results on environment factor *A* have been consolidated in Annex A of IEC 60076-7 Edition 2.0 [5]. Table 4 shows the results for non-thermally upgraded paper, demonstrating the influence of moisture content on the environmental factor.

Table 4 − Environment Factor A and Activation Energy E_A for hydrolysis and oxidation – non-thermally upgraded kraft paper – Reference values given by IEC [5].

Aging Parameter (Arrhenius relation)	**Free from air and 0.5 % moisture**	**Free from air and 1.5 % moisture**	**Free from air and 3.5 % moisture**	**With air and 0.5 % moisture**
***A* (h^{-1})**	4.1×10^{10}	1.5×10^{11}	4.5×10^{11}	4.6×10^{5}
E_A (kJ/mol)	128	128	128	89

For power transformers, there are two main moisture sources: the ingress of atmospheric air into the tank and the aging process by itself, since water is one of the degradation by-products. The typical rate of water contamination per year is about 0.03 % to 0.06 % of water in cellulosic materials for transformers with membrane-sealed conservator preservation systems and 0.2 % for transformers with an open-breathing conservator [2]. Instrument transformers are usually hermetically sealed, thus the ingress of atmospheric air into the tank occurs only in case of a leakage due to a defect. Thus, considering a suitable drying process for the paper and proper oil treatment, it is expected the moisture-in-oil content is lower than 10 ppm for new instrument transformers [19].

2.5.3.2 Oxidation

The scission of cellulose chains can also be caused by oxidation. According to Lundgaard et al [50], oxidative depolymerization is catalyzed by hidroxy-radicals (HO-) which are produced by decomposition of hydrogen peroxide H_2O_2 and organic hydroperoxides (ROOH). Matharage et al [53] suggests, when insulation moisture content is low and free from acidity, the deterioration of the paper may begin with oxidation. Oxidation in both paper and oil, produces acidity which progressively suppresses the oxidation while starting acid-catalyzed hydrolysis. For oil, oxidation is the most important aging process [19]. Oil oxidation may produce both water and acids, which can catalyze cellulosic degradation. Moisture and acids produced from oil and paper oxidation will initiate the self-acceleratory hydrolysis process. Thus, oxidation stability is a very important parameter for oil. Wiklund et al [46] give a brief explanation of oxidative aging of mineral insulating oils, which is summarized by them in *Figure 20*.

Reference values for the environmental factor *A* and Activation Energy E_A depending on air presence (oxygen), related to non-thermally upgraded kraft paper, are showed in Table 4.

Figure 20 − Simplified oxidation pattern for insulating oil.

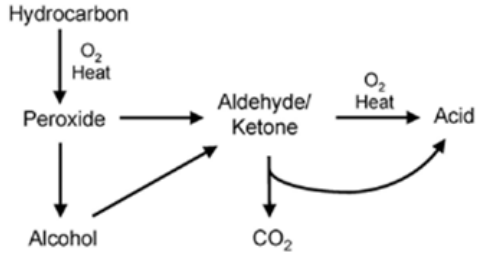

Source: [46]

An oil hydrocarbon molecule under heat and the presence of oxygen can form peroxides, which are inherently unstable. Peroxides can easily form alcohols or aldehydes or ketones, which are polar types of molecules that will change the properties of the oil medium in which all this happens. Oil interfacial tension will be affected and consequently, the solubility of water in the oil. Aldehydes and ketones can react again with oxygen to form acids directly or be oxidized and lose carbon dioxide to form acids. Carbon dioxide is in fact the most oxidized form of carbon and the absolute stop to the process. However, both aldehydes and acids can react with each other to form complex compounds that are not soluble in oil, i.e., sludge.

When the insulation oil is under electrical stress, free radicals can also be generated by the electronic excitation of hydrocarbon molecules caused by collision with free electrons liberated from the surface of the metal conductors [54]. New insulating oils, as normally refined, contain small amounts of chemical compounds that act as oxidation inhibitors, moderating or stopping the reactions of peroxides. Oxidation inhibitor additives are also used in mineral oils to improve oxidation stabilization properties by trapping oxidation byproducts (free radicals).

2.5.3.3 Pyrolysis

Pyrolysis is defined by [2] as thermal decomposition of materials at elevated temperatures involving an irreversible change of chemical composition. It is a process which can occur without the presence of water and/or oxygen. The temperature increase enhances the

action of the other agents as it causes an exponential acceleration of the rate of chemical reactions according to the Arrhenius formula.

This process is not considered relevant at normal operating temperatures. According to [2], it is not yet clear what the temperature range is in which pyrolysis becomes dominant. However, as mentioned by Lelekakis et al [44], this phenomenon occurs at temperatures above 140 °C. According to Zhang et al [3], pyrolysis is the main degradation process above 130 °C, however the direct degradation caused by pyrolysis is generally more obvious at temperatures above 200 °C.

Zhang et al [3] explains the pyrolysis process as follows: "*From the microscopic mechanism, the thermal stability of cellulose C-O bonds is much weaker than the C-H bonds of insulation oil. Under the effect of temperature, C-O bonds can be broken, de degree of polymerization of cellulose will be reduced, and the mechanical strength will be continuously reduced. Because insulating paper has a low thermal conductivity, heat easily accumulates in the paper. With the accumulation of heat, local chemical bonds are cleavage, and products as aldehydes, carboxyl groups, and carbon dioxide are produced.*" The main by-products originated in pyrolysis are *CO*, CO_2 and water.

2.5.3.4 Degradation products

In an impregnated paper-oil insulation system, oil and cellulosic insulation age together. Degradation processes of oil and cellulose form many different products. The interaction of these products with oil and cellulose may result in chain reactions which enhance the degradation processes. Content of paper and oil degradation by-products in oil is also used to assess insulation aging conditions. The ultimate degradation products are mainly water and carbon oxides. Water is formed by cellulose hydrolysis, and it is also an end product in the oxidation of both oil and paper [2]. Most of the water is retained in the solid insulation. A classical reference for the equilibrium between moisture content in paper and oil depending on the temperature is showed in *Figure 21*.

Carbon oxides, *CO* and CO_2, are oxidation products of oil and degradation products of cellulosic insulation. The content of such gases dissolved in oil and their relative amounts are used in the interpretation of dissolved gas analysis (DGA). Zhang et al [3] comments that the concentration in oil of *CO* and CO_2 is temperature dependent, i.e., at lower temperatures both are more easily absorbed into the solid insulation paper than at higher temperatures.

Besides water and carbon oxides, other important degradation products are methanol, furanic compounds, acids and sludge.

Figure 21 − Oommen curves for water content distribution between new oil and paper.

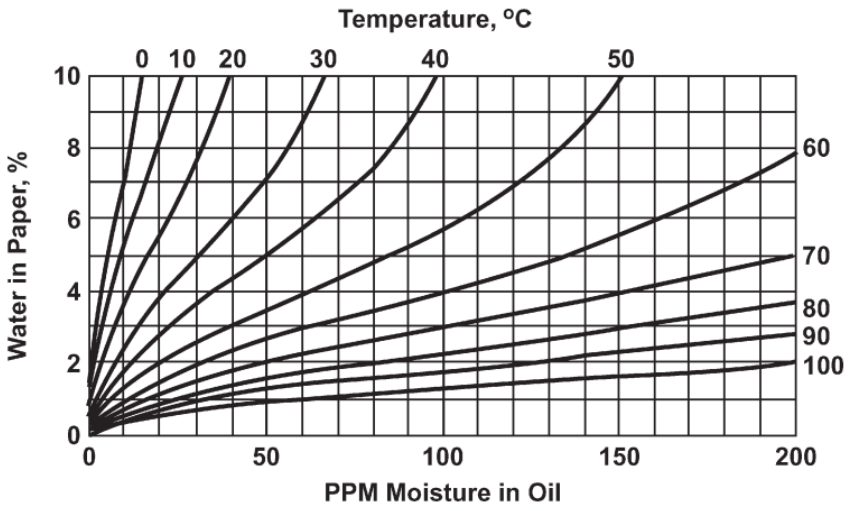

Source: [45]

Methanol is a by-product of cellulosic insulation pyrolysis. Matharage et al [53] have obtained in an experiment methanol in oil increasing linearly with the chain scission in paper. However, the mechanism involved with methanol production in cellulosic insulation degradation has not yet been fully understood and the use of methanol as an aging indicator of cellulosic insulation has yet a short history.

Acids are formed by cellulose hydrolysis and by oil and cellulose oxidation. Carboxylic acids are formed by a series of free radical reactions involving hydrocarbons and peroxides. These acids, with low molecular weight, are absorbed by cellulosic insulation and, together with moisture, degradate this insulation by acid hydrolysis.

Furanic compounds are liquid by-products of cellulosic insulation degradation. The formation of such products occurs in pyrolysis and hydrolysis processes. Furfuraldehyde (2FAL) is the most stable and oil soluble furanic compound. According to [2], the presence of furanic compounds is not generally considered to significantly influence the aging of oil or paper. However, the measurement of the furanic compound content, especially 2FAL, has found use in transformer diagnostics. Although it is clear that furanic compounds give information on paper degradation and many works have suggested a correlation between DP decrease and content in oil of the furanic compounds, according to [2], "*a general dependence between the 2-FAL and average degree of polymerization of the cellulosic insulation is not likely to exist,*

but will be dependent on several parameters including the operating conditions, the transformer's design , the type of paper etc."

Free radicals in oil participate in secondary chemical reactions resulting in soluble and insoluble decay products. Insoluble particulates in the oil formed by high electric stress constitutes the product called x-wax. X-wax formation is catalyzed by temperature, moisture, and the presence of copper or uncured resin [55]. According to [55], temperature has more influence on the formation of x-wax compared to the other factors. It is believed x-wax is prominent in sealed transformers, since "*in free breathing transformers, oxygen molecules having two unpaired electrons usually connect the large fractions and the coalescence of such insoluble suspension results in the formation of dark colored product called sludge*."

2.5.4 Electrical breakdown

Electrical breakdown of an insulation is a large (and in general abrupt) increase in electrical current resulting from a small increase in voltage (electrical field). On solid insulators, it involves the formation of a permanent conductive path behaving like a short circuit at a high enough applied voltage [56]. When electrical breakdown is caused mainly by free electrons at a very strong electric field condition, it is called electronic breakdown. In this case, a high enough electrical field raises the number of free electrons, resulting in a sudden increase in insulator temperature which initiates the breakdown. Electronic breakdown is a phenomenon that lasts between tens to hundreds of nanoseconds.

As presented in [57], different phenomena characterize the thermal breakdown. Dielectric losses due to an electrical field applied on an insulator causes a gradual temperature rise in the insulating material. Because of the temperature rise, there is an increase of material electrical conductivity affecting the dielectric losses in a positive feedback loop. If a thermal equilibrium is reached at a sustainable temperature not exceeding the critical temperature for the insulating material, the insulator is considered thermally stable at the applied electrical field.

In other way, if the electrical field exceeds a critical value, the positive feedback loop can lead the insulator gradually to a critical temperature condition, resulting in the thermal breakdown. Both the thermal breakdown and the electronic breakdown are related to temperature. While electronic breakdown is characterized by a sudden increase in temperature and a phenomenon of tens to hundreds of nanoseconds, thermal breakdown is a phenomenon resulting from a relatively slow and permanent heating that lasts from a few milliseconds to

tens of hours [56, 57]. Another electrical breakdown phenomenon, which lasts between hundreds of hours and tens of years, is electrochemical breakdown. In this case, a relatively low electrical field is applied to the insulator during an extended period. The breakdown occurs as a consequence of internal chemical processes, i.e., an aging process. At prescribed operating conditions, electrochemical breakdown process duration corresponds to the lifetime of the insulator.

Finally, another electrical breakdown phenomenon occurs when the mechanical strength of the material is exceeded, resulting in the rupture of the insulation leading to the electrical breakdown. This is the electromechanical breakdown. As discussed in [56], the electromechanical breakdown occurs "*when the electrostatic compression forces on the test specimen exceed its mechanical compressive strength."* This phenomenon is related with material electrostriction, i.e., dimensional modification due to displacement of ions caused by a high electrical field.

2.5.4.1 Intrinsic and practical breakdown strength

As defined in [40], "*the intrinsic breakdown of liquid and solid dielectrics is defined as the highest value of breakdown strength obtained after eliminating all known secondary effects, which may influence the breakdown*." Kufel et al [56] state that the intrinsic strength is achieved when the temperature and environmental conditions are carefully controlled and the material under test is pure and homogeneous. According to Kufel et al [56], the intrinsic strength is rarely reached. Ravindra and Mosch [40] consider the intrinsic breakdown as an ideal concept. In practical conditions, liquid and solid dielectric materials are not totally pure and homogenous. In other words, it is very difficult, in real life, to eliminate all possible secondary effects influencing the breakdown. To illustrate the difference between intrinsic and practical breakdown values, Ravindra and Mosch [40] state that the peak ac value of electrical breakdown strength for purified insulating oils is about 350 kV/cm while the intrinsic strength is on the order of 1 000 kV/cm and above.

For composite insulating systems as the oil-impregnated paper insulation, it is not reasonable to consider an intrinsic breakdown strength value. Ravindra and Mosch [40] give the following reference values for practical breakdown strength of paper-oil insulation systems:

- Cable: 50-80 kV/mm;
- Capacitor: 180 kV/mm.

Considering the similarities of materials and construction, it is reasonable to consider for instrument transformers the same range of values considered for cables. Similarities between paper-oil cables and CT are discussed in 2.7.

2.5.5 Main stresses on insulation systems and key aging acceleration agents

As discussed at the beginning of session 2.5, during the operation, insulation systems of electrical apparatus are subjected to different types of stresses, such as electrical, thermal, mechanical and environmental stresses. The application and operation conditions determine which of these stresses will be dominant for the degradation of the insulation system. The resulting degradation will also be affected by the interaction among different stresses acting simultaneously on the insulation system. The most common multi-stress case involves the combination of simultaneous electrical and thermal stresses [6].

Environmental stress refers to the environment surrounding the insulation system. For an oil-impregnated paper insulation system, the oil and substances dissolved or suspended therein constitute this medium. Thus, the presence of moisture, gases, acids and other contaminants in oil is relevant to assessing the environmental stresses.

From the various studies on the degradation processes/mechanisms of the oil-impregnated paper insulation system, it is commonly accepted that temperature, content of water, oxygen and acids are the main aging acceleration factors. For power transformers, electrical field and oil degradation by-products are usually considered as secondary importance factors. This statement seems to be applicable to power transformers since thermal aging is the predominant degradation process. Instrument transformers usually do not work at thermal limiting conditions. Thus, for this type of equipment, the electrical field might be considered as a relevant factor.

According to [2], free access to air and oxygen would reduce expected life by a factor of about 2, and a 2 % moisture content in paper would reduce life by a factor of around 10. The approach of the present work considers the insulation system inside a hermetically sealed housing and at initial conditions of moisture and oxygen content strongly limited due to suitable paper drying and oil treatment processes during the manufacturing of transformer. Thus, water and oxygen content will result from the aging process.

The degradation rate related to temperature is based on the Arrhenius Law. For kraft paper, the aging rate with respect to temperature has been studied by Montsinger [58, 59] and

such studies are the basis of the current IEC loading guide for oil-immersed transformers [5]. A similar approach, based on the Arrhenius law, has been applied to thermally upgraded paper and it is considered in the IEEE loading guide [60].

From an electrical stress perspective, aging studies intend to determine the time to breakdown of the insulation under applied electrical stress. During the operation, a power system apparatus is submitted to different electrical stresses: long duration or continuous operation voltage, short time duration overvoltages, fast and very fast transient overvoltages. The consideration of all types of dielectric stresses, and the contribution of each type of stress to the aging of one equipment is a task of great complexity. Aging models such as the Inverse Power Model and the Exponential Model are intended for the study of aging under continuous stress conditions [6].

The first researcher who included the influence of an applied electrical field on the activation energy in the Arrhenius equation was Thomas W. Dakin, who is cited by [6]. Crine et al [61] propose aging models based on disruption and recombination of chemical bonds inside the material. Kiersztyn [62] has proposed a model relating the inverse power law with the rate theory of chemical reactions. According to this model, aging of dielectrics obeys the same type of rate equation that governs the kinetics of chemical reactions.

Simoni [7] proposed the study of thermal and electrical insulation life based on the analysis of the life surface, a three-dimensional view of life depending on temperature and voltage. This model allows studying electrical lifetime at different continuous temperature conditions and thermal lifetime at different continuous electrical gradient conditions. Simoni also proposes the existence of both thermal and electrical threshold stresses [8], below them, the aging rate becomes negligible. Montanari et al [63] propose a probabilistic approach to the aging process using Weibull distribution applied on time-to-failure duration under thermal and electrical stresses, considering possible electrical threshold values.

Occhini et al [9] has published results of long-term field tests on EHV oil filled power cables performed at Waltz Mill test facilities based on an empirical equation which combines thermal and electrical stresses. This equation, in principle, is related to the Montsinger relation (to consider thermal aging) and Inverse Power Law (to take into consideration electrical aging).

Section 2.5.7 shows relevant multi-stress aging models with more details. The various models and approaches mentioned up to this point consider the temperature and electric field conditions under steady state conditions. In real-life operation, the insulation of equipment is also affected by transient stresses that can cause degradation resulting in accelerated aging.

2.5.6 Aging indicators for oil-impregnated paper CTs

One of the main aging indicators for oil-impregnated paper insulation systems is the degree of polymerization of paper (refer to 2.5.1). However, it is not possible to take insulating paper samples from a current transformer insulation without damaging the insulation. As discussed in section 2.5.3.4, paper and oil degradation processes form many different products. The content of these degradation products dissolved in oil can be used as degradation indicators. The most relevant is the analysis of dissolved gases in the oil. The content of furanic compounds and methanol are other by-products of cellulosic insulation used to investigate the aging conditions of the insulation. The determination of water content, acidity, dissipation factor, dielectric strength and interfacial tension are other relevant analysis of the oil to assess oil-impregnated paper aging conditions. However, the oil volume that can be removed from a current transformer is quite small considering the relative low oil volume of this equipment [19].

2.5.6.1 Analysis of dissolved gas-in-oil (DGA)

Dissolved gas-in-oil analysis (DGA) is a very often method used to identify damages in the oil-impregnated paper insulation. The content of relevant gases is used during type test campaigns, taking oil samples before and after tests, checking the increase of each gas content. Sometimes DGA is also used before and after routine dielectric tests, depending on the manufacturer´s quality control scheme or the specifications of customers. Besides this use for new equipment, DGA is used for an assessment of insulation aging conditions.

As indicated by CIGRE [19], the procedure and interpretation of the levels of dissolved gases can be treated with care involving aspects such as: suitable oil sampling, appropriate sensitivity of laboratory instruments and assessment of repeatability and reproducibility between laboratories. The time between an overstressing event and the oil sampling is a relevant factor. On this issue, IEC 61869-1 [25] determines the oil sampling before and three days after the test, which is also recommended by CIGRE [19]. For aging conditions assessment, it is recommended the use of DGA as part of a more embracing set of tests and analysis. Table 5 gives some guidance on the correspondence between gases and faults and/or defects. This table is a reduced version of a similar table given by CIGRE [19], including the gases mentioned in IEC 60599:2015 [64].

Table 5 − Dissolved gas-in-oil analysis – correspondence between gases and faults and/or defects.

Type of Gas		Overheating						Discharge of high energy/ Arcing		Partial discharge with low energy density	
		150-400 °C		400-900 °C		> 900°C					
		Oil	Oil+ paper	Oil	Oil+ paper	Oil	Oil+ paper	Oil	Oil+ Paper	Oil	Oil+ paper
Hydrogen	**H_2**				○	○	●	●	●	●	●
Methane	**CH_4**	●	●	○	○	○	○	○	○	○	○
Ethane	**C_2H_6**	●	●	○	○						
Ethylene	**C_2H_4**			●	●	●	●	○	○		
Acetylene	**C_2H_2**					●	●	●	●		
Carbon monoxide	**CO**		○		●		●		●		○
Carbon dioxide	**CO_2**		●		●		●		○		○

IEC 60599 [64] gives some typical concentration values observed in oil-impregnated paper current transformers. These values were obtained from several equipment of several networks and they are informed as a reference only.

Table 6 – Ranges of 90 % typical concentration values observed in current transformers [64]

H_2	CO	CO_2	CH_4	C_2H_6	C_2H_4	C_2H_2
6 - 300	250 – 1 100	800 – 4 000	11 - 120	7 - 130	3 - 40	1 - 5

Besides the content of each gas, it is also important to analyze the ratio between some gas content. When the CH_4/H_2 ratio is lower than 1/3, the indication is various low energy partial discharges. CH_4/H_2 ratio close to 1 can be an indication of thermal degradation at temperatures lower than 300 °C. C_2H_2/C_2H_4 ratio greater than 1 indicates high energy partial discharges. If this ratio is lower than 1, the indication is hot spots at mean or very high temperatures (300 to 1 100 °C). Table 7, which is based on Table 1 from [64] gives some guidance of the ratios CH_4/H_2, C_2H_2/C_2H_4 and C_2H_4/C_2H_6.

The ratio O_2/N_2 should reflect air composition. If this ratio is lower than 0.3, it is an indication that there is excessive consumption of oxygen in consequence of oil oxidation and/or paper aging. Another relevant ratio is CO_2/CO. In general, the formation of these gases depends on the temperature. Many times, CO formation is linked with excessive paper heating. For sealed systems, only the relevant increase of CO is expected. CO_2 formation can become relevant with moisture and oxygen presence. Some references given by IEC 60599 [64] are summarized in Table 8. However, there are some cases when CO is formed without any

degradation, leading to a value lower than 3 for the ratio CO_2/CO. Thus, it is important to analyze it by checking the formation of other gases as showed in Table 5.

Table 7 − Interpretation table considering content ratio of relevant gases [64].

Type	Fault	C_2H_2/C_2H_4	CH_4/H_2	C_2H_4/C_2H_6
PD	Partial discharges	Non-significant	< 0.1	< 0.2
D1	Discharges of low energy	> 1	0.1-0.5	> 1
D2	Discharges of high energy	0.6-2.5	0.1-1	> 2
T1	Thermal fault t < 300 °C	Non-significant	> 1	< 1
T2	Thermal fault 300 °C < t < 700 °C	< 0.1	> 1	1-4
T3	Thermal fault t > 700 °C	< 0.2	> 1	> 4

IEC 60599 [64] recommends considering CH_4/H_2 < 0.2 for partial discharges in instrument transformers.

Table 8 − CO_2/CO ratio and possible fault indication.

CO content Ppm	CO_2 content ppm	CO_2/CO ratio	Possible indication
≥ 1 000		< 3	Probable paper involvement in a fault, with possible carbonization, in the presence of other fault gases
	≥ 10 000	> 10	Paper overheating (<160 °C) or oil oxidation

IEC 60599 [64] also recommends the correction of CO_2 and CO content values before calculating the ratio. This correction is to take the background values into account. Therefore, it is desirable to have a previous result to check the increment of each gas content for a better assessment. If thermal degradation of the paper is suspected, further analysis (e.g., furanic compounds) is recommended.

It is important to remark that gases may also be generated as a result of other chemical reactions involving steel, galvanized steel, uncoated surfaces or protective paints [19, 64]. These cases, known as stray gassing, involve in general the formation of hydrogen and methane. As commented by [64], these occurrences can be detected by performing DGA on new equipment which has never been energized and by material compatibility tests.

Other DGA diagnostic method is the analysis of the Duval Triangle, developed by Michal Duval and based on the use of the content of three hydrocarbon gases (CH_4, C_2H_4 and

C_2H_2) in a triangle graphical representation to visualize different fault cases for oil-insulated high voltage equipment [65]. The Duval Triangle is showed in Figure 22. The fault types are the same presented in Table 7. *DT* means "Indeterminate or mixed thermal fault or electrical discharge". Each side of the triangle is an axis whose scales from 0 to 100 refer to the relative proportions of CH_4, C_2H_4 and C_2H_2. The three relative proportion of each gas are coordinates to determine the associated type of fault.

Figure 22 – Duval Triangle.

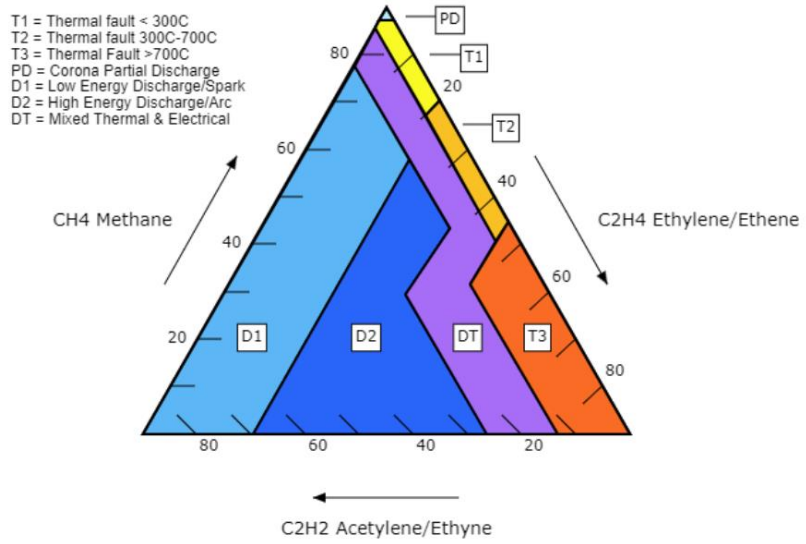

Source: [66]

2.5.6.2 Moisture content, dissipation factor and dielectric strength

Moisture in oil content for sealed systems is from 5 to 10 ppm. As discussed in 2.5.3.2, moisture is a degradation by-product for both paper and oil. Thus, for sealed systems, any moisture increase is a consequence of degradation. Most of the moisture is retained in the solid paper insulation. Figure 21 in 2.5.3.4 gives a reference to the equilibrium between moisture content in paper and oil depending on the temperature. The equilibrium is reached at a steady state condition. When using moisture in oil content for a degradation assessment, it is important to consider the oil temperature at the oil sampling instant. Moisture in oil also increases oil dissipation factor and it decreases the oil dielectric strength. As discussed by [19], the oil dissipation factor depends on ionic contamination and polar deterioration products (moisture, peroxide, alcohols, ketones, acids). According to [19], above 25-30 ppm of moisture in oil content, the moisture may not be soluble in oil and the dielectric performance can decrease,

mainly at low temperatures. Abdi et al [67] published a work with some experiments showing the impact of moisture in oil content on dielectric strength and dissipation factor. Figure 23 shows some results obtained by Abdi et al.

Figure 23 − Moisture in oil content and its impact on dielectric strength and dissipation factor for new insulating mineral oil.

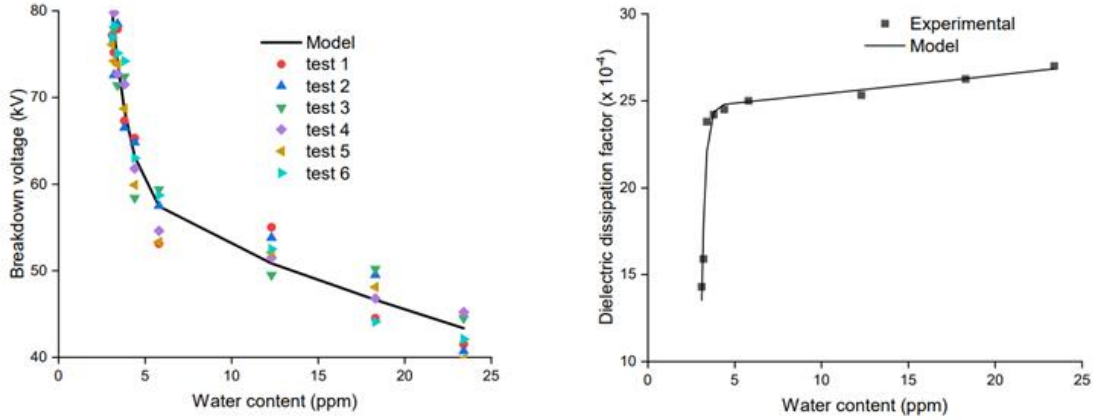

Source: [67]

The criteria recommended by IEC [68] for oil taken from instrument transformers for maximum voltage higher than 170 kV is informed in Table 9.

Table 9 − IEC mineral oil assessment criteria for oil taken from instrument transformers with maximum voltage higher than 170 kV [68].

Property	**New**	**In Service**		
		Good	**Fair**	**Poor**
Breakdown voltage (kV)	> 60	> 60	50-60	< 50
Water content (ppm)	< 10	< 20	20-30	> 30
Dissipation factor at 90 °C	< 0.01	< 0.01	0.01-0.03	> 0.03
Interfacial tension (dynes/cm)	≥ 35	Inhibited > 28 Uninhibited > 25	Inhibited 22-28 Uninhibited 20-25	Inhibited < 22 Uninhibited < 20
Acidity (mg KOH/g)	≤ 0.03	< 0.10	0.10-0.15	> 0.15

2.5.6.3 Interfacial tension and acidity

Acidity is used as an indicator of oil oxidation due to the formation of acidic compounds produced by degradation. The oxidation pattern is different for inhibited and

uninhibited oils, since the inhibitor addictive is consumed during the early service years, avoiding formation of oxidation products. Interfacial tension is affected by soluble polar contaminants and degradation products. The decrease of interfacial tension is used for both inhibited and uninhibited oils, as an oxidation indicator, but with a different formation pattern. For inhibited oils, periodic measurements of the inhibitor concentration are often used. Some guidance on applicable values can be verified in Table 9.

A study by Wiklund et al [46] based on analysis of many oil samples withdrawn from transformers from a few years to 45 years of service shows the decrease of interfacial tension and the increase of acidity for samples taken from transformers with longer service life. For inhibited oils, the acidity started relevant only for samples starting from 15 years of service life.

2.5.6.4 Furanic compounds

Furanic compounds are formed as insulating paper degradation by-products under overheating. The content in oil of 2FAL (2-furfuraldehyde) is the most important and sensitive furanic compound used for paper assessment. The analysis is usually performed by HPLC (High Performance Liquid Chromatography) [19]. The use of this analysis for instrument transformers is in general limited to diagnosis of suspect units together with CO dissolved in oil content. According to [19], the maximum concentration of 2FAL for a thermally aged CT is about 0.2 ppm, when measured CO content is about 700 ppm.

2.5.7 Aging models for oil-impregnated paper insulation

As discussed in 2.5.5, in the operation, the insulation of electrical apparatus works under different types of stresses. The main purpose of aging studies is to propose models to relate operational stresses and resulting insulation degradation to allow assessment of aging conditions and estimation of remaining life. An aging model involves the determination of the stress or stresses to be assessed using this model and the parameters that can affect the impact of the considered stress (or stresses) on the aging of the object under study. Validation of aging models is done through accelerated tests in which the specimen is subjected under controlled conditions of the parameters that affect the degradation process. As described by equation (22), the ratio between the life at normal operating condition (L_0) and the life at a higher stress condition (or accelerated life L_{acc}) is defined as acceleration factor AF.

$$A_F = \frac{L_0}{L_{acc}} \tag{22}$$

Since the model is considered as valid, results obtained from accelerated tests are applied to normal operating conditions. Cygan et al [6] states that the condition under thermal and electrical stresses acting simultaneously have been most commonly investigated, since the presence of both stresses is almost unavoidable in most applications. The present work considers a special focus on combined electrical and thermal stresses.

For the studies on insulation aging, it is also important to determine the quantity considered as the degradation parameter or the basic property for the aging evaluation. In [58], Montsinger analyzed the tensile strength of varnish cloth of conductors as the degradation parameter. Dakin [69] analyzed the decrease in tensile strength of cellulose paper in oil. As mentioned in [5], Lundgaard demonstrated a correlation between tensile strength and the degree of polymerization. Simoni [7] considered electric strength of the insulation system as the basic property for aging evaluation.

Besides the choice of a degradation parameter, an end-of-life criterion needs to be selected. This criterion corresponds to the value of the degradation parameter at which the insulation system is not able to perform or function as intended. Simoni [7] considered the electric strength as zero (i.e., when the dielectric breakdown occurs) as the end-of-life criterion in his studies.

As discussed in [2] and mentioned by Lundgaard et al [50], Oommen and Prevost [45], Lelekakis and al [44] and in IEC Power Transformer Loading Guide [5], the degree of polymerization (*DP*) of the paper is the most used basic property for oil-impregnated paper insulation evaluation and a DP of 200 (corresponding to a tensile strength of the paper around 35 %) is the most common end-of-life criterion adopted. It was previously presented in 2.5.1.

2.5.7.1 Life models for thermal stress

Thermal stress is considered as the major factor in limiting the life of electrical insulation. All the aging studies related to temperature are based on the Arrhenius equation [70]:

$$k(\theta) = A\, e^{-\frac{E_A}{R\theta}} \tag{23}$$

Where:

$k(\theta)$ is speed of the reaction.

θ is the absolute temperature in Kelvin.

A is the pre-exponential factor, or constant for each chemical reaction.

E_a is the activation energy for the reaction (in the same units as R_θ).

R is the universal gas constant.

The Arrhenius life-stress model can be described using the equation (24):

$$L(\theta) = C.\ e^{\frac{B}{\theta}} \tag{24}$$

Where:

$L(\theta)$ is the life at thermal stress θ.

C and B are the model parameters to be determined, B corresponds to equation (25).

$$B = \frac{E_A}{R} \tag{25}$$

The activation energy E_A is the quantity of energy that a molecule needs to start the reaction. For most real-life cases, this parameter is an unknown value, and B is determined empirically. Parameter B is a measure of the effect of temperature on life span.

From equations (22), (23) and (25), the acceleration factor for the Arrhenius model is:

$$A_F = \frac{C.\ e^{\frac{B}{\theta_0}}}{C.\ e^{\frac{B}{\theta_{acc}}}} = e^{\left(\frac{B}{\theta_0} - \frac{B}{\theta_{acc}}\right)} \tag{26}$$

Where:

θ_0 is the temperature at normal operating condition.

θ_{acc} is the temperature at aging accelerated condition.

The assessment of thermal aging of oil-impregnated paper insulation is focused on the loss of mechanical properties related to the degree of polymerization of cellulose. The kinetics of these reactions can be described according to the Arrhenius relation.

In the 1930's, Montsinger [58, 59] proposed a rule focused on thermal aging. According to Montsinger's rule, life is halved for every 6-10 degrees temperature increase depending on the material. This statement is described by the equation (27).

$$L(\theta) = e^{-p \cdot \theta} \quad (27)$$

Where:

$L(\theta)$ is the life duration at absolute temperature θ.

p is a constant (6 is suggested in the temperature interval from 80-140 °C [5]).

IEC 60076-7 [5] considers reference life temperature condition at 98 °C (per unit life) and the temperature step for which the rate of aging doubles as 6 for non-thermally upgraded paper. Thus, life halves or doubles for every 6 °C increase or decrease from 98 °C. However, once the Montsinger rule is considered valid from 80 to 140 °C, the decrease in the aging rate cannot be considered for temperature values lower than 80 °C. A similar approach, based on Arrhenius law, is adopted by IEEE loading guide [60] which considers a similar equation based on the Dakin's [69] application of Arrhenius equation to the thermal aging of insulation systems, however valid only for thermally upgraded paper for which, the unit life reference is at 110 °C. This is the equation (28).

$$L = e^{\left[\frac{15\,000}{\theta+273} - 27.064\right]} \quad (28)$$

The relative aging rates following IEC and IEEE approach are respectively determined as per equations (29) and (30):

$$v = 2^{\frac{\theta-98}{6}} \quad (29)$$

$$v = e^{\left[\frac{15\,000}{110+273} - \frac{15\,000}{\theta+273}\right]} \quad (30)$$

Table *10* shows some values for the acceleration factor v for non-thermally upgraded paper in the range from 80 °C to 140 °C, considering $v = 1$ at 98 °C.

Table 10 − Aging acceleration for non-thermally upgraded paper insulation.

$\boldsymbol{\theta}$ °C	$\boldsymbol{v}$	$\boldsymbol{\theta}$ °C	$\boldsymbol{v}$
80	0.125	116	8.0
86	0.25	122	16.0
92	0.5	128	32.0
98	1.0	134	64.0
104	2.0	140	128.0
110	4.0		

Occhini et al [9], Allam et al [10] and Gazzana-Priaroggia et al [71] have done similar studies on oil impregnated-paper power cables. Such studies are the basis of the approach considered in IEEE Std 1425-2001 [72], IEEE Guide for the evaluation of remaining life. According to this approach, the reference power cable life is 40 years at rated voltage and at 85 °C. The rate of deterioration doubles every 8 °C temperature increase ("8° C rule"), i.e., the Montsinger rule represented by equation (27) with a constant p = 8. Indeed, Montsinger mentions 8 °C increase in temperature as the temperature step to double the degradation in [59]. Thus, at 100 °C continuous operation at the same electrical gradient conditions, the life span of this cable would be about 10 years.

2.5.7.2 Life models for electrical stress

The time to breakdown of insulation under applied electrical stress is the major interesting finding in aging studies. From an electrical stress perspective, electrical aging can be defined as a progressive loss of dielectric strength arising from prolongated action of an electrical field [7]. The inverse power law proposed by Peek [73] and the exponential law are the most acceptable models relating continuous electrical stress with time to breakdown [6]. The inverse power law, which describes the aging under continuous stress, can be written as showed in equation (31).

$$L(V) = kV^{-n} \tag{31}$$

Where:

L(V) is the time to breakdown in hours at continuous applied voltage *V*.

k and *n* are parameters to be determined empirically.

The parameter *n* is a measure of the effect of electrical stress on life span. The higher ithe absolute value of *n*, the greater the effect of stress. If life is constant with stress, *n* = 0.

From equations (22) and (31), the acceleration factor for the inverse power relation is determined according to the equation (32) :

$$A_F = \frac{kV_0^{-n}}{kV_{acc}^{-n}} = \left(\frac{V_{acc}}{V_0}\right)^n \tag{32}$$

Other approach for the aging due to electrical stress is the exponential model. Its basic expression corresponds to the equation (33) :

$$L(V) = c \cdot e^{-kV} \tag{33}$$

Where:

L(V) is the time to breakdown in hours at continuous applied voltage *V*.

c and *k* are constants to be determined empirically.

From equations (22) and (33), the acceleration factor for exponential model is represented by equation (34):

$$A_F = \frac{c.e^{-kV_0}}{c.e^{-kV_{acc}}} = e^{k(V_{acc}-V_0)} \tag{34}$$

Since test results are available, the choice of the best model to consider is done by plotting test data of time to failure at different voltage levels. If data plotted in a log-log plot results in a straight line, the inverse power can be considered as suitable for the specific case. If data plotted in a semi-log graph, it results in a straight line, the use of the exponential model can be considered as correct [6]. As discussed by Cygan et al [6], following the approach proposed by Simoni et al [8] a threshold stress E_0 can be considered under which, aging due to electrical stress can be considered as negligible. The inverse power and the exponential law considering this threshold stress are described by equations (35) and (36).

$$L = L_0 \left[\frac{E}{E_0}\right]^{-n} \tag{35}$$

Where:

L_0 is the life at stress E_0.

E_0 is the threshold stress, under which aging by electrical stress is negligible.

E is the applied stress.

L is the life at stress *E*.

n is a constant to be determined empirically.

$$L = \frac{K_2}{E-E_0} exp[-k_1(E - E_0)] \tag{36}$$

Where:

L_0 is the life at stress E_0.

E_0 is the threshold stress, under which aging by electrical stress is negligible.

E is the applied stress.

L is the life at stress *E*.

k_1 and k_2 are constants to be determined empirically.

Thus, for insulation materials for which a threshold stress is considered, the equations (35) and (36) cannot be used if applied stress is lower than the threshold stress.

2.5.7.3 Life models for combined thermal and electrical stresses

Combined thermal and electrical stress are the main aging acceleration stresses for oil-impregnated paper insulation. Simoni [7] stated that experimental results lead to the conclusion that the simple superposition of electrical and thermal aging effects given by the sum of thermal aging rate and electrical aging rate cannot be accepted to represent the aging under simultaneous thermal and electrical stresses. From a physical point of view, this simple superposition does not take into consideration the synergy between both aging processes. Considering the electric strength as the basic property for the aging assessment and assuming the aging process as a cumulative quantity, Simoni [7] proposed that the decrease of the dielectric strength under simultaneous electrical and thermal stresses is obtained by the general equation of the Electric Strength Model – equation (37) . The model is based on the Inverse Power Law (for electrical aging) and Arrhenius relationship (for thermal aging).

$$\left[\frac{E_s}{E_{so}}\right]^{N+1} = 1 - \frac{t}{L_0}.\left(\frac{E}{E_0}\right)^N . e^{(B\,.\Delta\theta)} \tag{37}$$

Where:

E is the electric stress (effective value of the ac voltage gradient).

E_0 is the electric stress below which electrical aging ceases (threshold stress).

E_S is the electric strength after prestress for time t.

E_{S0} is initial value for the electric strength (before stressing the material).

L is the insulation life.

L_0 is the life at $E \leq E_0$ (no electrical aging) and at room temperature.

$N = n - b\,\Delta\theta$.

n is the voltage endurance coefficient, i.e., the exponent of electric stress in the inverse-power law.

b is a constant for the material (empirically determined).

t time.

$\Delta\theta = 1/\theta_0 - 1/\theta$ (thermal stress).

θ_0 is the absolute room temperature in K.

θ is the absolute (thermodynamic) temperature in K.

B is a constant in the thermal life equation.

When the insulation fails, $E_S = 0$ and $t = L$. Thus, equation (37) becomes the life equation for combined thermal and electrical stresses according to Simoni [7]:

$$\frac{L}{L_o} = \left(\frac{E}{E_0}\right)^{-N} . e^{(-B\,.\Delta\theta)} \tag{38}$$

From equation (38), if $\theta = \theta_0$, the electrical life is obtained as the equation (35), i.e., the inverse power law. By putting $E = E_0$, the thermal life is obtained as per the equation (39) which is a representation of the Arrhenius equation:

$$L = L_o\, e^{(-B\,.\Delta\theta)} \tag{39}$$

With the determination of electric strength for each combination of electrical and thermal stresses, Simoni [7] proposes the graphical representation by the line surface for combined stress, as showed in Figure 24.

The knowledge of both thermal and electric threshold stresses for the insulation medium is a key factor for a proper aging estimation. On electrical stress, in the scope of the present work, no publication has been found with a reference to the threshold electrical stress value associated with oil-impregnated paper insulation.

Figure 24 − Line surface for combined thermal and electrical stresses as proposed by Simoni.

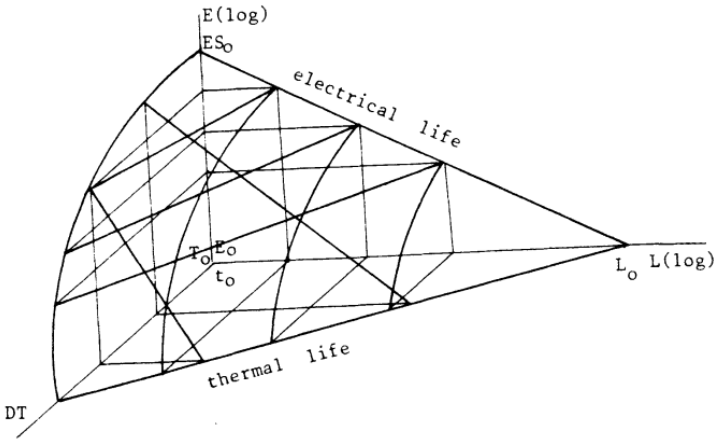

Source: [7]

On temperature, for oil-impregnated paper insulation, the Montsinger equation (reference for power transformers) as well as the approach adopted for power cables, both based on Arrhenius relation, have been discussed in 2.5.7.1. the Montsinger rule is generally considered valid for the temperature range from 80 °C to 140 °C. The IEEE Guide on the remaining life of oil-impregnated paper power cables [72] adopts 85 °C as the reference temperature for a lifespan of 40 years. Temperatures below 80 °C seem not enough to trigger a degradation acceleration of oil-impregnated paper insulation.

Occhini et al [9] published results of long-term field tests performed at Waltz Mill test site on EHV oil filled power cables based on an empirical equation which combines thermal and electrical stresses. This is the equation (40) which, in principle, is related to the Montsinger relation (to consider thermal aging) and Inverse Power Law (to take into consideration electrical aging).

$$L = \sum_{j=1}^{x} \left[\frac{E_j}{E_r}\right]^n \cdot t_j \cdot e^{\alpha(\theta_j - \theta_{op})} \tag{40}$$

Where:

$L(\theta_{op})$ is the total equivalent service life of the cable.

t_i is the duration of a test period.

θ_j is the insulation temperature of a test period.

θ_{op} is the rated service insulation temperature (85 °C).

E_j is applied test voltage during a test period.

E_r is the rated voltage (continuous).

n is the voltage aging exponent, empirically determined, in the range of 10 to 12 for oil impregnated paper power cables.

α is the temperature aging exponent, in the range of 0.07 to 0.087. This range is equivalent to assuming that the rate of aging is doubled for each 8 to 10 °C increase of insulation temperature above its maximum continuous operating temperature, 85 °C.

This equation can be applied to estimate the lifespan at any determined condition of voltage (or gradient) and temperature based on the knowledge of the lifespan at a reference condition. Thus, it can be written, as represented by equation (41).

$$L_{ref} = \sum_{p=1}^{x} \left[\frac{E_j}{E_{ref}}\right]^n \cdot t_j \cdot e^{\alpha(\theta_p - \theta_{ref})} \tag{41}$$

Where:

L_{ref} is the total equivalent lifespan at reference conditions $E = E_{ref}$ and $\theta = \theta_{ref}$.

t_j is the duration of a test period.

θ_j is the temperature of a test period.

E_j is applied test voltage (or gradient) during a test period.

E_{ref} is the reference voltage (or gradient).

n is the voltage aging exponent.

α is the temperature aging exponent.

For oil-impregnated paper insulation, the temperature 85 °C is assumed as the threshold temperature, i.e., the maximum temperature at which no aging acceleration is observed. Above 85 °C, the aging rate doubles for every temperature increment $\Delta\theta$. IEEE 1425 [72] states that the "8 °C rule", i.e., $\Delta\theta$ = 8 °C, is frequently assumed. This use of this equation is not recommended for temperature values above 140 °C, once different aging processes can be started, leading to a different aging rate.

In the scope of the work published by Occhini et al [9], the approach is equivalent to assuming E_0 as the rated continuous operating voltage of the cable insulation. The first part of the equation is clearly based on the inverse power law, for which Cygan et al [6] state that a threshold stress E_0 can be considered under which, aging due to electrical stress can be considered as negligible. It has been observed that a threshold electrical stress has not been considered for the aging tests performed on power cables. The present work proposes to consider this equation, however, considering the existence of a threshold stress E_0, as well as the threshold temperature assumed in the scope of this work as 80 °C. Thus, the use of equation (41) is recommended for the temperature range 80 °C $\leq \theta_p \leq$ 140 °C and for voltage (or gradient) values $E \geq E_0$.

2.6 FAILURES OF OIL-IMPREGNATED PAPER HIGH VOLTAGE CURRENT TRANSFORMERS

The expected service life for high voltage current transformers with oil-impregnated paper insulation is in the range from 25 to 30 years under the rated withstand requirements [19]. This expectation is based on the experience accumulated over decades of using this type of

equipment, taking into account it started from adequate initial conditions that are verified by the routine tests defined by the technical standards applicable to this equipment. Major failure of switchgear equipment is considered as a failure that causes the cessation of one or more of its fundamental functions [74]. The fundamental functions of a high voltage current transformer are current transducer and insulation. Failures causing fire and/or explosion are considered as part of major failures. Minor failure is any failure other than a major failure [74].

CIGRE Working Group A3.06 has published a report on an international enquiry on high voltage equipment reliability [74]. This enquiry includes results from 25 countries from 2004 to 2007. Internal dielectric failure represents 43 % of major failures and 70 % of failures involving fire and/or explosions. The most representative minor failure occurrence is leakage of the insulation media, which corresponds to 75 % of minor failures. According to the report [74], most major failures (76 %) occurred during normal operation. Considering failures involving fire and/or explosion only, 86 % of them occurred in normal service conditions. For current transformers only, internal dielectric failure corresponds to 55 % of major failures and 70 % of failures involving fire and/or explosion. Regarding the failure primary cause, "wear/aging" has been appointed for 52 % of the total of major failures and 38 % of failures involving fire and/or explosion. As mentioned in [74], most installed AIS (air-insulated switchgear) instrument transformers are hermetically sealed.

Major failures of oil-impregnated paper high voltage current transformers usually result in outages and sometimes cause damage to other equipment in the vicinity. For the top core type, failure of the main insulation usually occurs on the top of the active part head, but sometimes the failure occurs in the bushing. To mitigate the damage caused by instrument transformer failure on other switchgear equipment in the vicinity, both IEC and IEEE have introduced the internal arc fault test as a special test. The test consists of introducing a weak point in the main insulation and applying a prescribed fault current to the equipment. The objective is to limit the distance of projected parts reach after an explosion.

2.7 SIMILARITIES BETWEEN OIL-IMPREGNATED PAPER CURRENT TRANSFORMERS AND POWER CABLES

According to Gorur [75], oil-impregnated paper cables have been extensively used since the beginning of century XX. In the very beginning, these cables were constructed with a three-conductor belted copper core limited to 25 kV due to nonuniform electric field distribution. The addition of copper tape shielding around the individual conductors allowed to raise the voltage to 69 kV. With the use of low viscosity oils, this solution could be used up to 132 kV. Electrical field control using capacitive grading approach, the use of thinner papers and manufacture technology improvements allowed the use of oil-impregnated paper insulation for power cables for higher voltages as 550 kV and 750 kV. Many research works have been done in the 1980's and 1990's replacing laminated paper by combinations of paper and plastic films, like polypropylene, polymethylpentene and others. The most common solutions nowadays are polyethylene (PE), crosslinked PE (XLPE) and ethylene propylene rubber (EPR). Once the focus of the present work is the aging of oil-impregnated paper insulation applied to current transformers, the focus of the present comparison is with the oil-impregnated paper power cables.

Oil-impregnated paper cables are built with thin paper layers wrapped on the shielded conductors using capacitive grading with conductive (conducting tape screens) and/or semiconductive layers (using semiconductive carbon black paper) to maintain electrical field uniformity. The capacitive grading solution consists of controlling the capacitance of different layers of the insulation and, consequently, preventing regions of high electrical field concentration. For metallic shielding, metalized paper or metallic foil can be used. Figure 25 shows an example of an oil-impregnated paper insulated power cable.

Figure 25 − Example of oil-impregnated paper insulated power cable.

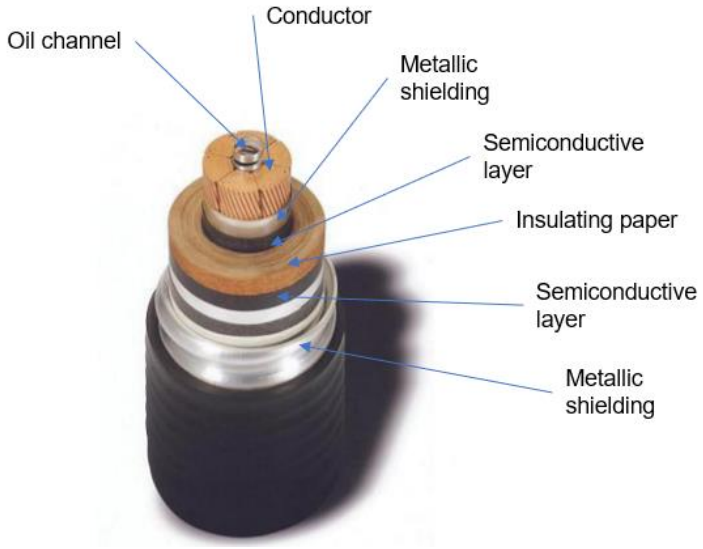

Source: own authorship

This construction can be considered similar to the oil-impregnated paper insulation system used for high voltage current transformers. An example of a top core oil-impregnated paper current transformer is showed in Figure 26. The insulation of oil-impregnated paper current transformers can be split in two main parts: the insulation built on the metallic core box (head of active part) and the insulation wrapped on the bushing stem. The metallic core box has a toroidal geometry (with an elliptical cross section) and the bushing stem, connected to the core box, is a pipe with a circular cross section. The bushing stem and core box are the metallic shielding connected to the ground potential. Insulation layers are split by semiconductive layers. However, as discussed in 2.1.2, conductive screens are placed on the semiconductive layer to provide a suitable surge impedance (improve electrical field grading at higher frequencies) and to conduct high frequency currents in the case of fast front transient overvoltages applied to the insulation. The construction of the insulation on the bushing stem is very similar to the construction of the oil-impregnated bushings of the power transformers and of the power cable termination bushings.

Figure 26 − Example of an active part of an oil-impregnated paper current transformer.

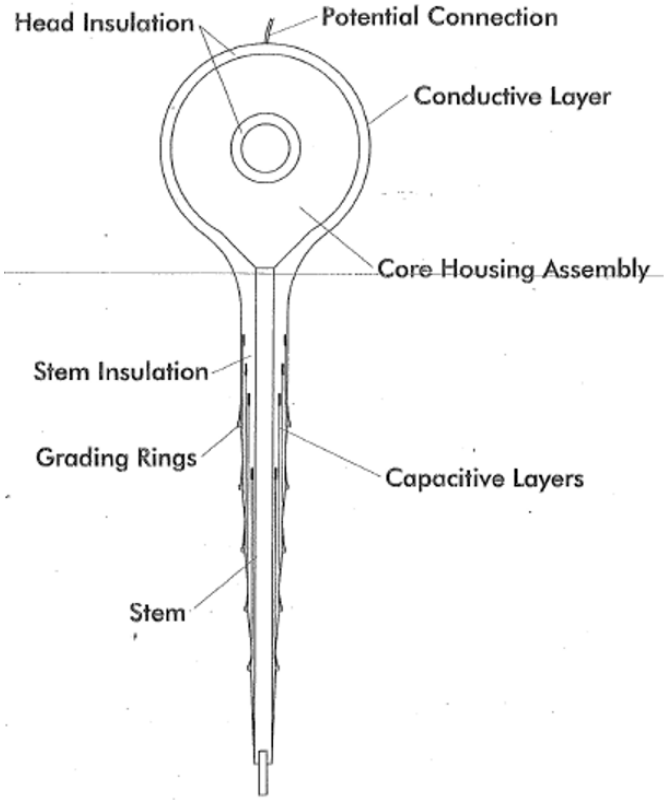

Source: [76]

For both power cable and current transformer insulation, it is necessary to control paper overlap to avoid oil channels. In the same way, the paper needs to be properly dried and impregnated with oil. The construction of layers of thin paper wrapped around a body with a circular (or elliptical) cross section, the compacting of the paper and the limited volume of oil are aspects of similarity between the insulation of power cables and the insulation of current transformers.

The main heat dissipation mechanism for the insulation of current transformers and for power cables is thermal conduction. Convection is considered as negligible due to the limited oil volume. The heat sources in power cables are the ohmic losses due to the current flowing through the cable conductors and the dielectric losses originated in the insulation. For the top core current transformer case, there are ohmic losses in the primary winding and the total heating from the secondary winding ohmic losses which are inside the core box, and the dielectric losses. For both cases, the insulation is simultaneously a thermal conductor for the ohmic losses and a heat source due to the dielectric losses.

2.8 AGING TESTS ON OIL-IMPREGNATED PAPER POWER CABLES

Thermal and electrical stresses are the most relevant contributions to the degradation of oil-impregnated paper power cables. A very significative contribution to the development of aging tests to assess power cable lifespan has been given by the researchers working at the EPRI Waltz Mill (US) test site. Equation (40) discussed in 2.5.7.3, that combines the Montsinger approach for thermal aging and the inverse power law for aging due to electrical stress, is applied by them.

Occhini et al [9] applied this equation, adopting the "8 °C rule" for thermal aging combined with a voltage exponent n = 10 for the lifespan estimation based on aging tests performed in Italy, which have been adopted by all researchers working at Waltz Mill as commented by Allam et all [10], in the discussion of the work done by Watanabe et al [77]. Watanabe et al [77] have used the same equation, but considering a temperature increase of 7 °C to correspond to a half-lifespan decrease, and a voltage exponent n = 16. The oil-filled cables used in the scope of the work done by Watanabe et all have been built with a laminated paper/plastic film/paper solution. However, these values have been adopted arbitrarily. The combined choice of "8 °C rule" and voltage exponent n = 10 seems to be used by most researchers related to the aging of oil-impregnated paper power cables.

An issue related to the use of the equation (40) intending a lifespan prediction is the application of the "8 °C rule" for thermal aging without considering a minimum temperature to consider this rule as valid. If the equation is applied for energization of the insulation at low temperatures (e.g., 20 to 40 °C), the calculation results may lead to unreasonable very long lifespan estimations. In the same way, no consideration of the existence of a threshold voltage stress, as proposed by Simoni et al [8], has been taken into account.

In the present work, the consideration of the threshold thermal and electrical stresses is considered as essential for correct lifespan estimations. Thus, in this investigation, the long duration tests performed on high voltage current transformer insulation mockups were analyzed based on Equation (41), which considers temperature and voltage threshold values.

3 LITERATURE REVIEW

The objective of this chapter is to present a brief review on the literature on aging models and their applicability in the case of oil-impregnated paper insulation, aiming at the analysis of the specific case of oil-impregnated paper current transformers.

IEC [78] defines aging as "*irreversible changes of the properties of an electrical insulation system due to action by one or more stresses*". An electrical insulation system is defined as an "*insulation structure containing one or more electrical insulation materials together with associated conducting parts employed in an electrotechnical device*" [78]. An important concept from these definitions is that the aging is not linked with the material itself, but with the insulation system (association of materials in a particular way) at defined stress conditions. The irreversible changes can be understood as the degradation of the insulation system. There are three main types of electrical insulation: gaseous, liquid and solid. As mentioned by Cygan and Laghari [6], "*electrical failure in solid insulation is of the non-reversible destructive type, whereas in gases and liquids it is of the reversible, non-destructive type.*" [2]

Oil-impregnated paper insulation is a composite insulation system with solid insulation (cellulose) impregnated and immersed in insulating oil. It is sometimes possible to replace the oil in an oil-impregnated paper apparatus. However, there is an interaction between the oil and the paper, resulting in cases in which the degradation products originating from the aging of the oil may have contaminated the solid insulation in such a way that irreversible degradation has already started. For oil-impregnated paper apparatus, there is a consensus that the life of the equipment is determined by the life its solid insulation [2].

According to Prevost and Oommen [39], the use of kraft paper impregnated with insulation oil began to be used in transformers in the 1920s and the period of the late 1920s and early 1930s was marked by many experiments seeking to improve the performance of paper

[2] According to the context of this statement, it must be understood that the occurrence of an arc in a liquid dielectric medium does not imply an irreversible destruction of the insulation given the movement of the liquid molecules, restoring dielectric strength in the region where the arc occurred. This does not mean that the occurrence of an arc in a liquid dielectric medium does not cause degradation in it (breakdown of molecules, generation of gases, acids and moisture).

insulation impregnated with insulating oil. A notable contribution related to the use of insulation with cellulose impregnated with insulating oil was made by Montsinger [2, 58].

In 1889, S. A. Arrhenius [70] introduced the temperature dependence of chemical reaction rates, and the concept of activation energy. This temperature dependence was represented by the remarkable model known as the Arrhenius equation (equation (23) in 2.5.7.1). From the knowledge of the influence of temperature on degradation processes (chemical reactions), Montsinger carried out experiments to determine empirically the effect of temperature on the aging of a paper-oil insulation system. Based on the results of his investigation, Montsinger proposed an empirical relation that is known as the Montsinger equation, which is the basis for the IEC loading power transformer guide [5]. According to Montsinger [58, 59], the life of transformers with oil-impregnated paper insulation is halved for every 6-10 °C temperature increase.

In 1948, Dakin [69] introduced the use of the Arrhenius equation to the aging of electrical insulation, aiming to give a theoretical basis for the relation found by Montsinger. Introducing his own proposition, Dakin stated "*the approximate 7 to 10 rule for the temperature coefficient of deterioration rate is replaced by a more accurate theoretical expression (…). The chemical rate theory interpretation of thermal aging offers a more satisfactory method for extrapolating the results of limited aging tests of insulating materials so they can be applied to predicting amounts of thermal aging in high temperature cycles*". Montsinger and Arrhenius' relations, as well as Dakin's adaption to the Arrhenius equation are presented in 2.5.7.1.

CIGRE Brochure 738 [2] summarizes the most important concepts of the degradation of oil-impregnated paper insulation system for power transformers. The cellulose degradation processes - hydrolysis, oxidation and pyrolysis - are described, as well as the temperature influence considering the Arrhenius relation application and the empirical model proposed by Montsinger. Thermal stress is recognized as the most relevant degradation factor for this type of equipment. The degree of polymerization and tensile strength of the paper are considered the ultimate properties to determine the aging conditions of insulation. However, thermal stress is not the only degradation stress for electrical insulation systems. In general, any insulation system is under electrical, thermal, mechanical, and environmental stresses, but some of the degrading stresses are prevalent depending on the equipment and the application [6]. According to Cygan and Laghari [6], "*one of the most frequently encountered situations in real*

applications are electrical and thermal stresses acting simultaneously." For instrument transformers, CIGRE Brochure 057 [4] published by WG 23-07 identifies the stresses on during service life as thermal, electrical, mechanical, environmental and transportation, but temperature and electric field are considered as the most relevant combined stresses. Thus, the combination of electrical and thermal stresses acting simultaneously on insulation systems is of major interest in aging studies of electrical insulation systems.

Thermal aging is considered as a relatively well understood mechanism. On the other hand, electrical aging is described by empirical relations, since the mechanism of action of the electrical field on the insulation structure is not yet fully understood [79]. From an electrical stress perspective, aging studies intend to determine the time to breakdown of the insulation under applied electrical stress. During the operation, a power system apparatus is submitted to different electrical stresses: long duration or continuous operation voltage, short time duration overvoltages, fast and very fast transient overvoltages. The consideration of all types of dielectric stresses, and the contribution of each type of stress to the aging of one equipment is a task of great complexity.

Gjaerde [79] mentioned that little is known about the nature of electrical aging, but it is common-sense that partial discharges play an important role in this process. Since a clear understanding of the physical and/or chemical aging mechanisms of insulation under electrical field has not yet been reached, empirical models have been developed. The Inverse Power Model and the Exponential Model are empirical models intended for the study of aging under continuous stress conditions [6]. As mentioned by Gjaerde [79], both models have proved to fit reasonably well with experimental data. Some researchers have tried to relate these empirical models with physical and/or chemical processes. According to Gjaerd [79], the first researcher who included the influence of applied electrical field on the activation energy in the Arrhenius equation was Thomas W. Dakin [80]. According to Dakin [80], the voltage endurance was linked with partial discharges and there is a given electrical field value at which no partial discharges occur, and life tends to become extremely long.

For a large number of investigations, electrical life is evaluated based on the Inverse Power Law Model and thermal life assessment is based on the Arrhenius model considering Dakin contribution and/or Montsinger equation, for the cases related to oil-impregnated paper insulation. For the application of the Inverse Power Law model, exponent *n* depends on the

insulation system, and it is empirically determined. For the application of the Arrhenius model, it is necessary to determine the activation energy (E_A) and the constant A. When the Montsinger equation is used, the temperature step to halve the lifespan needs to be determined. All of them are specific for each insulation system and they are empirically determined.

Simoni [7] proposed the study of thermal and electrical insulation life based on the analysis of the life surface, a three-dimensional view of life for temperature and voltage (see 2.5.7.3). This model allows studying electrical lifetime at different continuous temperature conditions and thermal lifetime at different continuous electrical gradient conditions. The expression of life at combined thermal and electrical stresses is the product of single stress life and a correction term which considers the synergy effects. Simoni also proposes the existence of both thermal and electrical threshold stresses below them, the aging rate becomes negligible. Montanari et al [63] propose a probabilistic approach to the aging process using Weibull distribution applied on time-to-failure duration under thermal and electrical stresses, considering possible electrical threshold values.

CIGRE Brochure 057 [4] included a chapter on the endurance and life of oil impregnated paper insulated instrument transformers. On thermal aging, reference is done to Montsinger's experimental research. The thermal stability test, which combines temperature and power frequency voltage stresses (as discussed in 2.3.4), is suggested as a suitable method to assess the thermal performance of the insulation. Recognizing the difficulties of performing such tests, it is recommended that the manufacturers perform long-duration tests on materials and establish an adequate quality control of the process in order to have proper values for the dielectric loss factor, according to their insulation technology. On the power frequency voltage stress, reference is done to the empirical inverse power and exponential models. A special focus on partial discharge is given. Moreover, Simoni's model is mentioned for an assessment of endurance under temperature and voltage stresses. However, there is no clear indication of how to apply the model for each specific case.

Occhini et al [9] has published results of long-term field tests on EHV oil filled power cables performed at Waltz Mill test facilities based on an empirical equation which combines thermal and electrical stresses. This equation, in principle, is related to the Montsinger relation (to consider thermal aging) and Inverse Power Law (to take electrical aging into consideration). This empirical equation has been used by many researchers working with power cables, even

for other insulation systems. Watanabe et al [77] performed tests to investigate the performance of laminated paper insulated self-contained oil-filled cables applying the same approach in order to obtain an equivalent 40-year life during a one and half year test with thermal and electrical aging acceleration. However, publications on aging tests on power cables identified in the scope of the present work do not consider the existence of thermal and electrical threshold stresses, as proposed by Simoni [7]. Occhini et al [9] adopted the exponent n = 10. Allam et al [10] mentioned the value of n in the range from 10 to 12. Both were investigating oil-impregnated paper power cables and they adopted the Montsinger equation with the temperature step to halve life as 8 °C (8 °C rule). Watanabe et al [77] adopted n = 16 and a temperature step to halve the lifespan of 7 °C.

Basu et al [81] has performed accelerated aging tests on several samples of high-pressure gas filled (*HPGH*) power cables with oil-impregnated paper insulation. The oil-paper samples were extracted from cables removed from service. The large number of samples available allowed to carry out several tests and the application of statistical analysis. Basu et al [81] commented on other investigations done by other authors like Chumura et al [26] and others. One relevant issue raised by Basu et al [81] is that many authors perform tests on *"samples produced from lab impregnation of the kraft paper with oil, which can behave differently over a bulk-produced cable in operation."* It is important to mention that the oil used in HPGH cables is highly viscous when compared to mineral oil. Thus, different results from the investigations with paper-oil insulation based on mineral oil are expected. Basu et al [81] found different values of n for different temperatures as follows: $n = 13.6$ at 45 °C, $n = 10.8$ at 60 °C and, $n = 7.4$ at 75 °C. Zhou et al [11] investigated thermal and electric combined deterioration mechanism of oil-paper insulation of a specific type of 220 kV current transformer. An investigation on the values for the life exponent n found values in the range from 4 to 6. Zhou et al [11] performed the tests on oil-paper samples. The tests were not performed on CT samples, but on oil-paper samples withdrawn from a CT.

The present work proposes the application of this empirical equation used for oil-impregnated power cables for long duration aging tests on reduced models of the insulation of high voltage oil-impregnated paper current transformers. Nevertheless, the present work proposes to consider the existence of the thermal and electrical threshold stresses. Based on the results, exponent n and the threshold electrical stress E_0 are estimated assuming the threshold temperature θ_0 = 80 °C and 8 °C rule as valid. In order to maintain insulation under conditions

similar to those of the real CT, the choice was made to carry out these tests on reduced models of CTs instead of simply carrying out tests on paper samples treated and impregnated in a laboratory, or even portions of insulation samples withdrawn from disassembled CTs. A summary of key research and publications is given in Table 11 .

Table 11 − Summary of key publications and research.

Year	Author/Reference	Main inputs
1889	S. A. Arrhenius [70]	• The Arrhenius equation: Temperature dependence of reaction rates.
1892		• According to Prevost and Oommen [39] , use of transformer oil had been introduced by General Electric (GE).
1915	F. W. Peek [73]	• Empirical results leading to inverse power law.
1920s		• Use of kraft paper impregnated with insulation oil began to be used in transformer according to Prevost and Oommen [39]
1930	V. Montsinger [58]	• Tests on transformers showing that the rate of aging is roughly double for every 8 °C increase in hot spot temperature.
1936	Ekenstam [47]	• Ekenstam proposed a direct relationship of degree of polymerization with time, as a first order process - left side of equation (19) in 2.5.3.
1948	T. W. Dakin [69]	• Aging by thermal stress: Introduction of the Arrhenius equation to the analysis of the aging of electrical insulation.
1978	Occhini et al [9]	• Accelerated aging tests on oil-impregnated paper power cables using empirical formula - equation (40) - based on the “8°C rule” (Montsinger [58]) and the inverse power law with voltage life exponent n = 10.
1971	T. W. Dakin [80]	• Aging by electrical stress: The endurance of electrical insulation is linked to the existence of partial discharges and there is a given electrical field value below which no partial discharge occurs, and life tends to become extremely long. This is equivalent to considering the electrical stress at discharge inception voltage as the electrical stress E_0, below which electrical aging is negligible.

Continuation of Table 11.

Year	Author/Reference	Main inputs
1984	L. Simoni [7]	• General equation of the decline in the electric strength for combined thermal and electrical stresses. The existence of the thermal and electrical threshold stresses is proposed.
1986	Allam et al [10]	• Accelerated aging tests on oil-impregnated paper power cables using same empirical formula used by Occhini et al - equation (40). Considering $10 \leq n \leq 12$ and temperature aging exponent $0.07 \leq \alpha \leq 0.087$, service life estimations were from 50 to 100 years.
1990	CIGRE WG07/SC23 [4]	• The brochure on Paper-Oil Insulated Instrument Transformers includes a chapter on endurance life tests. It refers to the Montsinger relation and to the Arrhenius law for thermal aging. It refers to the inverse power law and the exponential model for electrical aging, but without any reference to the empirical constants and exponents. Considers simultaneous electrical and thermal stresses as the most pertinent stress combination for instrument transformers and mentions the Simoni model [7]. • It recommends focusing on thermal stability and on keeping the level of partial discharges under control (levels below limits defined by IEC Standards).
1997	Emsley et al [49]	• Investigations on activation energy of oil-impregnated kraft paper insulation founding values in the range of 105 to 117 kJ/mol.
2004	Lundgaard [50]	• Investigations on activation energy of oil-impregnated kraft paper insulation founding values in the range of 96 to 125 kJ/mol.
2005	IEC 60076-5 Publication	• First edition of the IEC Loading guide for oil-immersed power transformers including the Montsinger equation and the relation between decrease of *DP* and the Arrhenius equation.
2009	Gilbert et al mentioned by [2]	• Investigations on activation energy of oil-impregnated kraft paper insulation founding values in the range of 96 to 107 kJ/mol.

Continuation of Table 11.

Year	Author/Reference	Main inputs
2009	Publication of CIGRE Brochure 394 [19]	• Reference for lifespan of instrument transformers under normal service conditions: 25 to 40 years. • Remaining life of instrument transformers: It mentions aging parameters and end-of-life criterion was under discussion for oil-impregnated papers insulation power transformers. Nothing clear was defined for instrument transformers. Thus, IT recommends diagnostic tests for the aging assessment (as discussed in 2.3. • Instrument transformers operates under thermal, electrical, mechanical, and environmental stresses. It recognizes so far, it is difficult to establish easy and acceptable relations to explain multi-stress aging of insulation systems.
2021	G. Zhou et al [11]	• Investigation on the thermal and electric combined deterioration mechanism of oil-paper insulation of a specific type of 220 kV CT. Tests were performed on insulation samples withdrawn from CTs. Values for the voltage life exponent n are in the range from 4 to 6. No comment on thermal and electrical threshold stresses.
2022	Basu et al [81]	• Investigation on oil-paper samples extracted from *HPGH* cables removed from service. different values of n for different temperature as follows: n = 13.6 at 45 °C, n = 10.8 at 60 °C and, n = 7.4 at 75 °C.
2023	F. Spressola [82]	• Accelerated aging tests on reduced models representing HV CTs with oil-impregnated paper insulation using equation (41). Testing results indicate: $1.3 < n < 3$, $1.17 \leq E_0 \leq 1.21$ p.u. and a life estimation around 50-55 years at rated conditions.

4 MATERIALS AND METHODS

This chapter describes the investigation on which this thesis is based: the methodology of the investigation, the definition of the test procedure, the design of the test samples, the definition of the test circuit and the preparation of the test facilities.

4.1 METHODOLOGY

The question that originated this research work was how one can, through a test, demonstrate that the insulation system of a high or extra-high voltage current transformer with oil-impregnated paper insulation has a design suitable to operate for 30 years (regulatory service life, refer to 1.1) at the maximum continuous operating voltage (U_m / $\sqrt{3}$) for which it was specified and at its maximum insulation temperature. Aiming to investigate the accelerated aging of an oil-impregnated paper current transformer under continuous and simultaneous thermal and electrical stresses and contributing to the knowledge on this topic, this investigation was organized with the following steps.

- Bibliographic research (chapters 2 and 3);
- Experimental stage: aging test (chapter 4);
- Analysis (chapter 5).

The bibliographic research carried out within the scope of this work was presented in chapters 2 and 3 of this thesis. It was found that the majority of the publications and research related to the aging of oil-impregnated paper insulation systems focuses on power transformer equipment and that the degradation caused by thermal stress is predominantly addressed, considering that this is the major relevant factor in determining the life of this equipment. Thermal degradation was discussed in 2.5.3.

Power cables are another type of component with paper-oil insulation for which there is a relevant number of publications related to accelerated aging. Many accelerated aging tests have been carried out on power cables with simultaneous application of thermal and electrical stresses. These tests consisted of the simultaneous application of continuous fixed values (steady state condition) of thermal and electrical stresses and lifespan estimation was done based on an empirical model combining Inverse Power Law and Montsinger relation to consider electrical and thermal stresses aging acceleration (as presented in 2.5.7.3).

In the literature on oil-paper insulation aging, a gap was found related to accelerated aging tests on current transformers, equipment whose insulation system suffers degradation predominantly under the effects of simultaneous thermal and electrical stress. Thus, considering the constructive similarities between the paper-oil insulation systems of power cables and current transformers (as discussed in 2.7), it was decided to carry out an experiment based on the empirical equation (41) of accelerated aging on thermal and electrical stresses in the case of oil-impregnated paper insulation of current transformers.

Thus, the equation applied to testing results is modified as follows in equation (42):

$$L(\theta_{op}) = \sum_{p=1}^{x} \left[\frac{E_j}{E_0}\right]^n \cdot t_j \cdot e^{\alpha(\theta_p - \theta_0)} \quad (42)$$

Where:

θ_0: Threshold insulation temperature value from which degradation is observed, assumed as 80 °C for oil-impregnated paper insulation.

E_0: Threshold electrical stress value from which degradation caused by electrical stress occurs.

4.2 EXPERIMENTAL STAGE

The defined test procedure consists of keeping the test samples energized under defined conditions of electrical and thermal stress until the breakdown of electrical insulation occurs. For this investigation, it was chosen a case of a 550 kV current transformer designed for a maximum continuous operation voltage U_m = 550/√3 and power frequency withstand voltage *PFWV* = 680 kV. In the design, the manufacturer limits the losses (losses in primary and secondary windings, and dielectric losses) so that the insulation temperature does not exceed 80 °C. Thus, maximum thermal and electrical stresses for steady-state continuous operation are related with insulation temperature of 80 °C and continuous power frequency voltage of 317.5 kV. For an accelerated aging condition, it is necessary to test the samples considering temperature and voltage values exceeding these values.

However, in practice, it is very difficult to find test facilities in which simultaneous high voltage and high temperature can be reached and kept for long duration tests, and, if any, it would be at an unfeasible cost. Thus, test samples have been designed as representative models of the 550 kV *CT* working at the same electrical stress but at a lower test voltage. To make this test feasible using an adapted industrial facility, the insulation of the active part of

the test samples has been designed so that at 70.7 kV the electrical stress in the insulation is the same electrical stress on the real 550 kV *CT* when it is energized at 317.5 kV. The choice of this value of 70.7 kV and the maximum continuous operation voltage of the test samples took into account the availability of existing material (i.e., metallic core box, head house tank and porcelain insulators) to build the test samples. The availability of material to build voltage transformers used to supply the test voltage to each sample and the dimensions of the available existing ovens in the facilities of the manufacturer were other factors analyzed to select the range for the test voltage values.

Table 12 shows a comparison of electrical stresses between the reference 550 kV *CT* and the test samples at different reference voltage conditions. The values of electrical stress are presented in p.u. to protect confidential design information of the manufacturer. The reference value 1 p.u. corresponds to the electrical stress in the real 550 kV CT when it is energized at maximum continuous operation voltage, U_m / √3. A calculation was made using the finite element analysis technique using the ANSYS Maxwell software. Figure 27 shows the result of this analysis. The electrical stress correspondence is considered between the innermost insulation layer of the 550 kV *CT* and the insulation of the designed test samples. A defined portion of the insulation has been chosen as a control region for the experiment as showed in Figure 27.

Table 12 − Voltage stress comparison - 550 kV reference CT versus test samples.

	550 kV CT	**Test samples**
Maximum Continuous Operation Voltage U_m/√3 (kV)	317.5	70.7
Voltage stress at U_m/√3 (p.u.)	1.00 *	
Power Frequency Withstand Voltage (kV)	680	152
Voltage stress at Power Frequency Withstand Voltage (p.u.)	2.14	
Partial discharge test voltage (kV)	381	85
Voltage stress at partial discharge test voltage (p.u.)	1.20	
Maximum voltage U_m (kV)	550	123
Voltage stress at U_m (p.u.)	1.73	
* 1 p.u. corresponds to the same voltage stress of the 550 kV CT when it is energized at maximum operation voltage Um / √3. Voltage stress values are informed in p.u. instead of kV/mm to protect intellectual property of the CT manufacturer.		

Figure 27 − FEA of electrical stress for the real 550 kV CT and for the test samples.

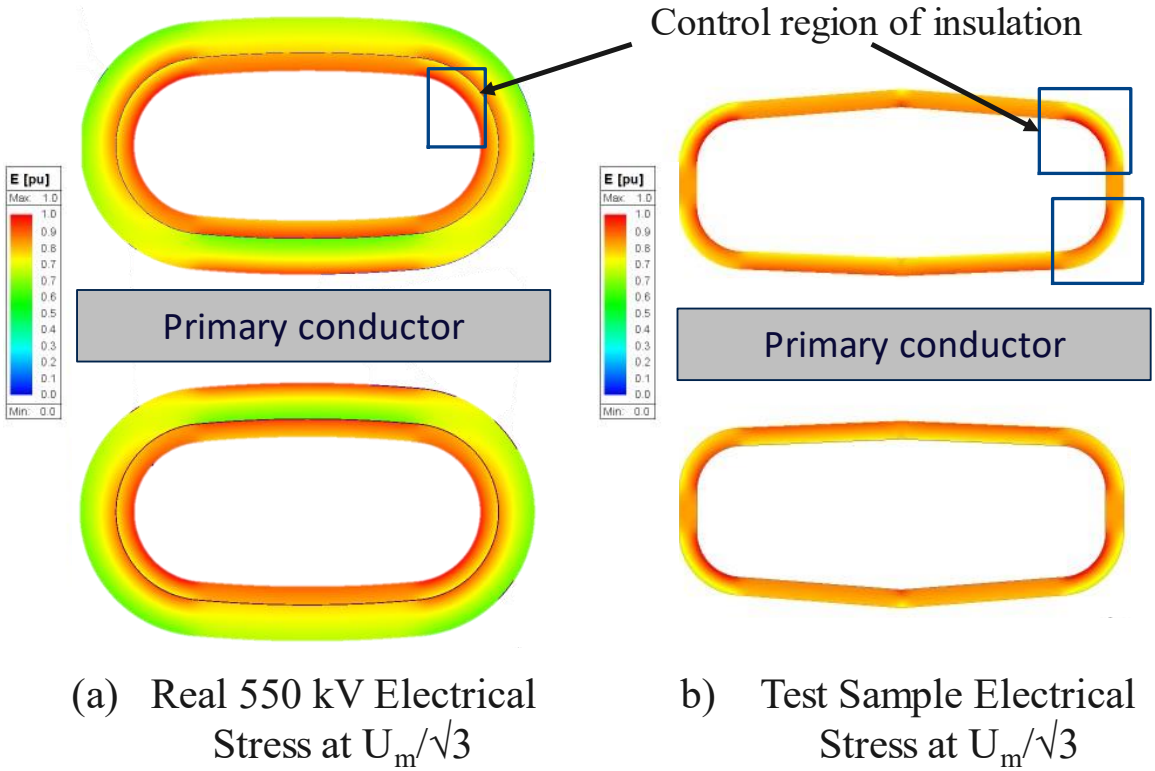

Source: own authorship

To achieve the test temperature of insulation for each test sample, the units have been placed inside an oven with a temperature of approximately 86 °C and a resistor (with ratings of 200 Ω / 100 W) has been installed inside the core box. This resistor was energized by an external voltage regulator at a suitable voltage controlling the losses inside the core box and causing an internal temperature rise (above oven ambient temperature) at a determined place on the wall of the metallic box that is under the control region of oil-paper insulation with the highest calculated voltage stress (see Figure 27). Thus, by using this resistor as a controlled heating source, it is possible to get a controlled fine setting of the temperature of the portion of the insulation considered as the control region (electrical and thermal stresses at controlled conditions).

Figure 28 (a) shows a general view of the designed test sample. *Figure 28* (b) presents a side cross section view showing the insulation built on the metallic core box and on the stem pipe. The insulation has been designed using the same papers and shielding materials and the same construction technology used for the original reference 550 kV *CT*. The resistor installed inside the metallic core box is showed in *Figure 28* (c). Fiber optical temperature probes have

been installed directly in contact with the inner side surface of the metallic box as showed in *Figure 28* (c). The temperature of the insulation on the outer side surface has been assumed as the same as the inner side surface, since the metallic box is built with aluminum, which is a good thermal conductor. After the assembly, each test sample was submitted to the drying and oil filling processes as defined by the standard drying and impregnation processes of the CT manufacturer. After finishing manufacturing, the test samples were subjected to routine dielectric tests. The results of these tests (see 5.1) show the conformity and uniformity in the manufacture of the samples. These results are also evidence of the similarity among test samples and the absence of manufacture defects.

Figure 28 – Test sample cross section view, position of fiber optical probes and resistor and general view of active part.

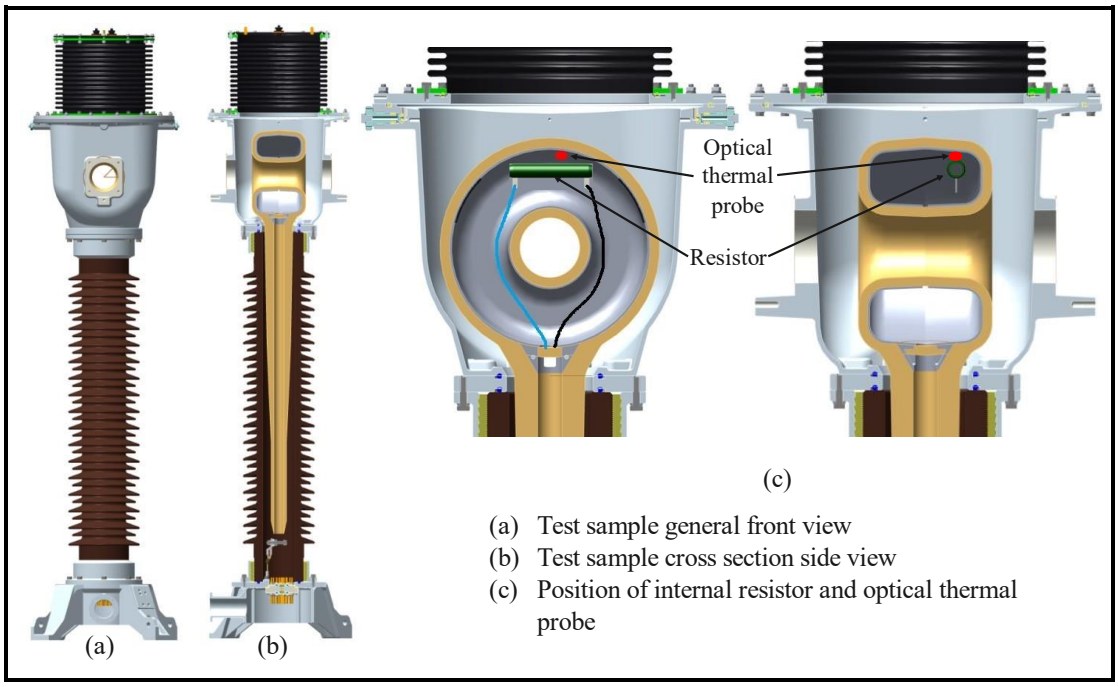

Source: Own authorship

Initially, three samples (*CT01, CT02 and CT03)* were built to be tested at three different test voltages. In a preliminary estimation of the test duration, the application of the equation (42) has been considered, assuming $n = 10$ and $E_0 = 1.0$ p.u.[3], resulting in test durations lower than 6 000 hours (for all test samples) to achieve an equivalent life of 40 years at reference service conditions. *Table 13* shows the reference service conditions, the defined test conditions

[3] A definition of values for exponent n and electrical stress E_0 is an objective of the present investigation. The scenario with $n = 10$ and $E_0 = 1.0$ p.u. has been considered for a preliminary estimation only, to evaluate a possible test duration.

for test samples *CT01*, *CT02* and *CT03* and, the estimation of the test time to reach an equivalent life of 40 years. As will be explained later (refer to 5.5), sample *CT03* was removed from the test and another test sample, *CT04*, was built to replace this unit.

Test voltages were supplied using three different voltage transformers (one for each test sample) with low voltage windings connected to a voltage regulator. Thus, the relative voltage difference among test samples is always the same. Therefore, test voltage is controlled by the input voltage in the low voltage winding of the voltage transformers and the internal test temperature is controlled by oven ambient temperature and by setting the voltage applied to the internal resistor installed inside the core box of each test sample. *Figure 29* shows a simplified diagram of the test circuit and the information on the ratios of each VT.

Table 13 − Electrical and thermal conditions for test samples CT01, CT02 and CT03.

	CT01	**CT02**	**CT03**	**Reference service conditions**
Test Voltage (kV)	86.9	82.7	76.0	70.7
Voltage stress at Test Voltage (p.u.)	1.23	1.17	1.08	1.00 *
Temperature of insulation (°C)	125	120	120	80
Preliminary estimation of test duration to achieve 40 years based on the equation (42) with n = 10 and E_0 = 1.0 p.u.	1 000 h (1.4 month)	2 535 h (3.5 months)	5 900 h (8.2 months)	40 years
* 1 p.u. corresponds to the same voltage stress of the 550 kV CT when it is energized at maximum operation voltage Um / √3. Voltage stress values are informed in p.u. instead of kV/mm to protect intellectual property of the CT manufacturer.				

All the test samples and VTs were grounded by a measuring impedance of a partial discharge detector. However, the measurement of partial discharge during the test is considered as a qualitative (and not quantitative measurement) because the test is carried out inside an industrial oven with many electromagnetic disturbances and high background noise. The purpose of this measurement was to give an indication that any component of the test circuit (test sample or VT) was on the verge of failing. *Figure 30* shows a general view of the test arrangement inside the oven.

During the investigation, the test was interrupted sometimes (depending on the availability of the high voltage laboratory existing in the manufacturer site facilities) to carry

out diagnostic tests on test samples. Additional interruptions occurred due to power blackouts or failure of anyone of the VTs used to supply the test voltage. Figure 31 shows a flow chart of the planned investigation activities.

The following measurements were defined to be carried out on test samples:

- Partial discharge measurement (PD);
- Capacitance and dielectric dissipation factor at power frequency;
- Dielectric frequency response (DFR);
- Dissolved gas analysis (DGA) on oil samples;
- Physical-chemical tests on oil samples (breakdown voltage, moisture content, dissipation factor at 90 °C, interfacial tension, acidity);
- Content of furanic compounds.

In addition, some PDC (polarization and depolarization current) measurements have been performed on the sample CT04 since the resources to perform these measurements have become available.

Figure 29 − Simplified diagram of test circuit.

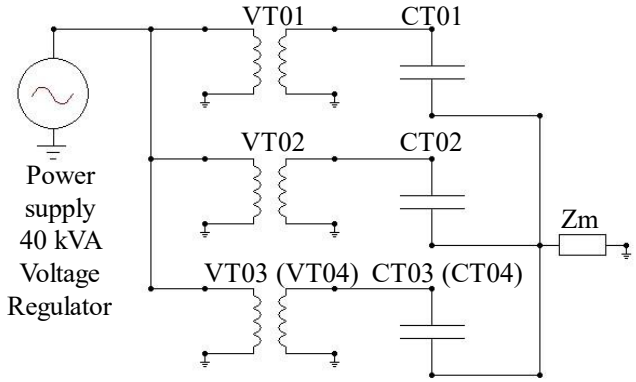

CT01, CT02, CT03 e CT04: Test samples

VT01 – 5 kVA Voltage transformer 110 – 86 900 V

VT02 – 5 kVA Voltage transformer 110 – 82 700 V

VT03 – 5 kVA Voltage transformer 110 – 76 000 V

VT04 – 2 x 8 kVA Voltage transformers 110 – 115 800 V

Zm – Measuring impedance for partial discharge monitoring

Source: Own authorship

Figure 30 − Test circuit arrangement inside oven.

Source: Own authorship

Figure 31 − Flow chart of the test investigation.

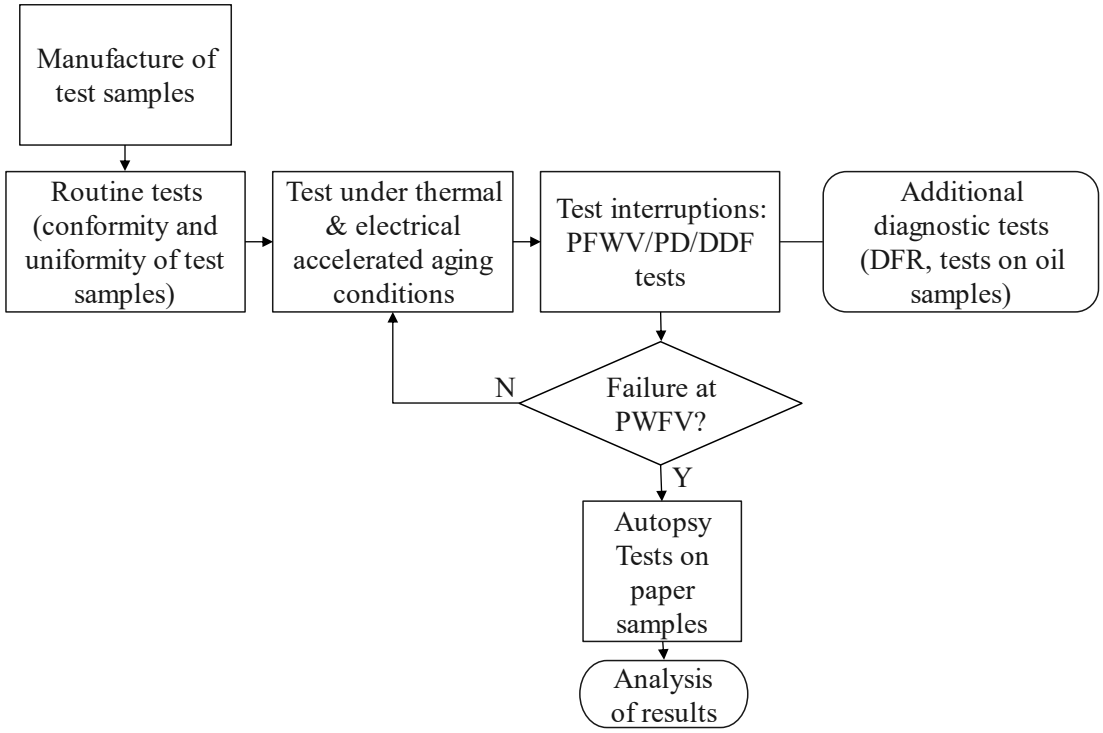

Source: Own authorship

It was defined to keep the test samples energized under accelerated aging conditions until the electrical breakdown occurs (along the energization inside the oven or even during

PFWV tests performed in the test interruptions) and teardown them for an inspection of the complete insulation structure after breakdown, taking paper samples for degree of polymerization tests.

However, an evaluation of the diagnostic test results after ~3 000 hours of test led to the decision to tear down the sample *CT03* and use part of the material (porcelain insulator, head house tank, core box, stem, and pedestal) to manufacture a new sample, *CT04*, to be energized at a higher stress. This is explained in 5.5. The definition of the *CT04* test voltage was based on the clearance of the oven used for the investigation and on the material available to manufacture a VT to supply the test voltage for this unit. *Table 14* shows electrical and thermal test conditions defined for all test samples.

Table 14 − Electrical and thermal conditions for all test samples.

	CT01	**CT02**	**CT03**	**CT04**	**Reference service conditions**
Test Voltage (kV)	86.9	82.7	76.0	115.8	70.7
Voltage stress at Test Voltage (p.u.)	1.23	1.17	1.08	1.64	1.00 *
Temperature of insulation (°C)	125	120	120	120	80
* 1 p.u. corresponds to the same voltage stress of the 550 kV CT when it is energized at maximum operation voltage U_m / √3. Voltage stress values are informed in p.u. instead of kV/mm to protect intellectual property of the CT manufacturer.					

Considering the methodology present in this chapter, the objectives targeted for this investigation can be achieved:

- Estimations for the empirical value *n* and E_0;
- Lifespan estimations for the CT insulation under continuous thermal and electrical stresses;
- Cross-analysis of the results of diagnostic tests related to the insulation aging conditions.

Regarding the cross-analysis of the diagnostic test results,

Table *15* presents a summary of the relationship between diagnostic tests and the respective degradation mechanisms associated with them.

Table 15 – Correspondence between diagnostic tests and mechanisms

Test	Paper thermal degradation	Paper electrical degradation	Oil thermal degradation	Oil electrical degradation	Remark
PD	○	●	○	●	
DDF	●	○	●	○	
DFR	●	○	●	○	
PDC	●	○	●	○	
Oil *DGA*	●	●	●	●	See Table 5
Oil *DDF*	●	○	●	○	
Oil *MC*	●	○	●	○	
Oil *BV*	○	●	○	●	
Oil *IT*	○	○	●	○	
Oil *Acidity*	○	○	●	●	
Oil HPLC	●	-	-	-	
Paper *DP*	●	-	-	-	
Paper *SEM-EDS*	●	○	-	-	

PD: Partial Discharge
DDF: Dielectric Dissipation Factor
DFR: Dielectric Frequency Response
PDC: Polarization & Depolarization current
DGA: Dissolved Gas Analysis
MC: Moisture Content
BV: Breakdown voltage
IT: Interfacial tension
HPLC: High Performance Liquid Chromatography (furanic compounds)
DP: Degree of Polymerization
SEM-EDS: Scanning Electron Microscopy with an Energy Dispersive X-ray Spectroscopy
● Primary relationship
○ Secondary relationship

5 ANALYSIS OF INVESTIGATION RESULTS

This chapter presents and discusses all the test results collected during this investigation, as well as the findings obtained from the inspection of insulation after the electrical breakdown. The well-known *PD* and *DDF* measurements were performed after every interruption in the long duration test under accelerated aging conditions. Oil samples were withdrawn for *DGA*, physical-chemical tests and content of furanic compounds. *DFR* measurements were also carried out. In addition, some *PDC* measurements were performed on the sample *CT04*.

Finally, the test duration, temperature and voltage were used for lifespan estimations and the results are analyzed and discussed.

5.1 INITIAL CONDITION OF TEST SAMPLES

All the test samples were manufactured following the same design, with the same materials and with the same manufacturing process. However, the manufacture of composite insulation systems, such as oil-impregnated paper, is subjected to the possibility of deviation. According to [25], routine tests are intended to reveal manufacturing defects. The routine tests intended to assess the insulation system are power frequency withstand voltage (*PFWV*) test, partial discharge (*PD*) measurements and the measurement of capacitance and dielectric dissipation factor (*DDF*). Partial discharge measurement combined with power frequency withstand voltage test reveals deviations in the insulation system construction and in the oil impregnation process. Deviations in capacitance reveal differences in the insulation system construction. Non-conformities in the drying process mainly affect *DDF* results.

Table 16 shows the initial results of partial discharge (*PD*) measurements for all test samples. Measured values at *PD* test voltages were recorded when increasing and decreasing the test voltage. *PD* level at *PFWV* was also recorded. A good practice to evaluate similarity of test samples is to record discharge inception voltage (*DIV*) and discharge extinction voltage (*DEV*). No *PD* has been detected in the initial tests of all samples. Thus, there is no *PD* inception or extinction. IEC Standard [25] allows $PD < 5$ pC at $1.2\ U_m/\sqrt{3}$ and $PD < 10$ pC at U_m.

Table 17 shows the initial measurements of capacitance and *DDF*. All the capacitance values are in the range from -2.2 % to 3.3 % in comparison with the average value. The average value and standard deviation for capacitance values at 80 kV are 1 149.625 ± 27.841 pF. The

capacitance values at 80 kV are inside the interval limited by the average value and twice the standard deviation. According to IEC Standard [25] *DDF* shall be lower than 0.5 %. The average DDF at 80 kV with standard deviation is 0.2008 ± 0.0022 %. Thus, all DDF values at 80 kV are inside the interval limited by the average value and twice the standard deviation.

Table 16 − Initial conditions − partial discharge measurements in pC.

Test sample	$1.2U_m/\sqrt{3}$ **87** kV	U_m **126** kV	**PFWV 152** kV	U_m **126** kV	$1.2U_m/\sqrt{3}$ **87** kV	**DIV kV/pC**	**DEV kV**	**Temp (°C)**
CT01	< 1	< 1	< 7	< 1	< 1	N/A	N/A	26
CT02	< 1	< 1	< 8.4	< 1	< 1	N/A	N/A	26
CT03	< 1	< 1	< 7	< 1	< 1	N/A	N/A	26
CT04	< 1.9	< 1.9	< 1.9	< 1.9	< 1.9	N/A	N/A	25

Table 17 − Initial conditions − capacitance and DDF measurements.

Test voltage		**10 kV**		**63 kV**		**80 kV**	
Test sample	**Temp (°C)**	**C (pF)**	**DDF (%)**	**C (pF)**	**DDF (%)**	**C (pF)**	**DDF (%)**
CT01	26	1152.7	0.170	1153.4	0.185	1154.0	0.203
CT02	26	1123.4	0.192	1124.0	0.195	1124.4	0.202
CT03	26	1186.2	0.183	1186.6	0.189	1187.0	0.200
CT04	25	1132.4	0.166	1132.7	0.181	1133.1	0.198

Therefore, routine test results demonstrate compliance and uniformity in the manufacture of test samples.

5.2 RESULTS OF DIAGNOSTIC TESTS

Session 2.3 presents the tests applicable for insulation performance of oil-impregnated paper *CTs*. Except for the temperature rise test, the other tests presented in 2.3 are many times also performed by users for the assessment of aging conditions during the *CT* lifetime to assess the conditions of insulation degradation. This session presents and discusses the results of these tests performed in some interruptions of the accelerated aging test.

5.2.1 Partial discharge measurements

According to [25], partial discharge measurement is carried out at U_m and $1.2U_m/\sqrt{3}$ when decreasing voltage after a pre-stress voltage applied for 1 minute. This pre-stress voltage is 80 % of the rated power frequency withstand voltage (*PFWV*) of the CT, when the

measurement is performed separated from *PFWV* test, or 100 % of *PFWV* when both tests are performed together. As presented in Table 16, the initial *PD* measurement was performed combined with *PFWV* test for all the test samples. Initially, *PD* measurements after the beginning of the accelerated aging test were performed with a pre-stress voltage of 80 % of *PFWV*. However, once no *PD* was detected, up to 80 % of *PFWV* for several measurements (i.e., *DIV* is higher than 80 % of *PFWV*), it was decided to perform *PD* measurements with 100 % of *PFWV* for the most recent *PD* measurements.

The measurement of partial discharges has been performed in a shielded high voltage laboratory using the test circuit indicated in [25] as showed in *Figure 32*. The *PD* measuring instrument was an *Omicron MPD-600 PD* detector.

Figure 32 − Partial discharge measurement test circuit.

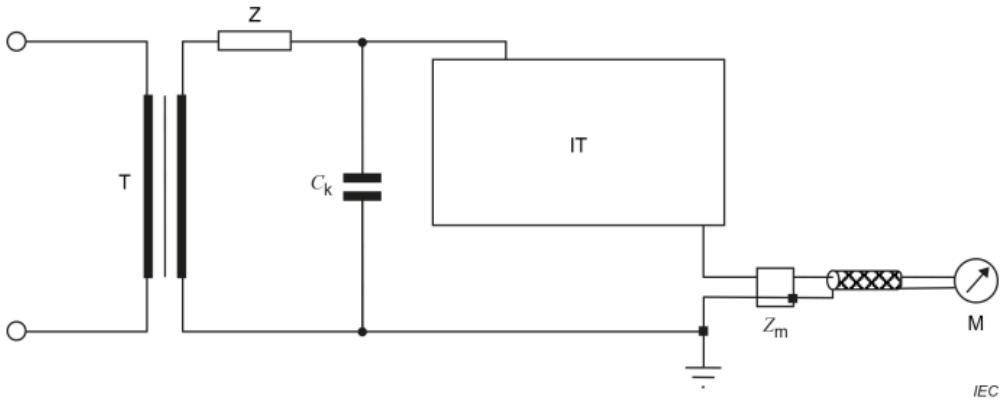

Key

T	test voltage generator
IT	instrument transformer to be tested
C_k	coupling capacitor
M	PD measuring instrument
Z_m	measuring impedance
Z	filter

Source: Figure 11 of [25],

CT01 failed at PFWV (pre-stress voltage for the *PD* measurement) that has been carried out after 7 864 hours under accelerated aging conditions. *CT02* failed during *PD* / *PFWV* tests after 13 994 hours. The results for each test sample are presented in Tables 18 to 21. *Figure 33* shows testing oscillograms of the last *PD* measurement on *CT01* and

Figure *34* shows the same for the last *PD* measurement on *CT02*.

These *PD* oscillograms showed in Figure 33 and

Figure *34* correspond to the typical patterns for internal *PD* in oil-impregnated paper insulation [83]. Discharge pulses occurred in advance to positive and negative peaks of the sinusoidal test voltage, and they are symmetrical in both half-cycles.

Table 18 − CT01 PD measurements in pC.

Test duration (h) (month)	**1.2U_m/√3 87** kV	**U_m 126** kV	**PFWV 152** kV	**U_m 126** kV	**1.2U_m/√3 87** kV	**DIV (kV)/(pC)**	**DEV (kV)**	**Temp (°C)**
Initial	< 1	< 1	< 7	< 1	< 1	N/A	N/A	26
1 232 1.71	< 1	< 1	N/A	< 1	< 1	N/A	N/A	22
2 000 2.78	< 1	< 1	N/A	< 1	< 1	N/A	N/A	26
2 521 3.50	< 1.6	< 1.7	N/A	< 1.7	< 1.6	N/A	N/A	20
3 273 4.55	< 1.6	< 1.6	< 1.6	< 1.6	< 1.6	N/A	N/A	25
3 476 4.83	< 1.9	< 1.9	1 700	520	270	152 / 1 700	60	22
3 476 (*) 4.83	< 2	< 2	N/A	< 2	< 2	N/A	N/A	22
6 487 9.01	< 1.8	< 1.8	720	400	300	152 / 720	32	24
7 864 10.92	< 1.8	6.4	327(**)	N/A	N/A	126 / 3	N/A	19
7 864 10.92	N/A	N/A	N/A	N/A	N/A	16 / 4 500	9	19

(*) Repetition after some days without energization

(**) Initially PD level was 327pC at 152 kV. PD level increased to a value above 1 000 pC after 2 seconds and the test lab protection tripped and turned off the test circuit. When re-energizing just after this occurrence, PD level was > 1 700pC at 12 kV

Table 19 − CT02 PD measurements in pC.

Test duration (h) (month)	**1.2U_m/√3 87** kV	**U_m 126** kV	**PFWV 152** kV	**U_m 126** kV	**1.2U_m/√3 87** kV	**DIV (kV)/(pC)**	**DEV (kV)**	**Temp (°C)**
Initial	< 1	< 1	< 8.4	< 1	< 1	N/A	N/A	26
1 256 1.74	< 1	< 1	N/A	< 1	< 1	N/A	N/A	23
2 316 3.22	< 1.8	< 1.8	N/A	< 1.8	< 1.8	N/A	N/A	15
7 793 10.82	< 2.1	4.3	7 500	4 500	1 400	126 / 4.3	32	22
7 793 10.82	< 2	5	N/A	5	2.1	126 / 5	62	22
9 173 12.74	< 1.8	7.2	223	180	108	126 / 7.2	56	26
10 804 15.01	< 1.9	3.5	10	4	< 1.9	120 / 3	87	24
12 843 17.84	3.4	3-8	9.2	4	3.5	66 / 3	40	19
13 392 18.60	2.5	3	7-9	3-5	2.6	76 / 2.5	53	23
13 994 19.44	< 1.6	4.6	1 992	1 062	493	117 / 3.6	33	25
13 994 19.44	N/A	N/A	N/A	N/A	N/A	5 / 500(*)	N/A	25

(*) After PD measurement, CT02 was energized at 5 kV revealing a very high PD level, that is an indicative of failure

Table 20 − CT03 PD measurements in pC.

Test duration (h) (month)	**1.2U_m/√3 87** kV	**U_m 126** kV	**PFWV 152** kV	**U_m 126** kV	**1.2U_m/√3 87** kV	**DIV (kV)/(pC)**	**DEV (kV)**	**Temp (°C)**
Initial	< 1	< 1	< 7	< 1	< 1	N/A	N/A	26
1 256 1.74	< 1	< 3	N/A	< 3	< 1	N/A	N/A	24
3 200 4.44	< 1.9	< 1.9	< 2	< 1.9	< 1.9	N/A	N/A	24

Table 21 − CT04 PD measurements in pC.

Test duration (h) (month)	**1.2U_m/√3 87** kV	**U_m 126** kV	**PFWV 152** kV	**U_m 126** kV	**1.2U_m/√3 87** kV	**DIV (kV)/(pC)**	**DEV (kV)**	**Temp (°C)**
Initial	< 1.9	< 1.9	< 1.9	< 1.9	< 1.9	N/A	N/A	22
2 420 3.36	< 1.6	< 1.7	< 2.0	< 1.8	< 1.6	N/A	N/A	25
3 200 4.44	< 1.8	< 1.9	< 1.9	< 1.9	< 1.8	N/A	N/A	18
3 760 5.22	< 1.2	< 1.2	< 1.2	< 1.2	< 1.2	N/A	N/A	19
4 430 6.15	< 2.3	< 2.3	< 2.4	< 2.3	< 2.3	N/A	N/A	22
4 873 6.77	< 1.6	< 1.6	< 1.7	< 1.6	< 1.6	N/A	N/A	16
5 190 7.21	< 1.6	< 1.6	< 1.6	< 1.6	< 1.6	N/A	N/A	14

No *PD* was detected in the initial measurements. *CT03* was dismantled without any *PD* detection. Throughout this investigation, the *CT04* remained *PD* free, and this unit remains energized under tests. *PD* was detected in *CT01* for the first-time during a *PD* test after 3 476 h. However, the discharge inception voltage (*DIV*) was 152 kV (i.e., *PFWV*), much higher than the voltage applied on this sample during the accelerated aging test. After 6 847 h, *DIV* was 152 kV with a lower *PD* level, but the discharge extinction voltage (*DEV*) was lower than the *DEV* of the test after 3 476 h. The reduction of *DEV* is an indication of aging.

This behavior is similar to the *CT02 PD* measurements, except for the measurement carried out after 9 173 hours in which the *DEV* was lower in comparison with the measurements performed later. Nevertheless, starting from the *PD* measurements performed after 10804 h, all measurements show a tendency to reduce the *DIV* and *DEV* values.

The failures of *CT01* and *CT02* during the last *PD/PFWV* tests were confirmed during the autopsy of these samples, as presented in 5.3

Figure 33 − CT01 PD measurements after 7 864 h.

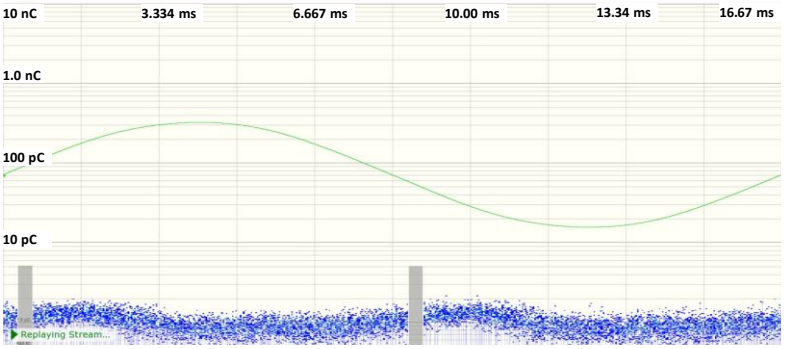

(a) CT01 after 7 864 h – PD measurement at 87 kV during voltage rise: <1.8 pC

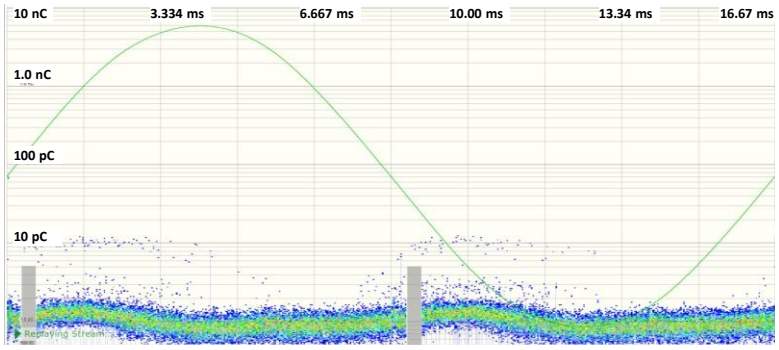

(b) CT01 after 7 864 h – PD measurement at 126 kV (DIV) during voltage rise: 6.4 pC

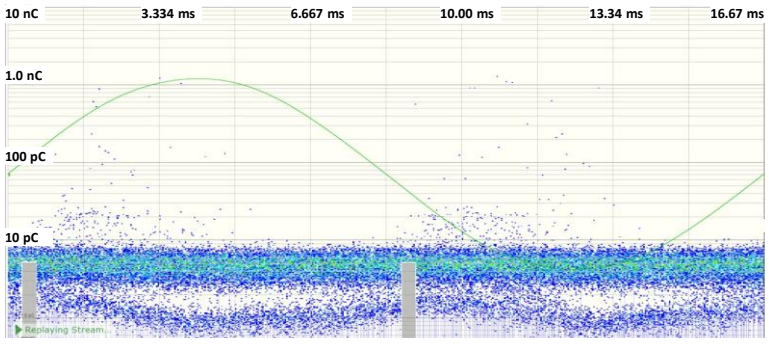

(c) CT01 after 7 864 h – PD measurement at 152 kV (PFWV) just before failure: 327 pC

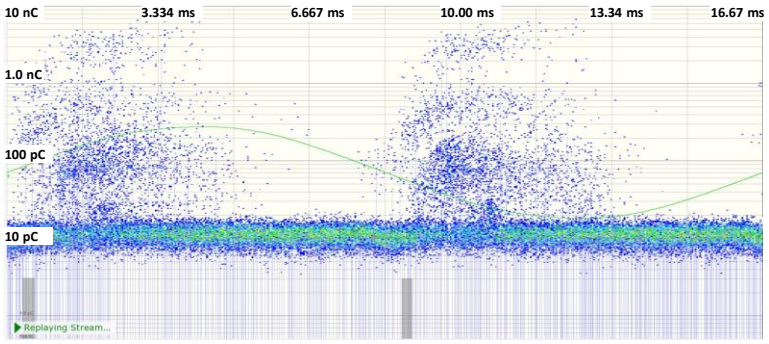

(d) CT01 after 7 864 h – PD measurement at 16 kV after failure: 4500 pC

Source: Own authorship

Figure 34 − CT02 PD measurements after 13 994 h.

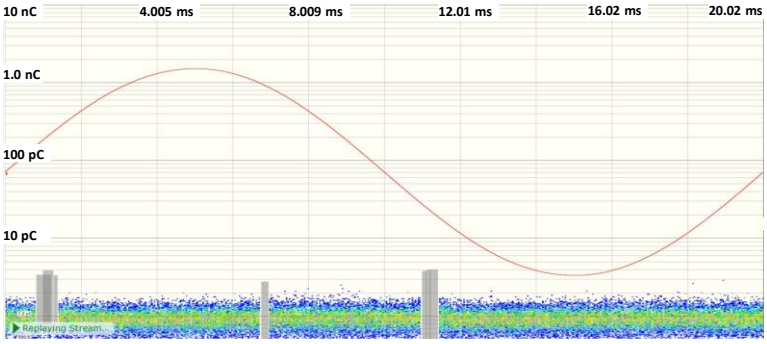

(a) CT02 after 13 994 h – PD measurement at 87 kV during voltage rise: <1.6 pC

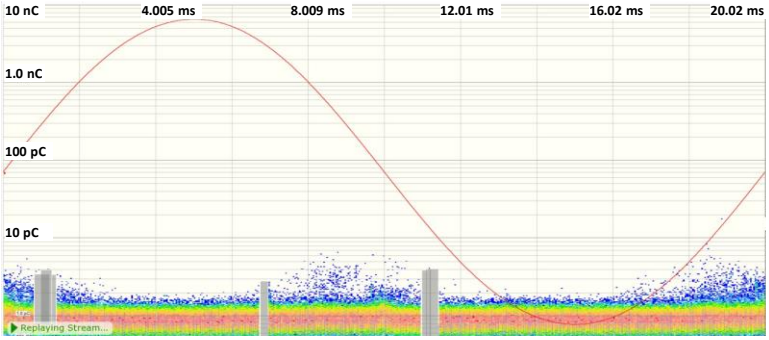

(b) CT02 after 13 994 h – PD measurement at 126 kV during voltage rise: 4.6 pC

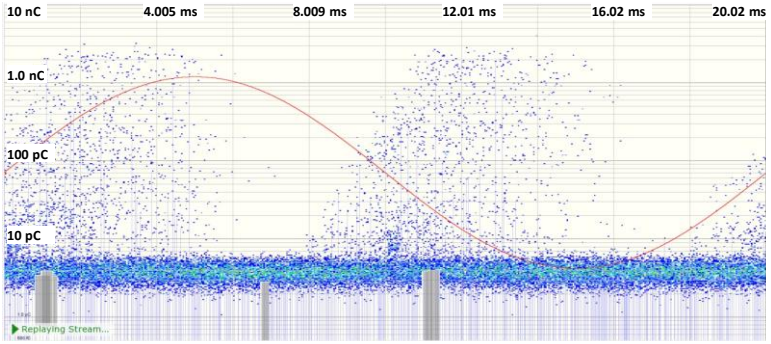

(c) CT02 after 13 994 h – PD measurement at 152 kV (PFWV): 1992 pC

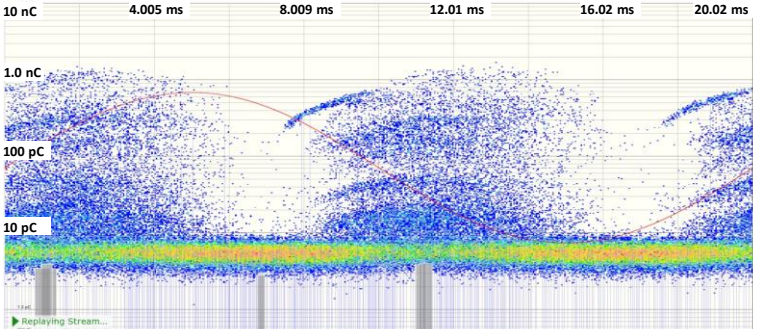

(d) CT02 after 13 994 h – PD measurement at 126 kV during voltage decrease: 1062 pC

Source: Own authorship

5.2.2 Capacitance and DDF measurements at power frequency

Tables 22 to 25 show the results of capacitance and *DDF* measurements performed at power frequency for each one of the test samples. *Figure 35* shows the evolution with testing hours of dielectric dissipation factor values measured at 80 kV for each equipment. To avoid issues with capacitance and DDF bridge, some DDF measurements were carried out at 10 kV only due to the high level of PD detected before these measurements.

Figure 35 – DDF at 80 kV versus aging test hours.

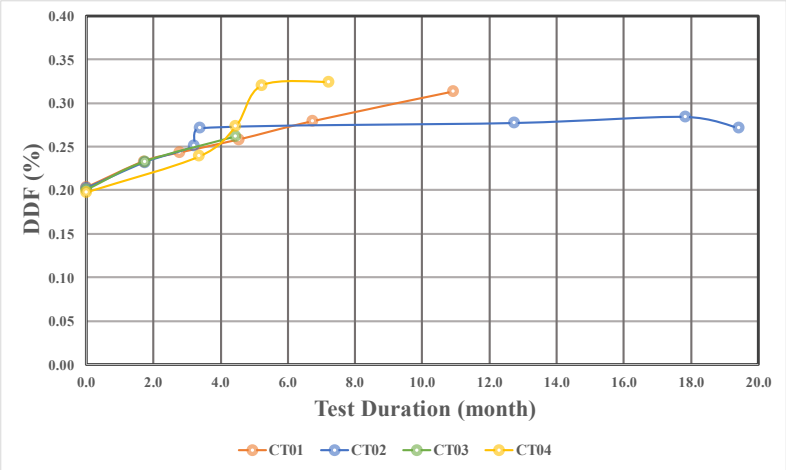

Source: Own authorship

Table 22 – Capacitance and DDF measurements at power frequency – CT01.

Test duration (h) (month)	10 kV		63 kV		80 kV		Temp (°C)
	C (pF)	DDF (%)	C (pF)	DDF (%)	C (pF)	DDF (%)	
Initial	1 152.7	0.170	1 153.4	0.185	1 154.0	0.203	26
1 232 1.71	1 169.4	0.228	1 169.6	0.230	1 170.1	0.233	22
2 000 2.78	1 171.1	0.237	1 171.8	0.242	1 172.2	0.243	26
2 521 3.50	1 172.4	0.266	1 173.1	0.269	1 173.5	0.270	20
3 273 4.55	1 179.9	0.254	1 180.6	0.257	1 181.0	0.258	25
3 476 4.83	1178.9	0.259	-	-	-	-	22
6 487 9.01	1 181.9	0.264	-	-	-	-	24
7 864 10.92	1 167.2	0.313	-	-	-	-	19

Table 23 − Capacitance and DDF measurements at power frequency – CT02.

Test duration (h) (month)	10 kV		63 kV		80 kV		Temp (°C)
	C (pF)	DDF (%)	C (pF)	DDF (%)	C (pF)	DDF (%)	
Initial	1 123.4	0.192	1 124.0	0.195	1 124.4	0.202	26
1 256 1.74	1 137.8	0.229	1 137.9	0.231	1 138.3	0.232	22
2 316 3.22	1 139.4	0.243	1 139.9	0.249	1 140.2	0.251	22
2 428 3.37	1 139.8	0.266	1 140.3	0.269	1 140.5	0.271	15
7 793 10.82	1 149.1	0.269	-	-	-	-	22
9 173 12.74	1 149.5	0.276	1 150.0	0.276	1 150.1	0.277	24
10 804 15.01	1 149.9	0.261	1 150.1	0.262	1 150.7	0.264	24
12 843 17.84	1 141.7	0.280	1 141.8	0.283	1 142.0	0.284	22
13 392 18.60	1 143.4	0.265	1 143.4	0.268	1 143.7	0.269	22

Table 24 - Capacitance and DDF measurements at power frequency – CT03.

Test duration (h) (month)	10 kV		63 kV		80 kV		Temp (°C)
	C (pF)	DDF (%)	C (pF)	DDF (%)	C (pF)	DDF (%)	
Initial	1186.2	0.183	1186.6	0.189	1187.0	0.200	26
1 255 1.74	1 201.6	0.227	1 202.1	0.232	1 201.8	0.233	24
3 200 4.44	1 206.1	0.257	1 206.5	0.261	1 206.9	0.262	24

Table 25 − Capacitance and DDF measurements at power frequency – CT04.

Test duration (h) (month)	10 kV		63 kV		80 kV		Temp (°C)
	C (pF)	DDF (%)	C (pF)	DDF (%)	C (pF)	DDF (%)	
Initial	1 132.4	0.166	1 132.7	0.181	1 133.1	0.198	25
2 420 3.36	1 137.2	0.236	1 137.7	0.238	1 137.9	0.239	22
3 200 4.44	1 138.6	0.272	1 139.1	0.272	1 139.4	0.273	18
3 760 5.22	1 130.1	0.199	1 132.4	0.314	1 132.4	0.320	19
4 430 6.15	1 132.0	0.271	1 133.0	0.274	1 134.0	0.275	22
4 873 6.77	1 132.0	0.300	1 133.0	0.303	1 133.0	0.304	16
5 190 7.21	1 132.0	0.320	1 133.0	0.323	1 133.0	0.324	14

As discussed in 5.1, the initial values for *DDF* were similar and in line with expected values, showing that the samples were manufactured with suitable drying and oil treatment processes. *DDF* values show a progressive increase as expected for thermally aged units. No appreciable difference between testing samples have been noticed. All measured values, even after thermal aging, are below the maximum value specified by IEC Std [25], which is 0.5 %.

5.2.3 *DDF* measurements at power frequency and high temperature

In addition to the *DDF* measurements at normal ambient temperature, *DDF* values have been measured at high temperature during some aging test interruptions. Table 26 shows the measured values with the respective coefficient α_c values.

Results of α coefficient for *CT01* and *CT04* do not indicate thermal instability. However, values for *CT02* lead to a negative value for α_c coefficient, which is not mentioned in the literature. As explained in 2.1.2, the coefficient α_c is represented by equation (4). A positive value of this coefficient means that the higher is the insulation temperature the higher is the respective *DDF* value. The negative value of coefficient α_c is a consequence of the decrease of the *DDF* value with the temperature increase showed for *CT02*. For oil-impregnated paper insulation, the total moisture content is partially present in the paper and partially present in oil. The distribution of this total amount in the paper and in the oil depends on the

temperature. The reference given by Oommen [45] (see *Figure 21* in 2.5.3.4) is valid when there is an equilibrium achieved when the temperature of the complete insulation system is the same. A possible hypothesis is that the equilibrium was not fully achieved when the *DDF* measurements at high temperature and/or at normal ambient temperature were carried out. However, in this case, one can consider this unit as thermally stable once the difference between the *DDF* values at normal and high temperatures is too low (the module of the α_c coefficient value is lower than 0.01.

Table 26 − DDF measurements at high temperature and respective coefficient α_c values.

Test voltage			**80 kV**		**Condition**
Test sample	**Temp (°C)**	**C (pF)**	***DDF* (%)**	**α_c x10^{-3}**	
CT01	24	1 181.9	0.279		After 4 856 h (6.74 months)
	80	1 182.5	0.380	5.5	
CT02	24	1 150.1	0.277		After 9 173 h (12.74 months)
	80	1 150.9	0.237	-2.8	
CT04	23	1 102.4	0.320		After 3 760 h (5.22 months)
	86	1 136.0	0.323	0.1	

5.2.4 DFR measurements

DFR was measured for all the test samples before the start of the accelerated aging test and during test interruptions along the investigation. The measurements were carried out using an insulation diagnostic analyzer IDAX 300. *DDF* x frequency curves are showed from *Figure 36* to *Figure 39*. These curves are showed without any temperature correction. Measurements were carried in the temperature range from 10 °C to 33 °C. For all the samples, it is possible to notice that *DDF* values from 10 Hz to 1 kHz are lower for the initial measurements in comparison with the other measurements after some hours at aging acceleration conditions. Such an increase in *DDF* values in this band is in line with the comments by Chunming et al [32] based on *Figure 14* showed in 2.3.5.2, i.e. the higher is the moisture content in solid insulation the higher are the *DDF* values at these frequencies.

IDAX 300 allows to apply a correction to the curves to consider all of them at the same reference temperature, i.e., 20 °C. The calculation of the curves translated to 20 °C is based on the same approach used by Zhang et al [35] using equation (17), as discussed in 2.3.5.2. IDAX

300 considers the activation energy E_A for impregnated kraft paper as 0.9 eV which is ~ 87 kJ/mol. *DDF* x frequency curves translated to 20 °C are showed from Figure 40 to Figure 43.

Figure 36 – DFR measurements – CT01.

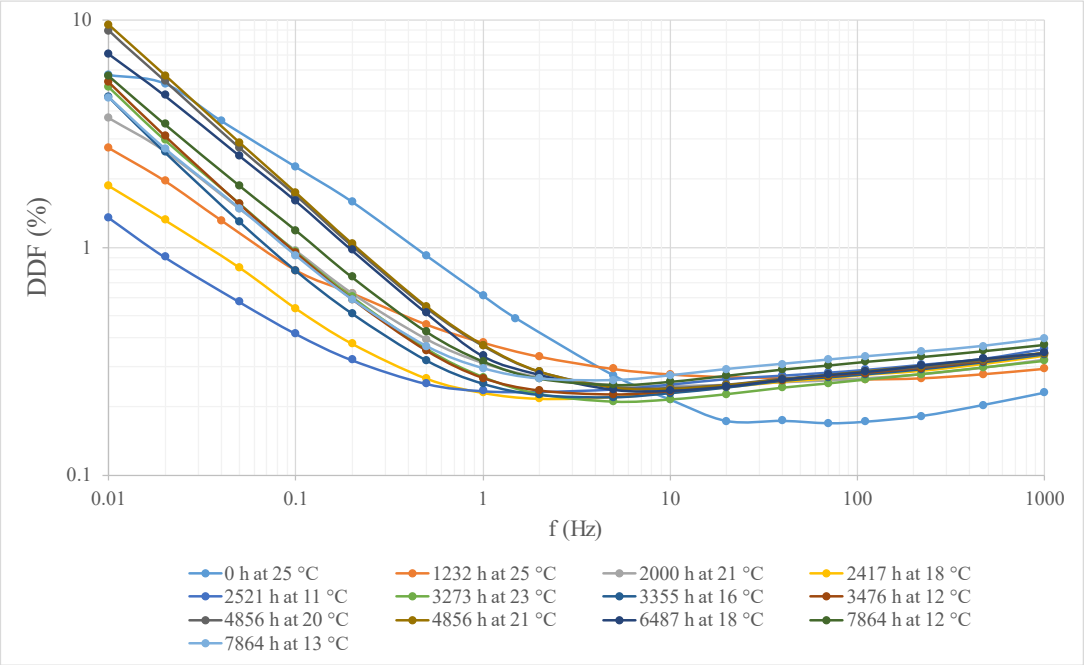

Source: Own authorship

Figure 37 – DFR measurements – CT02.

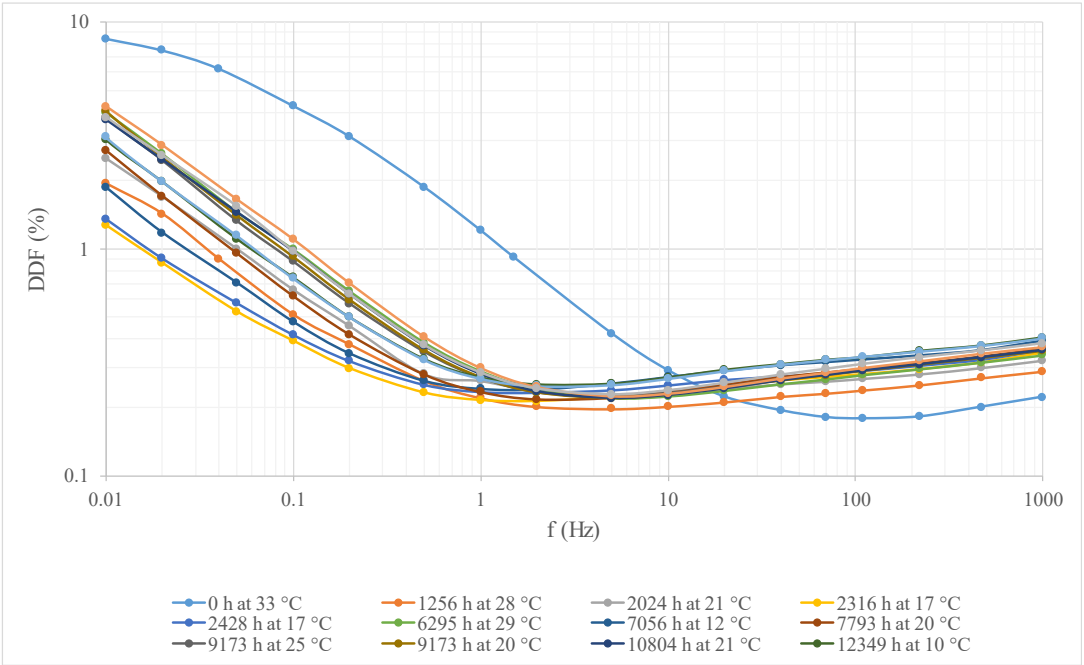

Source: Own authorship

Figure 38 – DFR measurements – CT03.

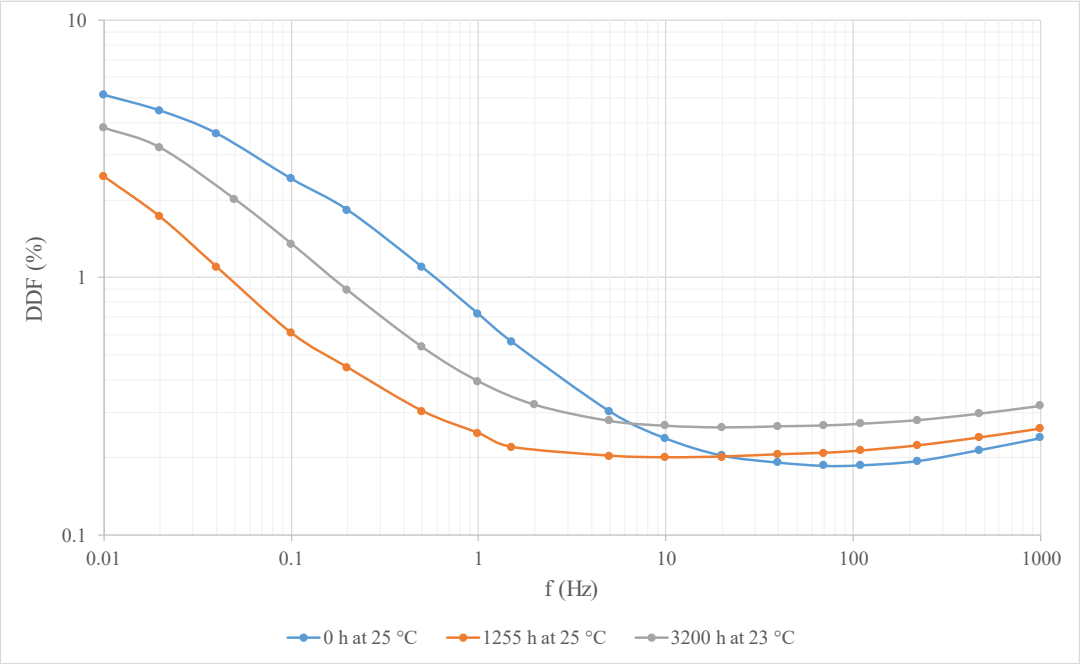

Source: Own authorship

Figure 39 – DFR measurements – CT04.

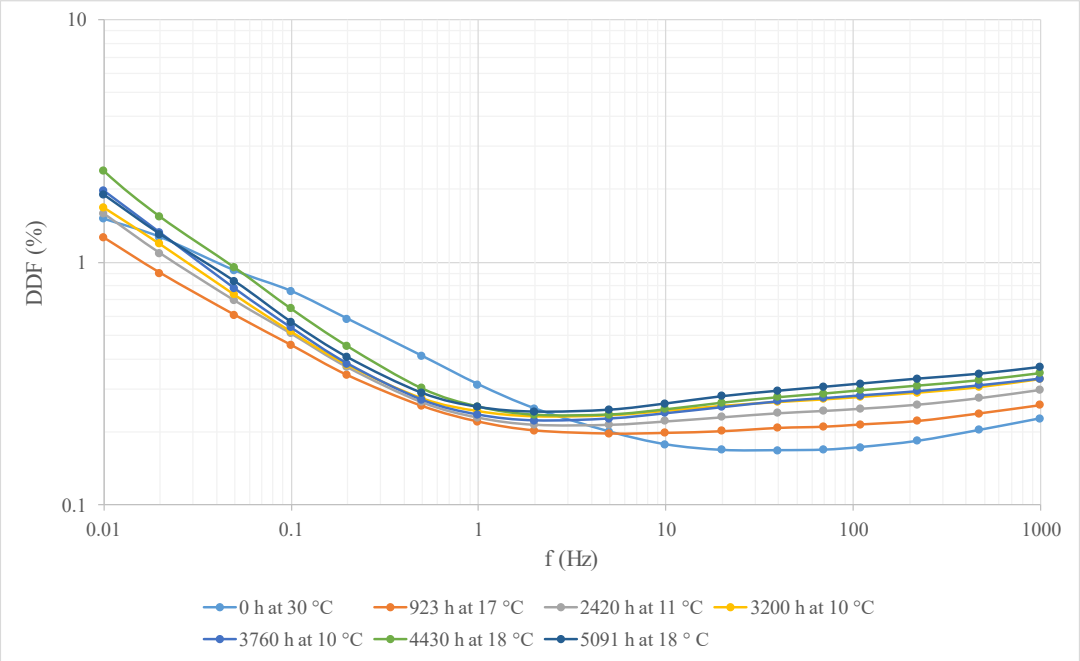

Source: Own authorship

Figure 40 – DFR measurements translated to 20 °C – CT01.

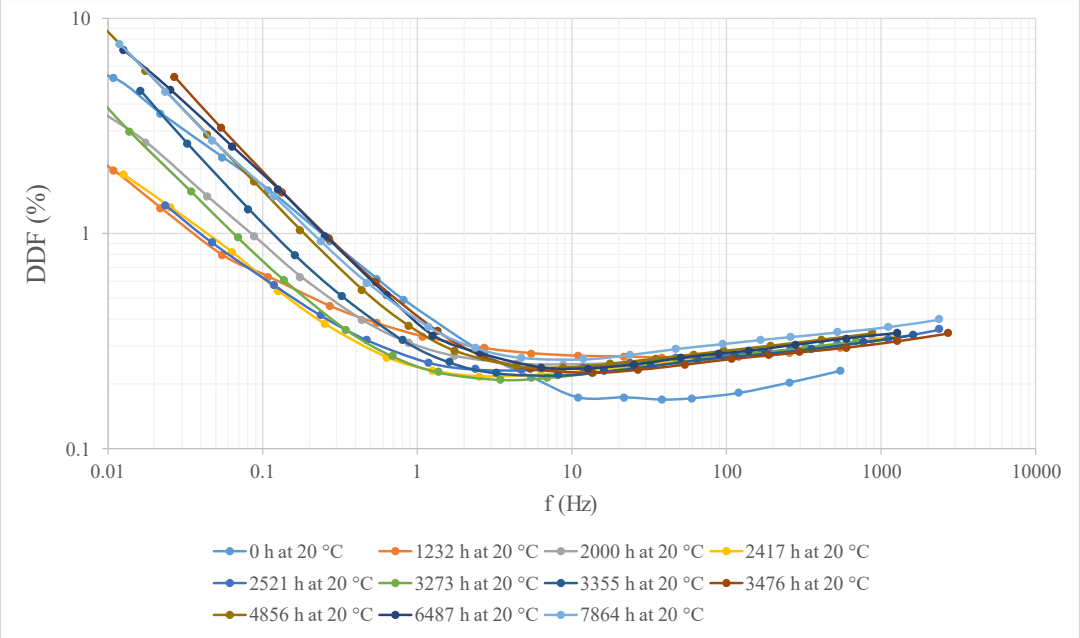

Source: Own authorship

Figure 41 – DFR measurements translated to 20 °C – CT02.

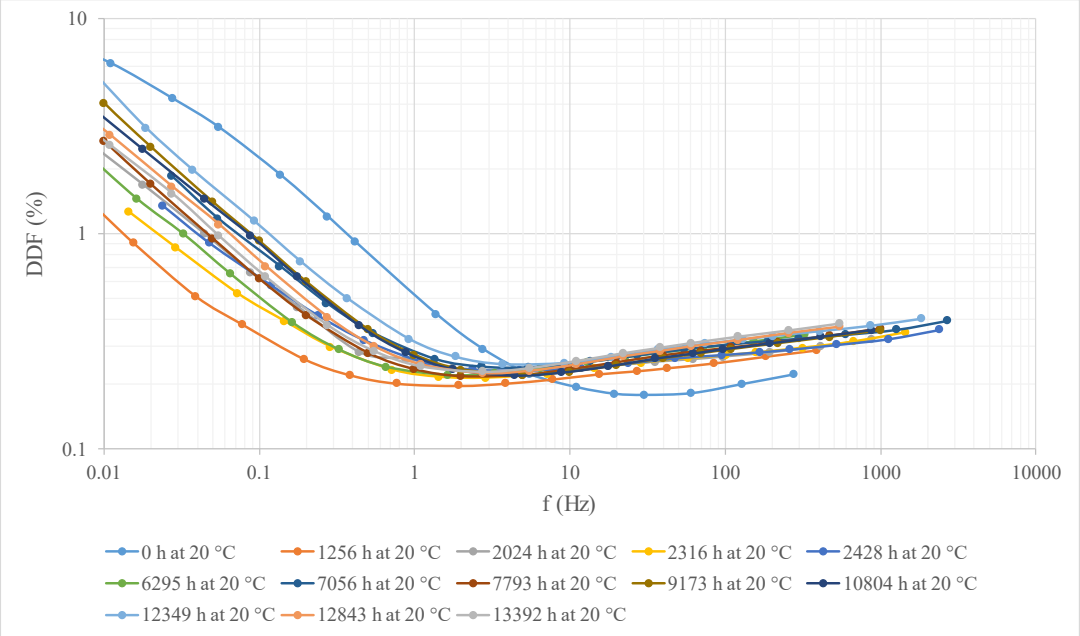

Source: Own authorship

Figure 42 − DFR measurements translated to 20 °C − CT03.

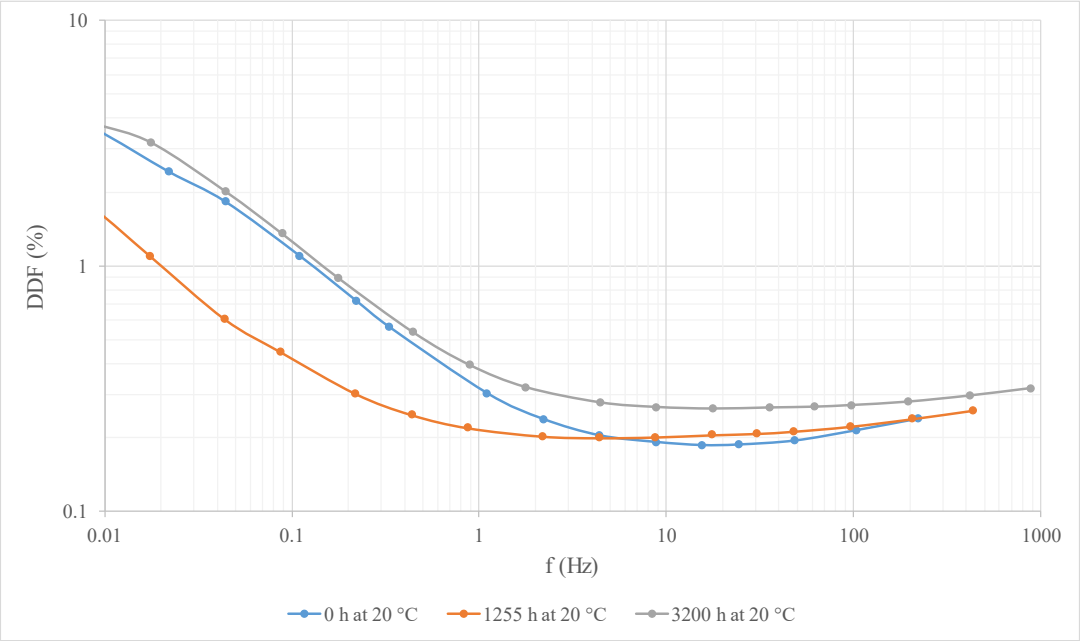

Source: Own authorship

Figure 43 − DFR measurements translated to 20 °C − CT04.

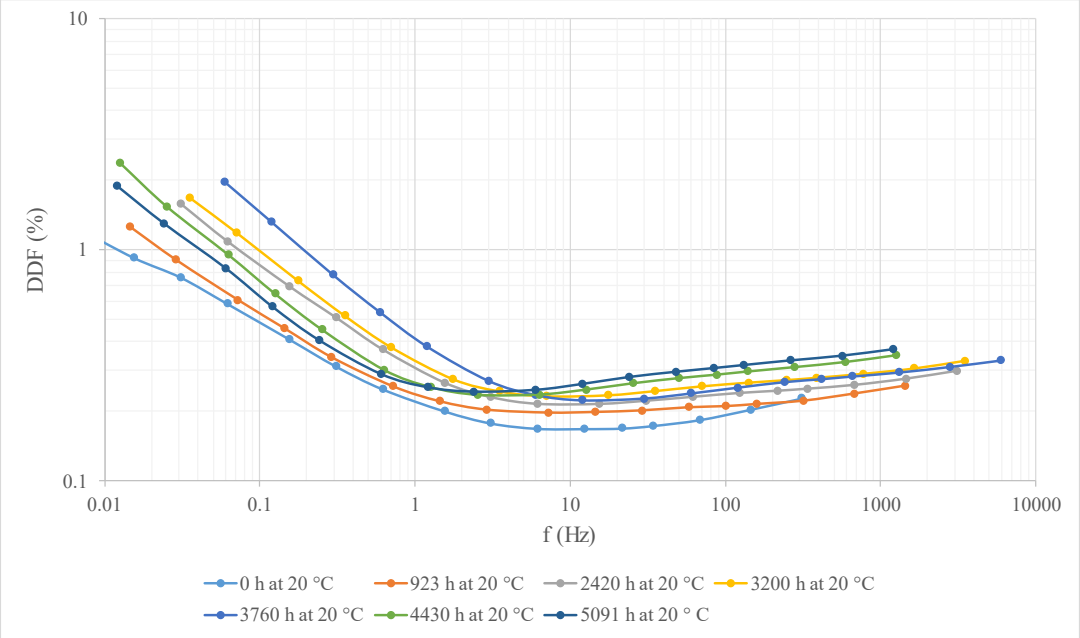

Source: Own authorship

IDAX 300 also allows estimation of moisture content in the paper based on the *DFR* measurements. However, this analysis and estimation is based on *XY* model (see 2.3.5.2.) which is successfully used for power transformers. In this work, this analysis has not been included

because the comparison between the curves obtained using *XY* model did not fit properly with the measured curves.

The figures 44 and 45 shows the *DFR* measurements for different test samples with approximately the same number of hours under test. A similar behavior is observed in the range from 10 Hz to 1 kHz in terms of *DDF* increase. *Figure 46* shows the initial and final *DFR* measurement for all samples, again with similar behavior in the range from 10 Hz to 1 kHz. It is clear that there is an impact in the results due to the aging of the insulation, however, it is not possible to quantify the aging based in this comparison.

Figure 44 − DFR measurements translated to 20 °C − 0 h and ~ 2 400 h.

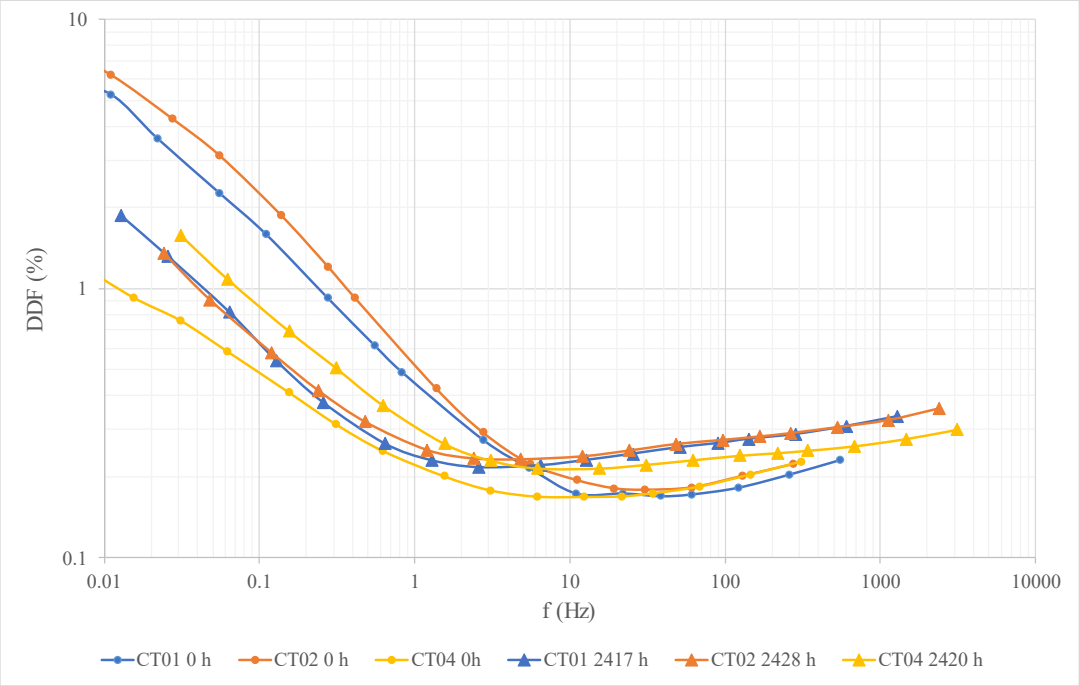

Source: Own authorship

Figure 45 − DFR measurements translated to 20 °C − 0 h and ~ 3 200 h.

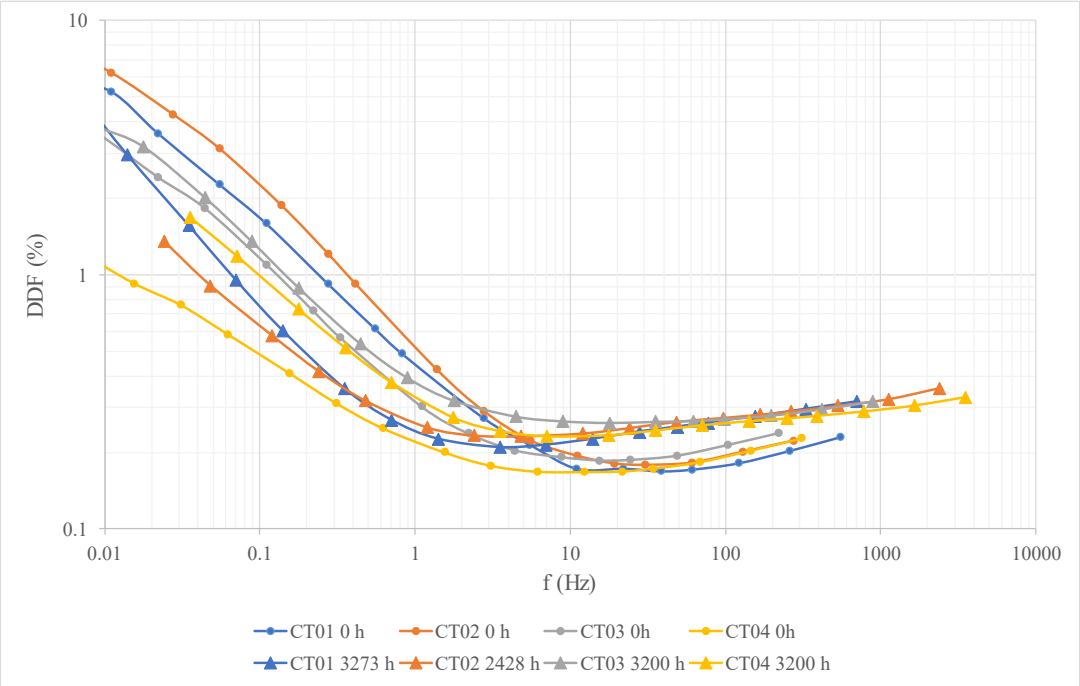

Source: Own authorship

Figure 46 − DFR measurements translated to 20 °C − 0 h and final measurements.

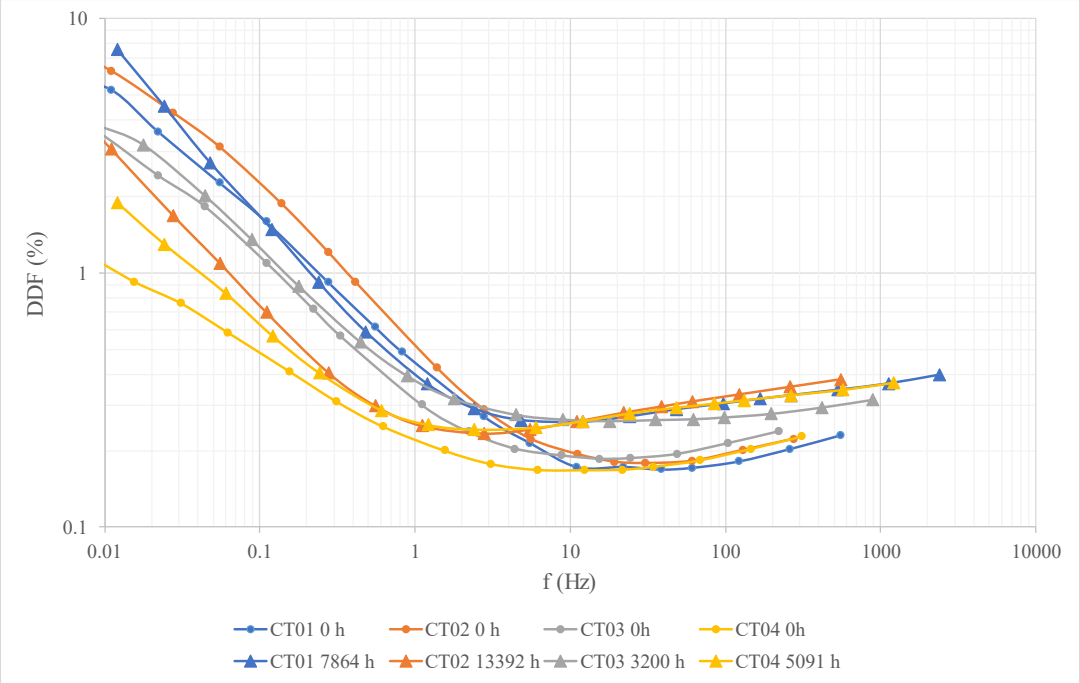

Source: Own authorship

5.2.5 PDC measurements

PDC (polarization and depolarization current) measurements have been performed on the sample CT04 since the resources to perform these measurements have become available. For comparison, a similar brand-new CT (available in the manufacturer's facilities) has also been measured. *Figure 47* shows the *PDC* measurement results. These measurements were carried out using IDAX 300. The DC voltage was set at 200 V.

Figure 47 − PDC measurements on CT04 after 4 873 h and on a brand-new similar unit.

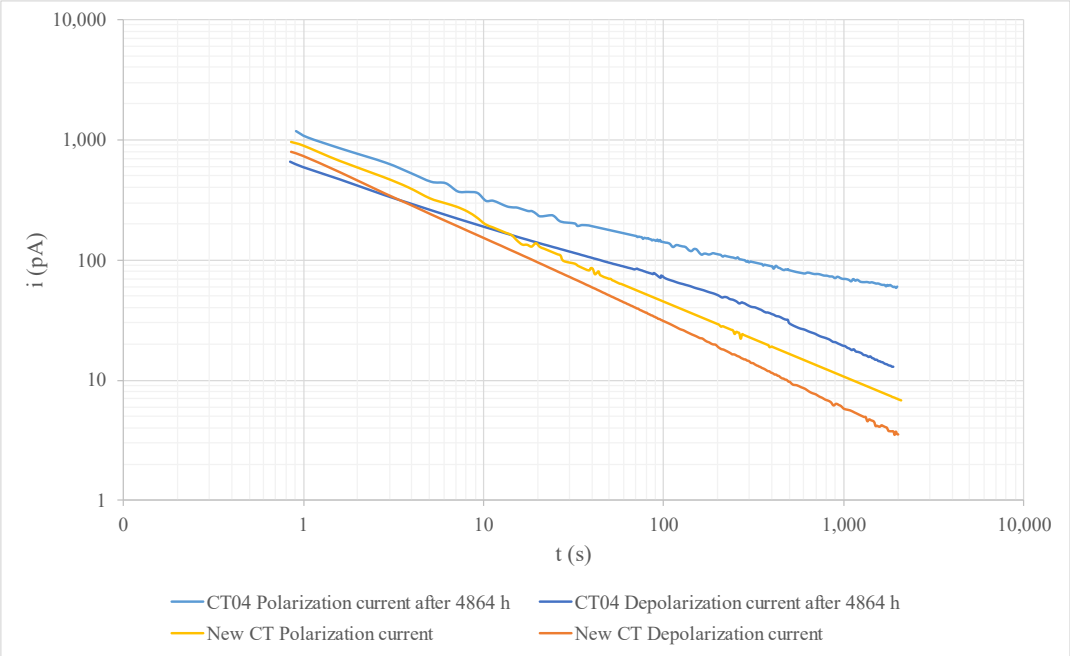

Source: Own authorship

As expected, polarization and depolarization current values are higher for the aged unit, CT04. Moreover, the difference between polarization and depolarization currents is also higher for the aged unit. As discussed in 2.3.5.1, Morsalin et al [29] states that the polarization current contains absorption and conduction components, and the depolarization current contains the absorption component only. Thus, there is a relative increase in the conduction current for the aged unit. The insulation DC resistance after 2000 s was around 3 TΩ for the aged sample and around 20 TΩ for the new sample. All these results are consistent with the expected behavior resulting from thermal degradation.

5.2.6 Tests on oil samples

The results of the tests on oil samples are showed from Tables 27 to 30.

Table 27 − CT01 results of tests on oil samples.

Sample CT01	Test hours	0	1232	2000	2274	2616	4856	7864
Test	**Date**	**27/11/2019**	**11/02/2020**	**30/03/2020**	**16/04/2020**	**27/07/2020**	**12/11/2021**	**18/08/2022**
Water Content	ppm	1.3	2.5	2.7	2.8	2.7	1.9	1.2
Density	g/cm3	0.863	0.863	0.863	0.863	0.863	0.864	0.867
Dissipation Factor at 90°C	%	0.21	0.25	0.28	0.35	0.15	0.18	0.16
Dielectric Strength	kV	78.8	76.6	75.5	74.5	74.3	78	66.7
Interfacial Tension	dina/cm	45.3	34.5	34.1	32.7	25.4	24	22.1
Oil Temperature	°C	22	25	23	35.7	25	22	22
Acidity	mgKOH/g	-	0.01	0.01	0.01	-	0.028	-
H2	ppm	1	43	62	74	68	57	931
O2	ppm	5246	1967	1713	1067	1316	2300	515
N2	ppm	14320	10047	10046	8636	9584	35600	13299
CO	ppm	5	526	795	950	944	2082	1038
CH4	ppm	0	9	13	16	18	51	109
CO2	ppm	36	2141	3425	4089	3308	15610	3909
C2H4	ppm	0	6.4	9.3	12.1	7.3	15	107
C2H6	ppm	0	2.9	5.9	8.6	6.2	36	19
C2H2	ppm	0	0	0	0	0	0	314
Total Gas Content	%	1.96	1.47	1.61	1.49	1.53	5.58	2.02
CO2/CO	-	7.20	4.07	4.31	4.30	3.50	7.50	3.77
C2H2/C2H4	-	-	0.00	0.00	0.00	0.00	0.00	2.93
CH4/H2	-	0.00	0.21	0.21	0.22	0.26	0.89	0.12
C2H4/C2H6	-	-	2.21	1.58	1.41	1.18	0.42	5.63
O2/N2	-	0.37	0.20	0.17	0.12	0.14	0.06	0.04
5HMF	ppm	-	0	0	0	0	0.06	-
2FAL	ppm	-	0.11	0.14	0.17	0.15	0.12	-
5MEF	ppm	-	0	0	0	0	0	-
2FOL	ppm	-	0	0	0	0	0.07	-
2ACF	ppm	-	0	0	0	0	0	-
Total	ppm	-	0.11	0.14	0.17	0.15	0.25	-

Table 28 − CT02 results of tests on oil samples.

Sample CT02	Test hours	0	1256	2024	2428	3139	9173	12349	13994
Test	**Date**	**27/11/2019**	**11/02/2020**	**30/03/2020**	**12/06/2020**	**20/11/2020**	**12/11/2021**	**01/07/2022**	**14/02/2023**
Water Content	ppm	1.6	1.4	1.5	2.6	1.2	5	2.4	2.5
Density	g/cm3	0.863	0.863	0.863	0.863	0.862	0.864	0.867	0.865
Dissipation Factor at 90°C	%	0.08	0.2	0.34	0.20	0.08	0.20	0.08	0.09
Dielectric Strength	kV	79.6	77.5	77.1	75.1	76.9	70	76.9	64.9
Interfacial Tension	dina/cm	45.3	33.9	33.4	29.5	16.7	19	29	20
Oil Temperature	°C	22	25	23	34.9	22	22	20	21
Acidity	mgKOH/g	-	0.01	0.01	-	-	0.034	-	0.064
H2	ppm	1	29	36	70	31	55	-	47
O2	ppm	4780	1827	1893	1338	2123	3500	-	4900
N2	ppm	12573	9676	10449	7821	10123	26100	-	40300
CO	ppm	8	634	823	744	800	2814	-	3759
CH4	ppm	0	9	13	13	12	63	-	100
CO2	ppm	39	2332	3236	2941	2526	15350	-	15840
C2H4	ppm	0	7.3	8.8	9.2	8	15	-	16
C2H6	ppm	0	3.3	6.1	6.1	6	64	-	82
C2H2	ppm	0	0	0	3.2	1	0	-	0
Total Gas Content	%	1.74	1.45	1.65	1.29	1.56	4.80	-	6.50
CO2/CO	-	4.88	3.68	3.93	3.95	3.16	5.45	-	4.21
C2H2/C2H4	-	-	0.00	0.00	0.35	0.13	0.00	-	0.00
CH4/H2	-	0.00	0.31	0.36	0.19	0.39	1.15	-	2.13
C2H4/C2H6	-	-	2.21	1.44	1.51	1.33	0.23	-	0.20
O2/N2	-	0.38	0.19	0.18	0.17	0.21	0.13	-	0.12
5HMF	ppm	-	0	0	0	-	0.05	-	-
2FAL	ppm	-	0.09	0.12	0.12	-	0.1	-	<25
5MEF	ppm	-	0	0	0	-	0	-	-
2FOL	ppm	-	0	0	0	-	0.06	-	-
2ACF	ppm	-	0	0	0	-	0	-	-
Total	ppm	-	0.09	0.12	0.12	-	0.21	-	-

Table 29 − CT03 results of tests on oil samples.

CT03	Test hours	0	342	1255	1547	3200
Test	**Date**	**27/11/2019**	**11/02/2020**	**30/03/2020**	**16/04/2020**	**27/07/2020**
Water Content	ppm	1.5	1.5	1.5	2.1	2
Density	g/cm3	0.863	0.863	0.863	0.863	0.863
Dissipation Factor at 90°C	%	0.07	0.18	0.18	0.27	0.14
Dielectric Strength	kV	79.1	77.9	76.8	75.4	75
Interfacial Tension	dina/cm	45.3	34.5	34.1	32.9	27.7
Oil Temperature	°C	22	25	23	36.1	25
Acidity	mgKOH/g	-	0.01	0.01	0.01	-
H2	ppm	0	17	27	35	30
O2	ppm	4789	1086	1527	1320	1679
N2	ppm	12535	6564	8592	8396	10079
CO	ppm	6	344	588	734	771
CH4	ppm	0	4	8	10	12
CO2	ppm	34	1007	2230	2873	2817
C2H4	ppm	0	2.8	6.3	9.2	7.3
C2H6	ppm	0	0.7	2.7	4.8	4.4
C2H2	ppm	0	0	0	0	0
Total Gas Content	%	1.70	0.90	1.30	1.30	1.50
CO2/CO	-	5.67	2.93	3.79	3.91	3.65
C2H2/C2H4	-	-	0.00	0.00	0.00	0.00
CH4/H2	-	-	0.24	0.30	0.29	0.40
C2H4/C2H6	-	-	4.00	2.33	1.92	1.66
O2/N2	-	0.38	0.17	0.18	0.16	0.17
5HMF	ppm	-	0	0	0	-
2FAL	ppm	-	0.08	0.11	0.11	-
5MEF	ppm	-	0	0	0	-
2FOL	ppm	-	0	0	0	-
2ACF	ppm	-	0	0	0	-
Total	ppm	-	0.08	0.11	0.11	-

Table 30 − CT04 results of tests on oil samples.

CT04	Test hours	0	1684	3200	4873
Test	**Date**	**20/11/2020**	**01/07/2021**	**21/07/2022**	**25/05/2023**
Water Content	ppm	1.2	0.7	0.6	0.8
Density	g/cm3	0.862	0.861	0.866	0.866
Dissipation Factor at 90°C	%	0.08	0.1	0.07	0.07
Dielectric Strength	kV	76.9	71.5	73.5	77.4
Interfacial Tension	dina/cm	45	33	35	36
Oil Temperature	°C	20	22	64.5	20
Acidity	mgKOH/g	-	-	-	-
H2	ppm	-	27	30	40
O2	ppm	-	1032	342	2200
N2	ppm	-	5827	4525	11200
CO	ppm	-	727	1058	1194
CH4	ppm	-	0	0	59
CO2	ppm	-	2383	3347	7730
C2H4	ppm	-	0	0	140
C2H6	ppm	-	0	0	58
C2H2	ppm	-	0	0	0
Total Gas Content	%	-	1.00	0.93	2.26
CO2/CO	-	-	3.28	3.16	6.47
C2H2/C2H4	-	-	-	-	0.00
CH4/H2	-	-	0	0	1.48
C2H4/C2H6	-	-	-	-	2.41
O2/N2	-	-	0.18	0.08	0.20
5HMF	ppm	-	0	-	-
2FAL	ppm	-	<0.02	<0.02	-
5MEF	ppm	-	0	0	-
2FOL	ppm	-	0	0	-
2ACF	ppm	-	0	0	-
Total	ppm	-	<0.02	<0.02	-

The initial measurements for all test samples show suitable values, better than the recommended limits for new units presented in 2.5.6.

Starting from the first oil sample after the first energization period of each test object, it can be noticed the ratio O_2/N_2 is lower than 0.5 which is an indicative of excessive consumption of oxygen as a result of oil oxidation and/or paper degradation. The increase of CO suggests paper degradation due to overheating, which is expected once the temperature has been increased to achieve a thermal aging acceleration. An increase in CO_2 is also noticed. The insulation of the testing samples is inside a sealed system and moisture and gases initial condition was suitable. Thus, CO_2 formation can be linked with the presence of moisture generated by paper degradation due to overheating.

The last oil sample withdrawn from *CT01* was collected after the *PD* measurement (after the effective failure). According to the analysis using the Duval Triangle, as showed in Figure 48, the detected gases are consistent with low energy density discharges followed by a high energy discharge. The same diagnosis can be considered from the combined analysis of the ratios C_2H_4/C_2H_6.

Figure 48 – Duval Triangle Analysis for the last oil sample withdrawn from CT01 (after failure).

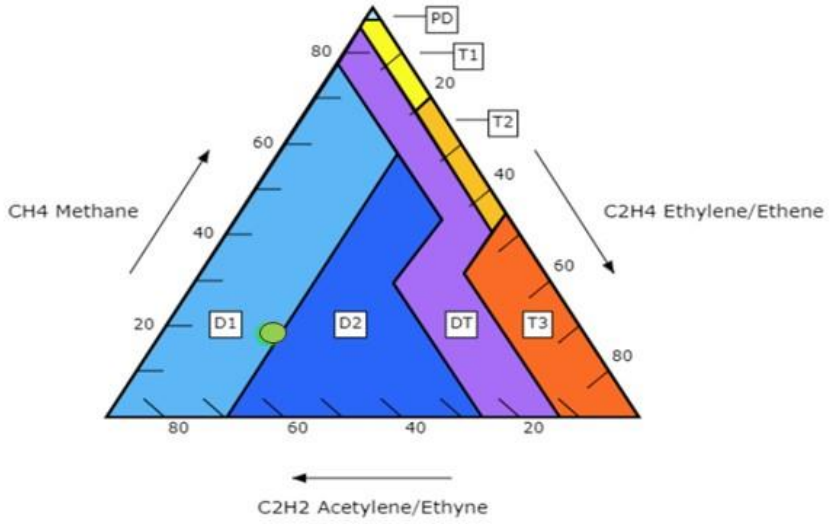

Source: Online tool available in [66]

The last oil sample withdrawn from *CT02* showed in *Table 28* was collected before the *PD* measurement (before the effective failure). Unhappily, the syringe of the oil sample that was withdrawn after the effective failure was damaged during transportation. According to the Duval Triangle analysis (see Figure 49), the results suggest thermal degradation, which is in line with other measurements (*DFR*, *DDF*, increase of CO) performed before the failure. The increase in H_2 with presence of CO, CO_2 and CH_4, and the ratio C_2H_4/C_2H_6 lower than 0.2

combined with a negligible ratio C_2H_2/C_2H_4 indicate possibility of PD. It is important to highlight that the Duval Triangle Analysis for the *CT01* corresponds to the analysis of the failure while for the *CT02*, it corresponds to the degradation stage before the failure.

Figure 49 – Duval Triangle Analysis for the last oil sample withdrawn from CT02 (before failure).

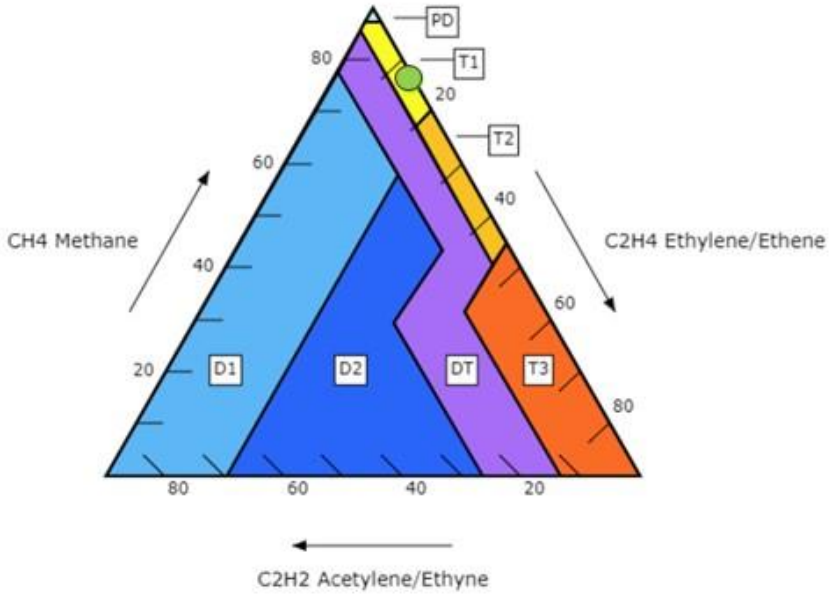

Source: Online tool available in [66]

Initial values of water content, dissipation factor and dielectric strength are in line with expected values for new sealed equipment. For all units, there is a small increase in moisture content in oil, but the value is still lower than 10 ppm. However, as discussed in 2.5.6.2, most of the moisture from degradation is retained in solid paper insulation. The values of *DDF* shown in 5.2.2 and 5.2.4 indicate moisture in the solid insulation. The small increase in moisture content is in line with the small variation in oil dissipation factor and oil dielectric strength.

The increase in oil acidity is a relevant degradation indicator. The last oil sampling for *CT01* and *CT02* indicated a relevant increase in acidity. However, all the values may be considered as "good" by the *IEC* (see Table 9). The results of interfacial tension have shown a progressive decrease. All the units started at ~ 45 dynes/cm. The results show a decrease in this quantity along the test hours, as shown in Figure 50.

Figure 50 − Interfacial tension variation along test hours.

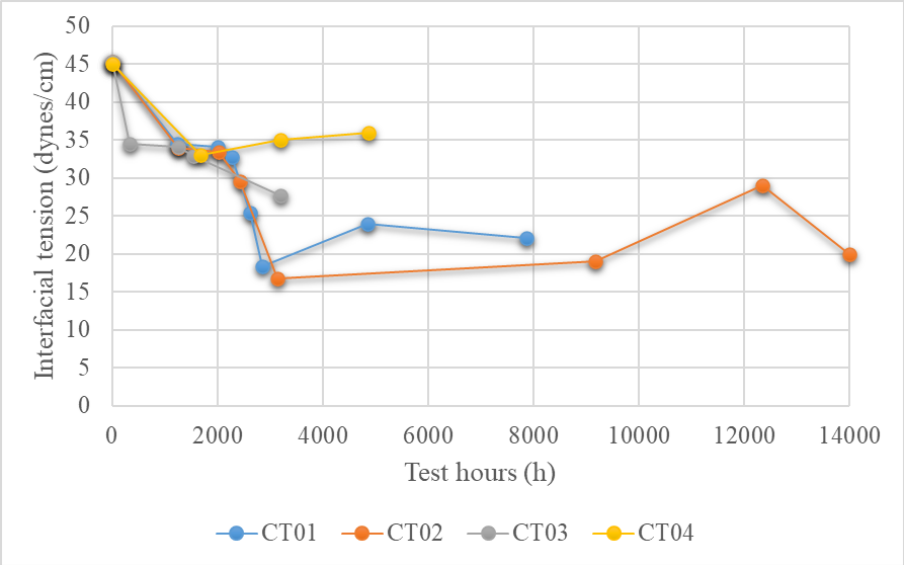

Source: Own authorship

Measurements of furanic compounds are rarely used for *CT*. In general, it is indicated when dissolved gas analysis shows high CO content. According to [19], the maximum concentration of 2FAL for a thermally aged *CT* is about 0.2 ppm when measured CO content is about 700 ppm. The aging test on *CT03* was interrupted after 3 200 hours. The last 2FAL measurement (after 1 547 testing hours) indicated 0.11 ppm and a respective CO content of 734 ppm. A similar scenario is observed for the results of *CT02* after 2 428 hours: 0.12 ppm of 2FAL and 744 ppm of CO. The most recent values for *CT02* are 0.10 ppm of 2FAL associated with 2 814 ppm of CO. Results for *CT01* show 0.15 ppm of 2FAL and 944 ppm of CO after 2 616 hours and 0.12 ppm of 2FAL with 2 082 ppm of CO after 4 856 h. All these results indicate thermal aging, as expected.

5.3 TEARDOWN OF TEST SAMPLES – VISUAL INSPECTION AND TESTS ON PAPER SAMPLES

Following the proposed investigation methodology, failed samples were torn down for visual inspection and withdrawal of paper samples for the analysis of the degree of polymerization. The objective of the visual inspection is to identify carbonization or tracking marks. Additionally, some paper samples were withdrawn for Scanning Electron Microscopy with an Energy Dispersive X-ray Spectroscopy (*SEM-EDS*) analysis. This analysis intends to

evaluate the morphology of paper fibers and, also identify possible residues presented on the surface of the paper.

The teardown examination was performed on samples *CT01, CT02* and *CT03*. *CT01* and *CT02* failed during *PFWV* tests and *CT03* has been dismantled after an evaluation of the aging conditions of the test samples after ~3000 hours under accelerated aging conditions to use some parts of this sample to build a brand new one: *CT04*. The sample *CT04* has not yet failed.

The sample *CT03* remained under accelerated aging conditions during 3 200 h and it was *PD* free before the teardown examination. Figure 51 shows a general view of the *CT03* active part and the identification of the place from where the paper samples were withdrawn. No carbonization or tracking marks were found on any part of the CT03 insulation. The coloring of the shielding screens revealed a normal appearance. Table 31 shows the results of the polymerization degree analysis of the *CT03* paper samples.

Figure 51 − Active part of the sample CT03 during teardown examination. Identification of paper samples withdrawn for degree of polymerization analysis.

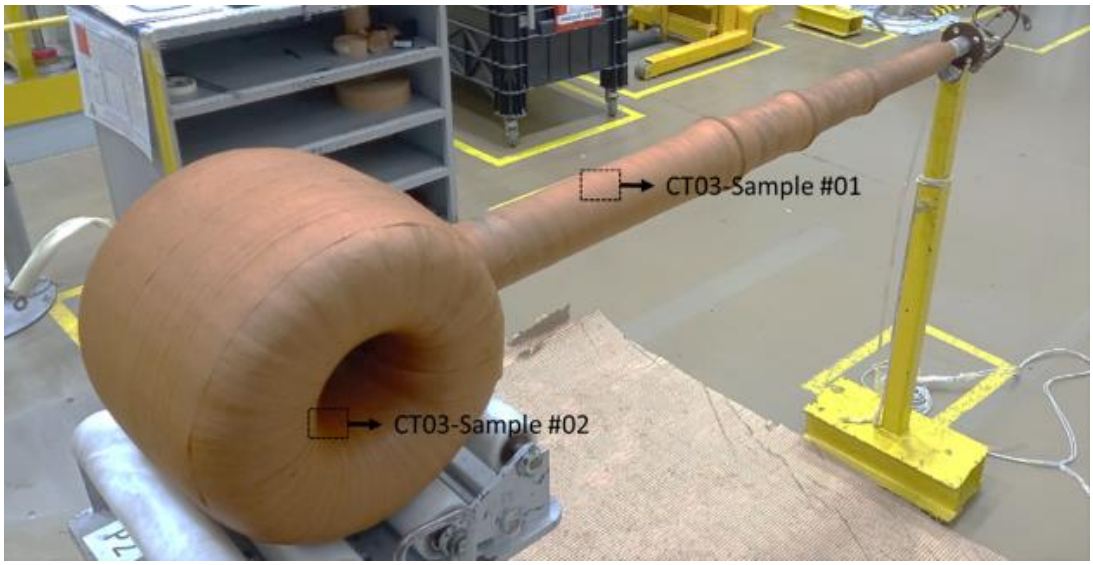

Source: Own authorship

Table 31 − CT03 − Degree of polymerization results.

Paper sample	Position (See Figure 51)	Polymerization degree (monomers)
CT03-Sample #01	Bushing	942
CT03-Sample #02	Head	718

The teardown examination of sample *CT01* was performed after 7 864 hours of testing under accelerated conditions. This unit failed during *PFWV/PD* tests. Nine paper samples were withdrawn from *CT01* as showed in *Figure 52*. The fault region is showed in *Figure 53*. The values of degree of polymerization were measured for 8 paper samples and they are in *Table 32*. One of the paper samples (CT01-Sample #08) was withdrawn for the *SEM-EDS* analysis. It was observed a normal morphological aspect (see *Figure 54*) as well as carbon and oxygen as the main elements found from the *SEM-EDS* analysis. A very small quantity of calcium and magnesium was found (see *Table 33*), and it was considered not relevant by Moscon and Wilhelm [84].

Figure 52 − Active part of the sample CT01 − Identification paper samples withdrawn for degree of polymerization and SEM-EDS analysis.

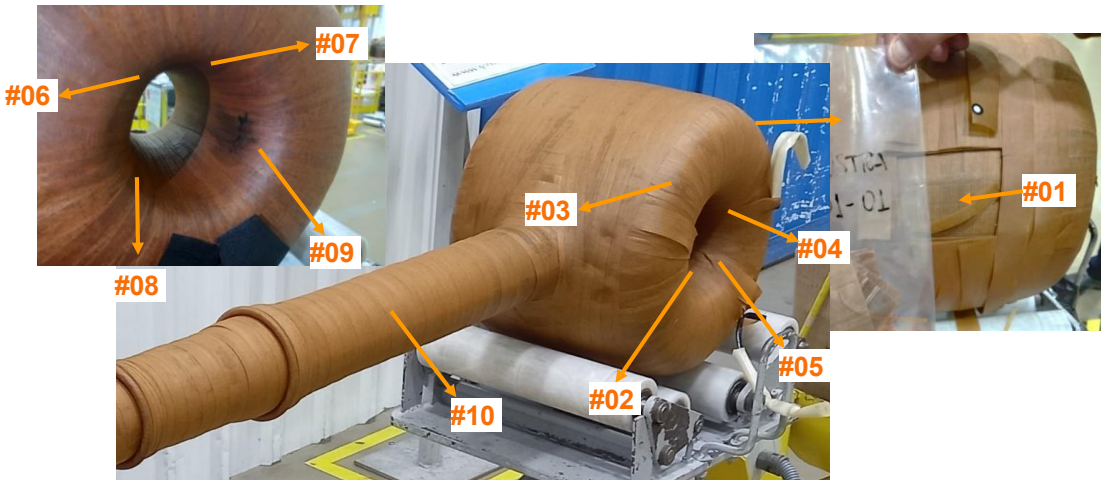

Source: Own authorship

Table 32 − CT01 − Degree of polymerization results.

Paper sample	Position (See Figure 51)	Polymerization degree (monomers)
CT01-Sample #01	Top of head	553
CT01-Sample #02	Head – Window curvature	520
CT01-Sample #03	Head – Border curvature	590
CT01-Sample #04	Head – Window curvature	573
CT01-Sample #05	Head – Window curvature	592
CT01-Sample #06	Head – Window curvature	535
CT01-Sample #07	Head – Window curvature	579
CT01-Sample #09	Head – Around failure	481
CT01-Sample #10	Bushing	611

Figure 53 − Active part of the sample CT01 during autopsy. Identification of fault region.

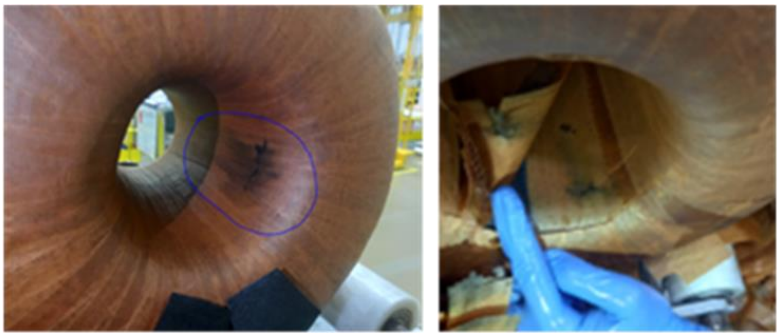

Source: Own authorship

Table 33 − CT01 − Elementary analysis by SEM-EDS in 4 regions of CT01-Sample #08 [84].

Element	**Elementary content (%)**			
	1	2	3	4
C	47.3	53.1	53.3	56.2
O	46.2	45.1	44.0	43.8
Mg	0.2	-	0.1	-
Ca	6.2	1.7	2.5	-

Figure 54 − Micrography of CT01-Sample #08. A: 600 X. B: 3500 X.

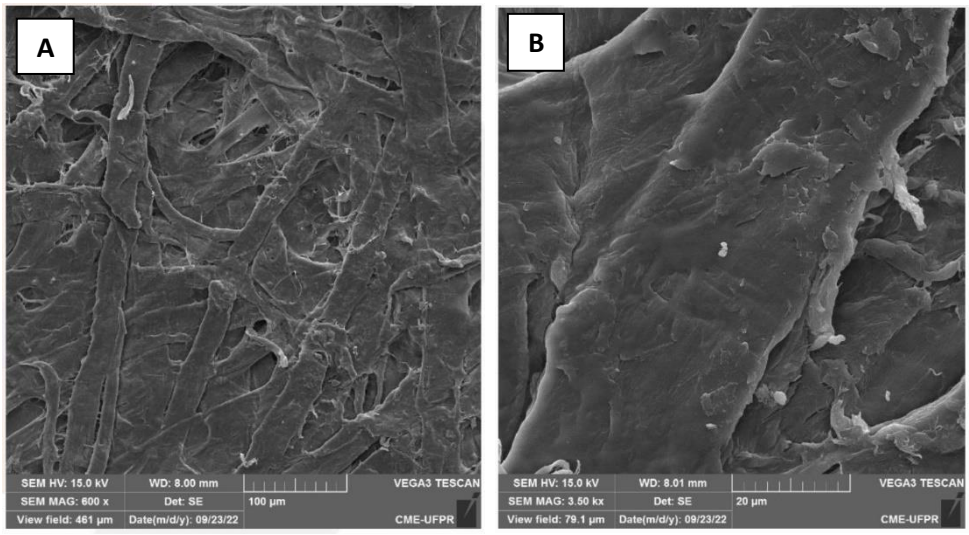

Source: Adapted from [84]

CT02 was torn down after 13 994 h under accelerated aging conditions. This sample also failed during *PWFV / PD* tests. Eight paper samples were withdrawn during the teardown examination, as showed in *Figure 55*. The fault region is showed in *Figure 56*. *Table 34* shows

the results of the degree of polymerization related to *CT02*. For the paper sample *CT02-Sample #08, SEM-EDS* analysis was carried out besides degree of polymerization. These results are in *Figure 57* and *Table 35* . As expected, the particulate materials are mostly composed of carbon and oxygen. A small amount of silicon, calcium, nickel, chromium, iron and aluminum have been detected. The differences between *SEM-EDS* for *CT01* and *CT02* paper samples were not considered relevant enough to lead to any conclusion in terms of difference in degradation.

The comparison among the results of the degree of polymerization indicated that the reduced model samples *CT01* and *CT02* can be considered at the same degradation level. For both cases, the values for the paper samples on the curvature of the window and in the failed region were respectively at the same magnitude.

Figure 55 − Active part of the sample CT02 − Identification paper samples withdrawn for degree of polymerization and SEM-EDS analysis.

Source: Own authorship

Figure 56 − Active part of the sample CT02 during autopsy. Identification of fault region.

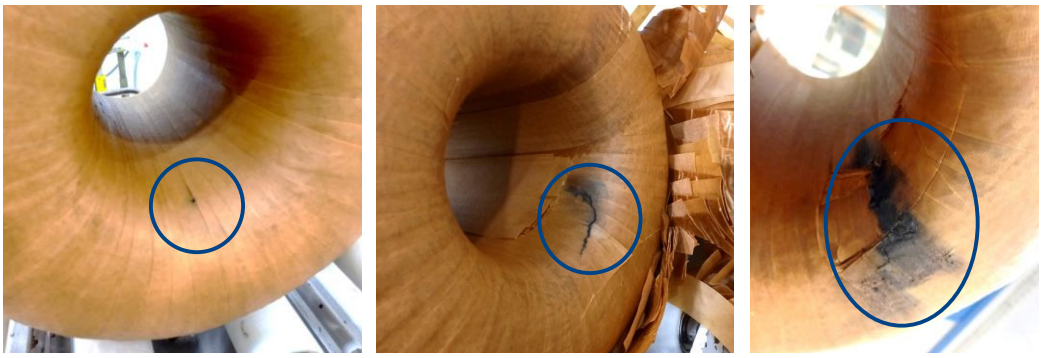

Source: Own authorship

Table 34 − CT02 − Degree of polymerization results.

Paper sample	**Position** (See)	**Polymerization degree (monomers)**
CT02-Sample #01	Top of head	640
CT02-Sample #02	Head – Window curvature	542
CT02-Sample #03	Head – Border curvature	662
CT02-Sample #04	Head – Window curvature	562
CT02-Sample #05	Bushing	762
CT02-Sample #06	Head – Around failure	496
CT02-Sample #07	Head – Around failure	476
CT02-Sample #08	Head – Around failure	465

Figure 57 − Micrography of CT02-Sample #08. A: 150 X. B: 2400 X.

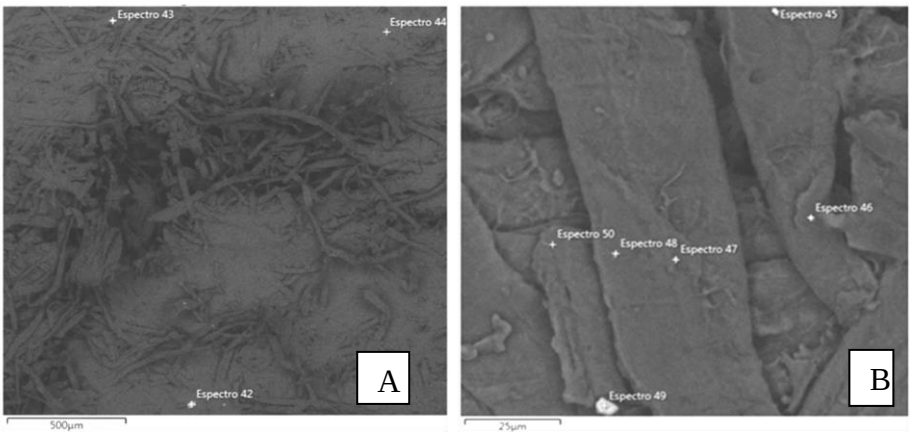

Source: Adapted from [85]

Table 35 − CT02 − Elementary analysis by SEM-EDS in 9 regions of CT02-Sample #08 [85].

Element	**Elementary content (%)**								
	42	43	44	45	46	47	48	49	50
C	54	60.7	46	54.7	61	53.2	59.4	61.6	61.7
O	32.5	31	40.2	19.1	32.6	38.7	38.5	37.7	38
Fe	1.9	2.4							
Si	11.7	2.0							
Ca			13.6			8.0			
Al		1.9					1.3		
Ni				6.3	1.8				
Mg		2.0							
Cr				5.4	1.2				

For both failed units, *CT01* and *CT02*, the fault occurs in the curvature of the active part window where the magnitude of the electrical field is higher, as expected. This fault region was close to the internal resistor and fiber optical thermal probe. This internal resistor is the heating source to increase the temperature of insulation at this point, above to the oven temperature.

The carbonization level of the fault region of *CT01* was visually more intense than the fault region of *CT02*. As presented in 5.2.1, Table 18, when *CT01* failed, the *PD* level suddenly increased from 327 pC to a value above 1 000 pC. The test lab protection tripped and turned off the test circuit when the test voltage was at *PFWV*. It was possible to listen a noise coming from the test object. The failure of *CT02* did not trigger lab protection. However, the *PD* level increased to 1 992 pC at the test voltage of 152 kV, which corresponds to the *PFWV*. The test voltage was decreased to zero. When trying to energize the unit again before to measuring *DDF*, the *PD* level was above 500 pC at 5 kV, and it was possible to hear a noise coming from the test object. Maybe this is the reason because the carbonization level of *CT01* was more intense.

5.4 SYNTHESIS OF THE RESULTS OF THE TESTS CARRIED OUT ON THE TEST SAMPLES – CROSS-ANALSYS

Several tests were performed on the test samples along the accelerated aging test and on insulation samples withdrawn during the teardown of the failed units. Besides the lifespan estimation and the investigation aiming to find empirical parameters of the aging model that

was chosen for this study, a cross-analysis of the results of diagnostic tests was proposed as an additional objective. Table 36 shows a synthesis of the main outputs obtained from the test results.

Table 36 – Synthesis of the test results

Test	Main outputs
PD	Even after the start of the DDF increase (primary indicator of thermal degradation), the test samples remained *PD* free for a long period. A reduction in PD inception and extinction voltage values was observed when the samples approached failure.
DDF	The increase of *DDF* values at rated frequency and normal ambient temperature was observed in the first measurements after the first interruption of the aging test as an impact of an initial thermal degradation. After this initial increase, there is a tendency of stabilization. *DDF* measurements at high temperature and the determination of the respective temperature coefficient α_c did not indicate thermal instability of the test samples.
DFR	The increase of *DDF* values in the range from 10 Hz to 1 kHz was observed for all test samples after some time at high temperature, a typical behavior related with thermal degradation. However, it was not possible to quantity the degradation level based on these results. The application of the *XY* model (developed for power transformers) did not result in consistent results and it could not be used to estimate the moisture content in the solid insulation.
PDC	The polarization and depolarization current values were higher for the aged sample. Moreover, the difference between polarization and depolarization current was also higher for the aged unit. These results indicate a relative increase in the conduction current for the aged unit which is consistent with thermal degradation.
Oil *DGA*	Ratio O_2/N_2 indicated oil and paper oxidation. CO and CO_2 contents were consistent with thermal degradation of the paper. The gas analysis after the failure of the sample *CT01* indicated occurrence of *PD* followed by a high energy discharge, as observed in *PD* measurement when the failure occurred.
Oil *DDF*	Small increase of oil *DDF*. The combined analysis of these measurements with the insulation *DDF* values, *DFR* and *PDC* measurements indicated that the moisture generated by degradation was in the solid insulation (paper).
Oil *MC*	Small increase of moisture content in oil. Most of the moisture generated by thermal degradation was retained in solid paper insulation.
Oil *BV*	In general, a tendency of decrease was observed. Only *CT01* and *CT02* achieved a remarkable decrease (respectively, 15 % and 18 %), despite still presented values classified as "good" by *IEC* [68].
Oil *IT*	Progressive decrease along test hours. Only the samples *CT01* and *CT02* achieved values classified as "poor" by *IEC* [68] when they were approaching the failure.
Oil *Acidity*	Increase of acidity has been detected only for the samples *CT01* and *CT02*, however the values remained in a range classified as "good" by *IEC* [68].
Oil HPLC	2FAL concentration remained < 0.2 ppm for all units. The values in the range 0.10 to 0.18 associated with the increase of CO content is an indication of thermal degradation.
Paper *DP*	No paper sample withdrawn from the test objects achieved the end-of-life criteria ($DP \leq$ 200). Measured values were lower for the samples withdrawn from the head than those from the bushing indicating a higher degradation level of the solid insulation where thermal and electrical stresses are higher, as expected. The comparison between *CT01* and *CT02 DP* values indicates the same degradation level for both samples.
Paper *SEM-EDS*	A normal morphological aspect was observed indicating that despite of an initial thermal degradation, the thermal end-of-life was not achieved.

PD: Partial Discharge	*IT*: Interfacial tension
DDF: Dielectric Dissipation Factor	*HPLC*: High Performance Liquid Chromatography (furanic compounds)
DFR: Dielectric Frequency Response	*DP*: Degree of Polymerization
PDC: Polarization & Depolarization current	*SEM-EDS*: Scanning Electron Microscopy with an Energy Dispersive X-ray Spectroscopy
DGA: Dissolved Gas Analysis	
MC: Moisture Content	
BV: Breakdown voltage	

When subjecting oil-impregnated paper insulation to high thermal stress, the degradation processes described in 2.5.3 associated with thermal stress are triggered depending on the temperature and initial conditions of the insulation. The chemical reactions involved in these processes cause the cellulose chains to break, the oil to oxidize and trigger the generation of by-products (moisture, acids, gases) that feed back into the degradation mechanisms. These degradation by-products impact electrical properties of the insulation such as the dielectric dissipation factor, discharge inception and extinction voltage values and dielectric strength.

The simultaneous application of electrical stress to the insulation combined with thermal stress acts synergistically resulting in a reduction in the life of the insulation. When insulation fails under the combined action of both stresses, this synergy must be taken into account to determine the root cause of the failure.

The cross-analysis of the test results showed in the Table 36 indicates the progressive thermal degradation of all the test samples, however, *DP* values of the paper samples (even those related with the samples withdrawn close to the fault region, see Tables 32 and 34) are higher than the end-of-life criteria. The morphological analysis of the paper samples confirmed an acceptable condition of cellulose chains. The cross-analysis clearly indicates that the failure of *CT01* and *CT02* test samples cannot be considered as a thermal failure caused by the continuous steady-state thermal stress applied to these samples. Even with the increase in *DDF*, these samples remained thermally stable.

On the other hand, these samples showed a decrease in the inception and extinction voltages of partial discharges (an indication of the degeneration of their capability to withstand electrical stress) until there was a high growth of partial discharges, finally resulting in the dielectric breakdown of the insulation.

Therefore, it can be stated that the failure of the samples was a dielectric failure caused by the combined action of electrical and thermal stresses. Although, thermally, the samples could still have a relatively long remaining life, the by-products of thermal degradation contributed to the reduction of the inception and extinction voltages of partial discharges and the increase in the level of partial discharges progressed to the electrical breakdown of the insulation.

5.5 TIME TO BREAKDOWN UNDER TEST CONDITIONS AND LIFESPAN ESTIMATION AT REFERENCE OPERATION CONDITIONS

This work aims to investigate the accelerated aging of *CTs* built with oil-impregnated paper insulation under simultaneous thermal and electrical stresses. A long-duration power frequency test is performed on reduced models of 550 kV *CTs* with controlled voltage and temperature conditions. Equation (42) is applied to the test results, aiming to find values for the voltage exponent n and for the threshold electrical stress E_0 to get a convergence among the experimental results.

In a preliminary assessment, testing hours were estimated based on equation (42) and assuming service life at 1.0 p.u. as 40 years with n = 10 and E_0 = 1.0 p.u., based on the use of this equation for paper-oil power cables (see Table 13). However, after ~ 3 000 testing hours, *CT01*, *CT02* and *CT03* remained free of *PD*. These preliminary results raised the question about the possibility of n being less than 10 and E_0 being greater than 1.0 p.u. If so, there would be the possibility of the test duration for *CT03* being too long. Thus, it was decided to stop the test on *CT03* and to use its main materials (insulator, head housing, core box, stem tube, pedestal, and oil compensation bellow) to manufacture a brand-new test sample, *CT04*, to be tested at higher voltage (refer to Table 14).

As presented in 5.3, *CT03* was torn down. The visual inspection did not reveal any carbonization or any evidence of excessive degradation. Moreover, the results of the polymerization degree analysis also indicate that this sample was at a very low aging level. With this confirmation about *CT03*, the test voltage to be applied on the sample *CT04* was defined based on the maximum voltage that was possible to apply considering the clearances of the test oven and the voltage transformer that could be designed and manufactured to be used as a test transformer, taking into account the available material. All the chosen test voltages are showed in Table 14. Table 37 shows the weighted average values of voltage, electrical stress and temperature for each test sample. Annex A shows a summary of voltage and temperature values for all test cycles.

Table 37 − Actual aging conditions: weighted average values of voltage, electrical stress and temperature.

	CT01	***CT02***	***CT03***	***CT04***
Average value of actual test voltage (kV)	87.9	83.5	76.6	116.4
Electrical stress (p.u.)	1.24	1.18	1.08	1.65
Average value of insulation temperature (°C)	125.3	120.0	119.6	120.2
Test duration (hours)	7 864	13 994	3 200	5 190
Test duration (months)	10.92	19.44	4.44	7.21

Equation (42) has been applied to the results of *CT01*, *CT02* and *CT04* as showed in *Table 38*. The results for *CT01* and *CT02* correspond to the lifespan estimation. For *CT04*, it is an estimation of achieved life until the present moment since this unit has not yet failed.

For the contribution of thermal stress, θ_0 has been assumed as 80 °C and $\alpha = 0.087$ ("8°C rule"). For the contribution of electrical stress, it has been considered $1 \leq n \leq 10$ and $1.0 \leq E_0 \leq 1.23$ p.u. for this preliminary analysis showed in Table 38 . The choice of 1.23 p.u. is justified because *CT01* (energized at 1.24 p.u.) failed after a much lower number of hours than *CT02* (energized at ~ 1.18 p.u.), which indicates a contribution of aging due to electrical stress for the sample *CT01* (i.e. $E_0 < 1.24$ p.u).

The minimum life expectancy of oil-impregnated paper *CTs* is about 25 to 30 years [19]. However, several units surpassed a 40-year-service life in the world. *CTs* are under other electrical stress (e.g., high frequency), besides power frequency voltage stress impacting their service life. Based on a conservative approach, all the scenarios considering lifespan higher than 70 years have been disregarded (i.e., $Lmax = 70$). Thus, due to the present results, the exponent n must be lower than 5.

Since *CT04* have not failed until the publication of this thesis, it is reasonable to assume that the *CT04* achieved life would not be higher than the *CT01* and *CT02* lifespan estimates while comparing them with the estimation of achieved life for *CT04*. Thus, the scenarios with values of *CT04* achieving life estimation higher than *CT01* and *CT02* lifespan estimation may also been disregarded. All disregarded values in *Table 38* are on a grey background.

Table 38 − Life estimation for CT01 and CT01 and achieved life estimation for CT04 for different values of n and E_0.

Test sample	*n*	10	9	8	7	6	5	4	3	2	1
	E_0										
CT01	*1.00*	408.1	327.4	262.6	210.8	169.2	135.8	109.0	87.6	70.4	56.5
CT01	*1.05*	250.5	211.0	177.8	149.8	126.2	106.4	89.7	75.7	63.8	53.9
CT01	*1.10*	157.4	138.9	122.5	108.2	95.5	84.3	74.5	65.8	58.2	51.4
CT01	*1.15*	101.0	93.2	86.0	79.3	73.2	67.6	62.4	57.6	53.2	49.2
CT01	*1.18*	78.1	74.0	70.0	66.3	62.8	59.5	56.3	53.4	50.6	47.9
CT01	*1.19*	71.9	68.6	65.5	62.6	59.7	57.0	54.5	52.1	49.8	47.6
CT01	*1.20*	66.2	63.8	61.4	59.1	56.9	54.8	52.7	50.8	48.2	47.2
CT01	*1.21*	61.1	59.3	57.5	55.8	54.2	52.6	51.1	49.6	47.4	46.8
CT01	*1.22*	56.4	55.1	53.9	52.8	51.6	50.5	49.5	48.4	46.7	46.4
CT01	*1.23*	52.2	51.4	50.7	50.0	49.3	48.6	48.0	47.3	45.7	46.1
CT02	*1.00*	273.5	231.1	195.3	165.1	139.6	118.0	99.8	84.4	71.5	60.5
CT02	*1.05*	167.9	149.0	132.2	117.3	104.1	92.5	82.1	72.9	64.8	57.6
CT02	*1.10*	105.5	98.0	91.1	84.7	78.8	73.3	68.2	63.4	59.1	55.0
CT02	*1.15*	67.6	65.7	63.8	62.1	60.3	58.7	57.1	55.5	54.0	52.6
CT02	*1.18*	54.4	54.1	53.7	53.4	53.0	52.7	52.4	52.1	51.8	51.5
CT02	*1.19*	53.0	52.8	52.6	52.4	52.2	52.0	51.9	51.7	51.5	51.4
CT02	*1.20*	52.1	52.0	51.9	51.8	51.7	51.6	51.5	51.4	51.3	51.3
CT02	*1.21*	51.5	51.5	51.5	51.4	51.4	51.4	51.3	51.3	51.3	51.2
CT02	*1.22*	51.4	51.3	51.3	51.3	51.3	51.3	51.3	51.2	51.2	51.2
CT02	*1.23*	51.3	51.3	51.3	51.3	51.2	51.2	51.2	51.2	51.2	51.2
CT04	*1.00*	2 730.2	1 659.5	1 008.8	613.2	372.8	226.6	137.7	83.7	50.9	30.9
CT04	*1.05*	1 676.1	1 069.8	682.8	435.8	278.2	177.5	113.3	72.3	46.2	29.5
CT04	*1.10*	1 052.6	703.8	470.6	314.7	210.4	140.7	94.1	62.9	42.1	28.1
CT04	*1.15*	674.9	471.7	329.8	230.5	161.2	112.7	78.8	55.1	38.5	26.9
CT04	*1.18*	521.6	374.2	268.4	192.5	138.1	99.0	71.0	51.0	36.6	26.2
CT04	*1.19*	479.4	346.8	250.9	181.5	131.3	95.0	68.7	49.7	35.9	26.0
CT04	*1.20*	440.9	321.6	234.6	171.1	124.8	91.1	66.4	48.5	35.4	25.8
CT04	*1.21*	405.8	298.5	219.5	161.5	118.8	87.4	64.3	47.3	34.8	25.6
CT04	*1.22*	373.8	277.2	205.5	152.4	113.0	83.8	62.2	46.1	34.2	25.4
CT04	*1.23*	344.5	257.5	192.6	144.0	107.6	80.5	60.2	45.0	33.6	25.2

The results of *CT01* and *CT02* have also been analyzed using Arrhenius and Montsinger laws. Both models do not consider the contribution of electrical stress to the aging acceleration. The Arrhenius equation has been applied following the same approach applied by Zhou et al [11], as per equation (43). Montsinger has been applied as per equation (44). Table 39 shows this analysis result.

$$L(\theta_{op}) = L_{ac} e^{\left[\frac{-E_a}{R}\left(\frac{1}{\theta_{ac}} - \frac{1}{\theta_{op}}\right)\right]} \quad (43)$$

Where:

$L(\theta_{op})$: Lifespan at continuous temperature operation θ_{op}.
θ_{ac}: Insulation temperature at accelerated aging condition.
L_{ac} : Lifespan at temperature θ_{ac}.
E_a : Activation energy.
R: Universal gas constant = 8.314462618.

$$L(\theta_{op}) = L_{ac} 2^{\left[\frac{\theta_{ac}-\theta_{op}}{p}\right]} \quad (44)$$

Where:

$L(\theta_{op})$: Lifespan at continuous temperature operation θ_{op}.
θ_{ac}: Insulation temperature at accelerated aging condition.
L_{ac} : Lifespan at temperature θ_{ac}.
p: Constant which corresponds to the temperature increase necessary to reduce lifespan by half, p = 8.

Table 39 − Equivalent age (years) for CT01 and CT02 based on thermal aging acceleration only using Montsinger and Arrhenius models.

Test samples	Equivalent age based on Montsinger	Equivalent age based on Arrhenius
CT01	45.5	43.2
CT02	51.3	51.2

From the analysis of Table 38, it is also possible to notice an increased tendency of difference between the life estimation for *CT01* and *CT02* when $E_0 >$ 1.22 p.u. The values for *CT01* in Table 39 are lower than the respective values for this sample in Table 38. For *CT02*, values in Table 38 are in convergence with values in Table 39. This is an indication that the electrical stress at the *CT02* test voltage is probably lower than E_0. But E_0 is probably lower than the electrical stress at the test voltage for *CT01*.

Finally, an exhaustive calculation of life estimation was performed using a script written in GNU Octave (see Annex B), and the charts presented in Figures 58 and 59 were obtained. The following conditions were considered for the construction of these graphs: $1 \leq n \leq 4$; $1.17 \leq E_0 \leq 1.22$ p.u; L_{CT01}, L_{CT02} and $L_{CT04} \leq L_{max} = 70$ years. In addition, based on the conformity and uniformity of the test samples, it was considered a maximum admissible difference between L_{CT01} and L_{CT02} of 5 %.

Figure 58 − Life estimation for CT01 (L_{CT01}) and CT02 (L_{CT02}) versus possible values for E_0 and n.

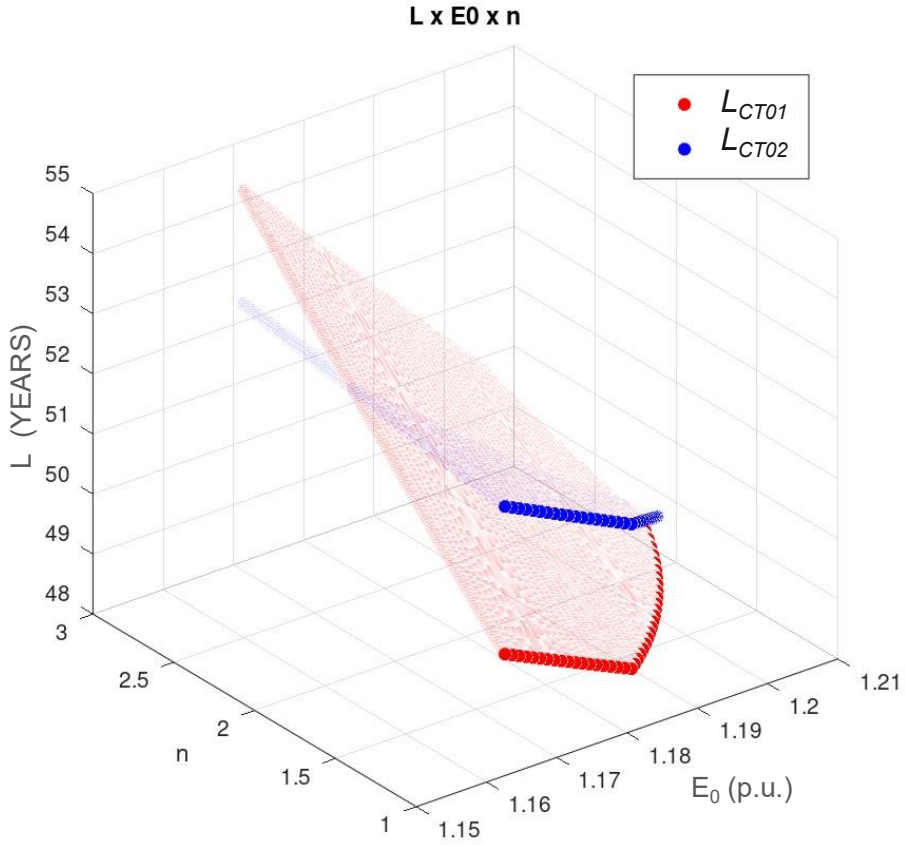

Source: Own authorship

Figure 59 − Combination of values of E_0 and n satisfying the conditions considered and the experimental values.

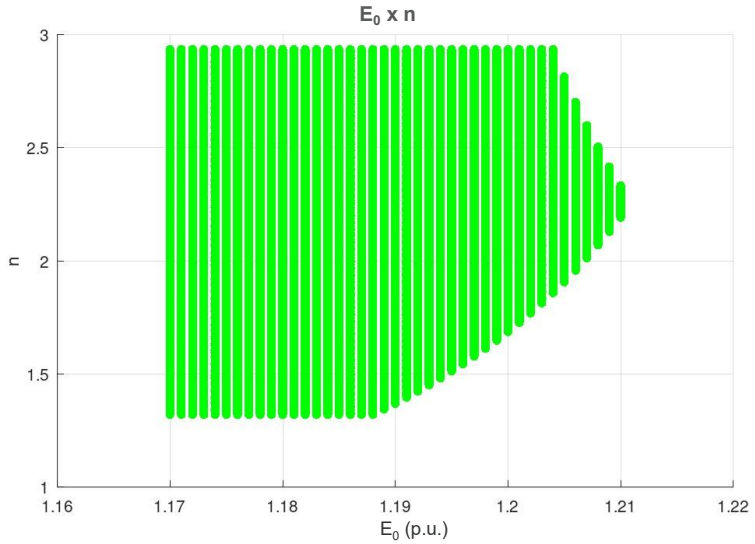

Source: Own authorship

The green area in Figure 59 corresponds to the intersection between the red and blue surfaces in Figure 58, i.e., the possible combinations of n and E_0 satisfying the conditions $1 \leq n \leq 4$; $1.17 \leq E_0 \leq 1.22$ p.u; L_{CT01}, L_{CT02} and $L_{CT04} \leq L_{max} = 70$ years and a maximum admissible difference between L_{CT01} and L_{CT02} of 5 %.

The possible values for the voltage exponent n are in the range from 1.307 to 2.950. These values are significantly lower than the values found in the literature about oil-impregnated paper power cable ($10 \leq n \leq 12$), or even the values found in by G. Zhou et al [11] in a recent publication related to oil-impregnated paper *CT* ($4 \leq n \leq 6$). Regarding the values found in power cable literature, it is important to highlight that the researchers at that time did not consider the existence of the threshold value E_0, as proposed by Simoni [7]. This fact may lead to the empirical determination of much higher values for the exponent n. Concerning to the research done by G. Zhou et al [11] , although there is reference to the Simoni's model, no reference was found in this work to the use of a threshold value of electrical stress below which aging acceleration caused by electrical stress becomes negligible. On the other hand, the results found here for samples CT01 and CT02 rise as evidence of the existence of this threshold value E_0.

Based on the results of this investigation, a test procedure can be defined considering conservative values for n and E_0 (consider n and E_0 so that the number of testing hours is maximized), as showed in Table 40 .

Table 40 – Example of parameters for an endurance accelerated aging test considering conservative values for n and E_0 to reach 30 years of equivalent lifespan

Equation parameters $E_0 = 1.21$ $\theta_0 = 80\ °C$ $\alpha = 0.086$ $n = 1.307$

Duration (hours)	Duration (months)	Voltage stress E_j (p.u.)	Test insulation temperature θj (°C)	Equivalent life (years)
2000	2.8	2.56	125.0	30.0
3000	4.2	1.88	125.0	30.0
4000	5.6	1.51	125.0	30.0
5000	6.9	1.27	125.0	30.0

In order to avoid a test voltage with a value close to the rated power frequency withstand voltage of the *CT*, a test with duration between 3000 and 4000 hours at a test voltage between 1.5 to 1.9 p.u. can be a suitable alternative.

6 CONCLUSION AND FUTURE WORK

This thesis presented an investigation based on a long-duration test carried out on reduced models of oil-impregnated paper insulation system of a 550 kV CT. The test samples were under controlled conditions in terms of thermal and power-frequency electrical stresses. The test samples are similar units based on the results of the initial dielectric routine tests. The tests were performed until the failure of two test samples (named *CT01* and *CT02*). Another test sample (*CT04*) remains under test until the publication of this thesis since its failure has not occurred before it. Life estimations have been calculated using a thermal and electrical multi-stress model based on the Montsinger rule and Inverse Power Law. The existence of threshold values for electrical and thermal stresses, E_0 and θ_0, has also been considered. Ranges of possible values for the threshold electrical stress E_0 and for voltage exponent n have been found based on the test output.

There was a significant difference in the lifespan estimates of samples *CT01* and *CT02* based on the Montsinger and Arrhenius models that consider thermal stress only. Nevertheless, the use of the proposed thermoelectrical multi-stress model, taking into account the existence of a threshold value E_0 for electrical stress, results in convergent lifespan estimates for these samples for scenarios in which E_0 is greater than the electrical stress applied to the sample *CT02*.

The application of the thermoelectrical multi-stress model to the results of this investigation indicates that the estimated lifespan for the test samples *CT01* and *CT02* is about 50 years, that the exponent related to electrical stress n is in the range of 1.307- 2.950 and that the electrical stress threshold E_0 is in the range of 1.17 to 1.21 p.u. These results consider that the parameters E_0 and n are constant for the temperature range covered by this investigation (from 80 °C to 125 °C). It is recognized that these parameters may be impacted by temperature variation.

The output of this investigation contributes to the development of an endurance test procedure that can be applied to *CTs* with paper-oil insulation. These tests can be carried out both on real *CTs* and on reduced models designed to represent the real *CT*. For the reduced model to suitably represent the real *CT*, it is necessary to use the same materials (same paper with the same thickness, same insulating oil), the same construction technology (method of wrapping the paper over the tube and over the core box, same paper overlapping rules ensuring the same level of paper compaction), same manufacturing process (paper drying processes, oil

treatment and impregnation), in addition to demonstrating the similarity of electrical stress through simulation of electric field (finite element calculation).

Although this investigation points to a possible and promising path for the development of an endurance test, it is still not possible to propose a test that can be included in a technical standard for equipment, as standardized tests require the adoption of criteria that can be used for the different solutions of each manufacturer in the market. Although there is great similarity between CTs with paper-oil insulation from different manufacturers, there is no standardization in relation to electrical stress values (electric field at each voltage rating condition) or even in terms of the paper thickness adopted or the impregnating oil used. There are minimum requirements defined in technical standards for paper and impregnating oils, but still allowing manufacturers to choose from countless combinations. These innumerable combinations may result in different values of E_0 and n.

Nevertheless, investigations adopting the procedures used in this work can be of great value for manufacturers to evaluate modifications/improvements in equipment designs that are based on constructive solutions for which the lifespan based on service experience is already known. New manufacturers can also use the methodology of this investigation to determine safe thermal and electrical stress levels so that equipment is designed to achieve a suitable duration in service life. This is a relevant contribution once more and more users are asking for equipment designed for 25 or 30 years in their technical specifications.

As an example, based on the results found in this investigation, and consider conservative values for n and E_0, a test with duration between 3000 and 4000 hours at a test voltage between 1.5 to 1.9 p.u. can be a suitable alternative (see Table 40).

Besides the contribution related to lifespan estimation, the investigation included diagnosis tests performed along with the aging test to check the insulation condition. The results of these tests were discussed, indicating that they are useful to assess the degradation level of oil-impregnated paper CTs.

The results of diagnostic tests carried out as part of this investigation revealed relevant variation of several parameters along the aging test. The main conclusions obtained from a cross-analysis of the results of these diagnostic tests are listed as follows:

- The decrease of the discharge inception and/or extinction voltage values is a very relevant parameter related to the insulation aging conditions.
- The increase of *DDF* at normal ambient temperature is an important indicator of thermal aging, however, it does not give a complete information related with

the thermal stability of the *CT*. The increase of *DDF* at normal temperature needs to be analyzed together with complementary measurements.

- A complementary measurement to evaluate the thermal stability of a *CT* is the measurement of the *DDF* at normal and high temperature to calculate the thermal coefficient α_c.
- *DFR* is a useful measurement to evaluate the thermal aging of oil-impregnated paper insulation. When using these measurements, it is recommended to be careful with the application of the *XY* model (based on power transformer construction) to assess moisture in solid insulation. In this investigation, it was not possible to find a suitable combination of the values for *X* and *Y* parameters to obtain consistent results. However, the comparison of the results measured along the life of the equipment and the comparison between sister units are of great value to monitor the progress of insulation aging.
- *PDC* measurement is a promising test to be periodically carried out on *CT* insulation. In the same way as *DFR*, periodic measurements on the same unit as well the comparison of the results of one equipment with sister units may allow to identify abnormal aging acceleration cases.
- *DGA* in oil samples, as a non-invasive test, may be used to support to decision to do a deeper analysis on units with results differing from sister units. Besides the content of each gas, individually analyzed, the verification of the ratio of specific gases may allow, together with other measurements, to diagnose the aging conditions of a *CT* in operation.
- Physical-chemical tests on oil samples may also be used to complement analysis of aged equipment, highlighting oil acidity and interfacial tension.
- Oil *HPLC* can be used as an additional information to evaluate the possibility of thermal aging. The results of such test may be evaluated together with *DGA* (highlighting CO and CO_2 contents), *DFR* and *DDF*.
- The autopsy of failed units is an important practice, mainly if other measurements (mentioned above) were earlier performed. A visual inspection and the determination of the polymerization degree of paper samples can be analyzed and, together with the other measurement results if available, to allow the determination of the type of failure occurred, besides to be used in the

construction of a database to be used in the continuous evaluation of *CT*s of the same family.

Following these conclusions, the variations of these parameters are of great value for evaluating the degradation conditions of the insulation over its service life. It is useful to highlight the importance of the cross-analysis of several different parameters to assess the degradation condition of the insulation, as well as the evolution of the values of such parameters along the service life.

Monitoring *PD* is an extremely important parameter for evaluating the level of degradation of the insulation system. Tests on units removed from service to evaluate the inception and extinction voltages of discharges may support decision-making regarding keeping the units in service.

The combined analysis of several different diagnostic tests (*PD*, *DDF*, *DFR*, *PDC* and tests on oil samples) is recommended for decision-making regarding the replacement of equipment in service.

6.1 PUBLICATION

F. E. Spressola, Z. Roman, R. G. Oliveira, F. M. Lagos and E. T. W. Neto, *"Aging of Oil-impregnated Paper High Voltage Current Transformers: Long Duration Test and Lifespan Estimation,"* in *IEEE Transactions on Dielectrics and Electrical Insulation*, vol. 31, no. 1, pp. 358-365, Feb. 2024, doi: 10.1109/TDEI.2023.3321283.

6.2 FUTURE WORK

As mentioned in the conclusion of this work, the parameters E_0 and n were considered as constant values for the temperature range covered by this investigation (from 80 °C to 125 °C). It is recognized that these parameters may be impacted by temperature variation. Therefore, a specific investigation into this topic may be a next step towards a consolidated procedure which can be used as future normative reference. Besides the temperature influence on these parameters, the combination of transient overvoltages along the test (e.g., lightning impulse shots at regular test time intervals) is another step to be considered after the knowledge consolidation on the contribution of the continuous steady-state stresses to the aging of CT oil-paper insulation.

CT04 will remain energized until its failure in order to complete this investigation. The failure of CT04 is expected to occur before ~ 8 600 testing hours.

BIBLIOGRAPHY

[1] V. Gurin and T. O'Hanlon, "The SDIPF reliability curve of old EHV power transformers - A historical review for utilities when developing specifications for new transformers - Part I," *Transformers Magazine,* pp. 56-60, Vol 9, Issue 4 2022.

[2] CIGRE WG D1.53, "Brochure 738 - Ageing of Liquid Impregnated Cellulose for Power Transformers," CIGRE, 2018.

[3] E. Zhang, L. Jiang, C. Zhang, P. Zheng, Y. Nakanishi and T. Wu, "State-of-Art review on chemical indicators for monitoring the aging status of oil-immersed transformer paper insulation," *Energies,* p. https://doi.org/10.3390/, 30 January 2023.

[4] CIGRE WG 07/Study Committee 23, "Brochure 57 - The paper-oil insulated measurement transformer," CIGRE, Paris, 1990.

[5] IEC - International Electrotechnical Commission, *IEC 60076-7:2018 Power transformers - Part 7: Loading guide for mineral-oil-immersed power transformers,* IEC, 2018.

[6] P. Cygan and J. Lagary, "Models for insulation aging under electrical and thermal multistresses," *IEEE Transactions on Electrical Insulation,* vol. 25, pp. 923-934, 1990.

[7] L. Simoni, "General equation of the decline in the electric strength for combined thermal and electrical stresses," *IEEE Transactions on Electrical Insulation,* Vols. EI-19, pp. 45-52, 1984.

[8] L. Simoni, G. Mazzanti, G. C. Montanari and L. Lefebre, "A general multi-stress life model for insulating materials with or without evidence of threshholds," *IEEE Transactions on Electrical Insulation,* pp. 349-364, June 1993.

[9] E. Occhini, G. Lanfranconi, M. Tellarini and G. Maschio, "Self contained oil filled cable systems for 750 and 1100 kV. Design and tests.," in *CIGRÉ ICLHVS,* Paris, 1978.

[10] E. M. Allam, J. H. Cooper and J. .. Shimshock, "Development and long-term testing of a low-loss 765 kV high pressure oil-filled pipe cable," in *International Conference on Large High Voltage Electric Systems,* Paris, 1986.

[11] G. Zhou, Q. Wang, Y. Shi and X. Chen, "Research on deterioration mechanism of oil-paper insulation of 220 kV current transformers," in *IEEE 5th Conference on Energy*

Internet and Energy System Integration (EI2), doi: 10.1109/EI252483.2021.9713025, 2021.

[12] GT Modernização do Setor Elétrico Portaria MME n° 187/2019, "Relatório do Grupo Temático Sustentabilidade da Transmissão," MME, Ministry of Mines and Energy - Brazil, 2019.

[13] H. Peng, M. Dong, M. Ren, J. Miao and Z. Zhang, "Insulation diagnosis for 220kV oil-immersed current transformer by frequency dielectric spectroscopy," in *2011 Electrical Insulation Conference (EIC)*, Annapolis, Maryland, 2011.

[14] ANEEL, "Análise de Impacto Regulatório - AIR da necessidade de aprimoramento dos comandos regulamentares afetos à "vida útil regulatória" de equipamentos de transmissão," ANEEL - Agência Nacional de Energia Elétrica, 2019.

[15] ANEEL, "Avalição das contribuições recebidas durante a Consulta Pública nº5, de 2020, e atualização do Relatório de Análise de Impacto Regulatório nº5/2016-ANEEL," ANEEL (Electric Energy National Agency), 2021.

[16] IEC - International Electrotechnical Commission, *IEC 60071-1:2019 Insulation co-ordination - Part 1: Definitions, principles and rules*, IEC, 2019.

[17] IEC - International Electrotechnical Commission, "Electropedia," [Online]. Available: www.electropedia.org.

[18] GE Grid Solutions, *OSKF Oil-Insulated Current Transformers 72.5 to 800 kV (Catalogue)*, GE Grid Solutions.

[19] CIGRE Study Committe A3, "Brochure 394 - State of the art of instrument transformers," CIGRE, 2009.

[20] W. Hou, L. Yang, Y. Mo, Y. Huang and X. Zheng, "Static dielectric constant and dielectric loss of cellulose insulation: Molecular dynamics simulations," *High Voltage*, p. https://doi.org/10.1049/hve2.12087, 22 March 2021.

[21] J. P. Vandeleene, *Theoretical aspects of instrument transformers*, Alstom T&D, 2001.

[22] E. F. Fuchs and M. A. S. Masoum, Power Quality in Power Systems and Electrical Machines (Second Edition), Academic Press, 2015.

[23] F. E. Spressola, "Avaliação do comportamente térmico de transformadores de corrente de extra-alta tensão isolados a papel e óleo," UNIFEI, Itajubá, 2011.

[24] G. Gorlini, W. Mosca and M. Tellarini, "The evaluation of aging conditions of high voltage current transformer," CESI, 1976.

[25] IEC - International Electrotechnical Commission, "IEC 61869-1:2023 Instrument transformers - Part 1: General requirements," IEC, Geneva, Switzerland, 2023.

[26] L. Chmura, D. Boorn, P. Morshuis and J. J. Smit, "Life curves for new and thermally aged oil-impregnated paper insulation," in *Electrical Insulation Conference*, Ottawa, Canada, 2013.

[27] IEC - International Electrotechnical Commission, *IEC 61869-2 Instrument transformers - Part 2: Additional requirements for current transformers*, Geneva, Switzerland: IEC, 2012.

[28] IEEE, *IEEE Std C 57.13.5-2019, IEEE Standard for performance and test requirements for instrument transformers of a nominal system voltage of 115 kV and above*, New York, USA: IEEE Standards Association, 2019.

[29] S. Morsalin, T. B. Phung, M. Danikas and D. Mawad, "Diagnostic challenges in dielectric loss assessment and interpretation: a review," *IET Science, Measurement & Technology vol 13*, pp. 767-782, doi: 10.1049/iet-smt.2018.5597, 2019.

[30] Megger, A stitch in time - The complete guide to electrical insulation test, Megger, 2020.

[31] A. Kumar and S. M. Mahajan, "Time domain spectroscopy measurements for the insulation diagnosis of a current transformer," *IEEE Transactions on Dielectrics and Electrical Insulation vol 18. No. 5*, pp. 1803-1811, October 2011.

[32] Z. Chunming, X. Wenxie and D. Zhaohong, "Transformer oil-paper insulation aging evaluation system based on different aging characteristics," in *6th International conference on control, robotics and cybernetics (CRC)*, Shanghai, 2021.

[33] T. K. Saha and P. Purkait, "Investigation of polarization and depolarization current measurements for the assessment of oil-paper insulation of aged transformers," *IEEE Transactions on Dielectrics and Electrical Insulation, vol 11 no. 1*, pp. 144-154, doi: 10.1109/TDEI.2004.1266329., Feb 2004.

[34] R. Liao, J. Liu, L. Yang, J. Gao, Y. Zhang, Y. Lv and H. Zheng, "Understanding and analysis on frequency dielectric parameter for quantitative diagnosis of moisture content in paper-oil insulation system," *IET Electric Power Applications Vol. 9 Iss. 3*, pp. 213-222, doi: 10.1049/iet-epa.2014.0101, 2015.

[35] M. Zhang, J. Liu, P. Qi, Q. Chen, L. Liao, X. Chen and M. Yin, "Measurement of dielectric response of transformer moisture content," *IET Science, Measurement & Technology Vol.12 Iss. 5,* pp. 594-602, doi: 10.1049/iet-smt.2017.0419, 2018.

[36] S. Raetzke, M. Koch and M. Anglhuber, "Modern insulation condition assessment for instrument transformers," in *IEEE International Conference on Condition Monitoring and Diagnosis,* Bali, Indonesia, 2012.

[37] M. Anglhuber and M. Koch, "Experiences with measurement and analysis of hte dielectric response of instrument transformers," in *IEEE International Conference on High Voltage Engineering and Application (ICHVE),* Athens, Greece, 2018.

[38] D. M. Robalino and I. Güner, "Investigation of EHV current transformer failure by dielectric frequense response technique," in *IEEE Electrical Insulation Conference (EIC),* Virtual Event, 2020.

[39] T. A. Prevost and T. V. Oommen, "Celluose insulation in oil-filled power transformers: part I - history and development," *IEEE Electrical Insulation Magazine,* pp. 28-35, January/February 2006.

[40] A. Ravindra and W. Mosch, High Voltage and Electrical Insulation Engineering, Wiley & IEEE Press, 2011.

[41] C. Krause, "Power transformer insulation - history, technology and design," *IEEE Transactions on Dielectrics and Electrical Insulation,* pp. 1941-1947, December 2012.

[42] IEEE, *IEEE C57.12.80-2010 - IEEE Standard Terminology for Power and Distribution Tranformers,* New York: IEEE Standards Association, 2010.

[43] IEEE, *IEEE C57.100-2011 - IEEE Standard Test Procedure for Thermal Evaluation of Insulation Systems for Liquid-Immersed Distribution and Power Transformers,* IEEE Standards Association, 2012.

[44] N. Lelekakis, W. Guo, D. Martin, J. Wijaya and D. Susa, "A field study of aging in paper-oil insulation systems," *IEEE Electrical Insulation Magazine,* pp. 12-19, Jan/Feb 2012.

[45] T. V. Oommen and T. A. Prevost, "Cellulose insulation in oil-filled power transformers: part II - maintaining isulation integrity and life," *IEEE Electrical Insulation Magazine,* pp. 5-14, March/April 2006.

[46] P. Wiklund, B. Pahlavanpour and J. Nunes, "Properties of aging mineral insulaing oils in service," in *Cigré SCD1 Colloquium; Trends in Technology, Materials, Testing and Diagnostics Applied to Electric Power Systems*, Rio de Janeiro, 2015.

[47] A. Ekenstam, "The behaviour of cellulose in mineral acid solutions: Kinetic study of the decomposition of cellulose in acid solutions," *Berichte der deutchen chemischen Gesellschaft*, pp. 553-559, vol. 69 1936.

[48] D. C. P. Araujo, G. d. S. P. Gomes, M. B. de Morais and R. P. Fehlberg, "Métodos para cálculo do envelhecimento de transformadores isolados a óleo mineral: uma revisão do estado da arte," in *XXV SNPTEE*, Belo Horizonte - MG, Brazil, 2019.

[49] A. M. Emsley, R. J. Heywood and M. Ali, "On the kinetics of degradation of cellulose," *Cellulose 4*, p. https://doi.org/10.1023/A:1018408515574, March 1997.

[50] L. Lundgaard, W. Hansen, D. Linhjell and T. Painter, "Aging of Oil-Impregnated Paper in Power Transformers," *IEEE Transactions on Power Delivery*, vol. 19, pp. 230-239, 2004.

[51] M. Martins, "Envelhecimento térmico do papel isolante de transformadores. Investigação experimental. Modelos de degradação.," *Ciência e Tecnologia dos Materiais*, pp. 77-86, 1/2 2010.

[52] L. Lundgaard, W. Hansen, S. Ingebrigtsen, D. Linhjell and M. Dahlund, "Aging of kraft paper by acid catalyzed hydrolysis," in *IEEE Internation Conference on Dielectric Liquids, ICDL*, Coimbra, Portugal, 2005.

[53] S. Matharage, Q. Liu, P. Mayrommatis, G. Wilson, Z. Wang and P. Jarman, "Ageing assessment of transformer paper insulation through detection of methanol in oil," in *IEEE ICPADM*, Sydney, Australia, 2015.

[54] S. J. Tee, "Ageing assessment of transformer insulation through oil test database analysis," The University of Manchester, Manchester, 2016.

[55] T. Asokan and S. Bandaru, "X-was formation in transformer liquid dielectrics," in *ICDL*, Coimbra, Portugal, 2005.

[56] E. Kuffel, W. Zaengl and J. Kuffel, High Voltage Engineering - Fundamentals, 2nd Edition, Newnes, 2000.

[57] N. Malik, A. Al-Arainy and M. Qureshi, Electrical insulation in power systems, New York: Marcel Dekker, 1998.

[58] V. Montsinger, "Loading transformers by temperature," *Transactions of the American Institute of Electrical Engineers,* vol. 49, pp. 776-790, 1930.

[59] V. Montsinger, "Effect of load factor on operation of power transformers by temperature," *Transactions of the American Institute of Electrical Engineers,* vol. 59, pp. 632-636, 1940.

[60] IEEE, *IEEE C57.91-2011 - IEEE Guide for Loanding Mineral-Oil-Immersed Transformers and Step-Voltage Regulators*, IEEE Standards Association, 2011.

[61] J. Crine, J. Parpal and C. Dang, "A new approach to the electric aging of dielectrics," in *Proceedings of CEIDP*, Leesburg, Virginia, USA, 1989.

[62] S. Kiersztyn, "Formal theoretical foundation of electrical aging of dielectrics," *IEEE Transactions on Power Apparatus and Systems,* Vols. PAS-100, pp. 4333-4340, 1981.

[63] G. Montanari and M. Cacciari, "A Probabilistic Life Model for Insulating Materials Showing Electrical Thresholds," *IEEE Transactions on Electrical Insulation,* vol. 24, pp. 127-134, 1989.

[64] IEC - International Eletrotechnical Commission, *IEC 60599:2015 - Mineral oil-filled electrical equipment in service - Guidance on the interpretation of dissolved and free gases analysis,* Geneva, Switzerland: IEC, 2015.

[65] S. S. Dessouky, A. E. Kalas, R. A. Abd El-Aal and M. M. H. Abdel, "Modification of Duval Triangle for Diagnostic Transformer Fault through a Procedure of Dissolved Gases Analysis," *Transactions on Environment and Electrical Engineering ISSN 2450-5730 Vol 1, No 3*, 2016.

[66] Oil Analysis Laboratories, "DGA Helper," Oil Analysis Laboratories, [Online]. Available: https://oilanalysislab.com/Oil_Analysis_Downloads/LW/DGA/. [Accessed 5 October 2023].

[67] S. Abdi, N. Harid, L. Safiddine, A. Boubakeur and A. Haddad, "The correlation of transformer oil electrical properties with water content using a regression approach," *Energies,* no. April 2021, 2021.

[68] IEC - International Electrotechnical Comission, *IEC 60422 - Mineral insulating oils in electrical equipment - Supervision and maintenance guidance,* Geneva, Switzerland: IEC, 2013.

[69] T. W. Dakin, "Electrical insulation deterioration treated as a chemical rate phenomenon," *Transactios of the American Institute of Electrical Engineers,* pp. 113-122, doi: 10.1109/T-AIEE.1948.5059649, Jan 1948.

[70] S. A. Arrhenius, "Über die Dissociationswärme und den Einfluss der Temperatur auf den Dissociationsgrad der Elektrolyte," *Journal of Physical Chemistry,* pp. 96-116, doi:10.1515/zpch-1889-0408 1889.

[71] P. Gazzana-Priaroggia, G. Palandri and U. Pelagatti, "The influence of ageing on the characteristics of oil-filled cable dielectric," *The Institution of Electrical Engineers,* pp. 467-479, November 1960.

[72] IEEE, *IEEE Std 1425-2001, IEEE Guide for The Evaluation of the Remaining Life of Impregnated Paper-Insulated Transmission Cable Systems,* New York: IEEE Power Engineering Society, 2002.

[73] F. W. Peek, "Dielectric Phenomena in High Voltage Engineering," New York, McGraw-Hill, 1915, p. 179.

[74] CIGRE WG A3.06, "Final Report of the 2004-2007 International Enquiry on Reliability of High Voltage Equipment, Part 4 - Instrument Transformers," CIGRE, 2012.

[75] R. S. Gorur, "High-Voltage Transmission," in *The Electrical Engineering Handbook*, WAI-KAI CHEN, Academic Press, 2005, pp. 737-748.

[76] Z. Roman, *Current and Voltage Transformers,* Alstom Grid, 2013.

[77] Y. Watanabe, H. Fukagawa, Z. Iwata, R. Hata, S. Yoshida, H. Saitoh and Y. Fujiwara, "Development of new 500 kV laminated paper insulated self-contained oil-filled calbe and its accessories," *IEEE Transactions on Power Delivery,* vol. 3, no. January 1988, pp. 47-62, 1988.

[78] IEC - International Electrotechnical Comission, *IEC 60505 Evaluation and qualification of electrical insulation systems,* Geneva: IEC, 2011.

[79] A. C. Gjaerde, "Multi-factor ageing models-origin and similarities," in *Proceedings of 1995 Conference on Electrical Insulation and Dielectric Phenomena,*, 1995.

[80] T. W. Dakin, "The endurance of electrical insulation," in *Proceedings of the 4th Symposium on Insulating Materials*, p. 147, 1971.

[81] D. Basu, B. Gholizad, R. Ross and S. M. Gargari, "Temperature Effect on Electrical Aging Model for Field-Aged Oil Impregnated Paper Insulation," in *IEEE Conference on Electrical Insulation and Dielectric Phenomena*, Denver, 2022.

[82] F. E. Spressola, Z. Roman, R. G. Oliveira and F. M. E. T. W. N. Lagos, "Aging of Oil-impregnated Paper High Voltage Current Transformers: Long Duration Test and Lifespan Estimation," *IEEE Transactions on Dielectrics and Electrical Insulation*, p. doi: 10.1109/TDEI.2023.3321283, February 2024.

[83] IEEE, *IEEE PC57.160/D7.2 Draft for Guide for the Electrical Measurement of Partial Discharges in High Voltage Bushings and Instrument Transformers*, New York: The Institute of Electrical and Electronics Engineers, 2018.

[84] K. G. Moscon and H. M. Wilhelm, "Study of insulating kraft paper sample impregnated in mineral insulating oil surface using SEM-EDS," Vegoor Tecnologia Aplicada, Colombo, PR, Brazil, 2022.

[85] H. M. Wilhem, "Análises de MEV-EDS em amostra de papel kraft isolante impregnada com óleo," Vegoor Tecnologia Aplicada, Colombo, PR, Brazil, 2023.

APPENDIX A – Summary of test cycles

Table 41 – Summary of test cycles

Test cycle	CT01				CT02				CT03				CT04			
	Duration (hours)	U_meas (kV)	E_meas (p.u.)	θ_meas (°C)	Duração (horas)	U_med (kV)	E_meas (p.u.)	θ_med (°C)	Duração (horas)	U_med (kV)	E_meas (p.u.)	θ_med (°C)	Duração (horas)	U_med (kV)	E_meas (p.u.)	θ_med (°C)
Total	7864	87.97	1.24	125.3	13994	83.49	1.18	120.0	3200	76.64	1.08	119.6	5190	116.29	1.64	120.2
01	265	86.97	1.23	125.9	265	82.67	1.17	117.6								
02	112	86.96	1.23	125.7	112	82.65	1.17	117.7								
03	124	86.37	1.22	125.6	124	82.10	1.16	117.5								
04	36	87.37	1.24	125.5	36	83.05	1.17	117.5								
05	378	86.88	1.23	125.2	378	82.59	1.17	117.7								
06	26	87.20	1.23	125.7	26	82.89	1.17	119.7	26	76.30	1.08	119.2				
07	46	86.90	1.23	125.5	46	82.60	1.17	119.5	46	76.00	1.07	118.9				
08	50	86.48	1.22	125.4	50	82.20	1.16	119.4	50	75.75	1.07	118.8				
09	129	86.71	1.23	125.2	129	82.40	1.17	119.3	129	76.05	1.08	118.7				
10	5	86.24	1.22	125.4	5	81.98	1.16	119.5	5	75.43	1.07	119.1				
11	3	87.35	1.24	125.3	3	83.03	1.17	119.3	3	76.35	1.08	119.1				
12	79	87.15	1.23	125.2	79	82.84	1.17	119.1	79	76.21	1.08	118.5				
13	4	86.11	1.22	125.3	4	81.85	1.16	120.8	4	75.31	1.07	119.1				
14		0.00		0.0					146	76.20	1.08	118.8				
15	233	87.23	1.23	125.4	233	82.91	1.17	119.2	233	76.14	1.08	118.8				
16	294	87.07	1.23	125.1	294	82.76	1.17	119.3	294	76.13	1.08	118.8				
17	116	87.01	1.23	124.8	129	82.71	1.17	119.2	129	76.10	1.08	118.6				
18	112	87.30	1.23	124.9	112	82.98	1.17	120.9	112	76.30	1.08	119.0				
19	274	87.52	1.24	125.9	274	83.19	1.18	120.9	274	76.63	1.08	120.8				
20	17	87.79	1.24	126.8	17	83.45	1.18	121.1	17	76.90	1.09	121.4				
21	114	87.37	1.24	125.8					114	76.50	1.08	121.3				
22	104	87.16	1.23	125.6												
23					112	83.49	1.18	120.0								
24	57	87.01	1.23	125.7												
25	50	77.03	1.09	125.9					50	88.00	1.24	123.8				
26									250	76.76	1.09	120.0				
27									4	76.00	1.07	118.1				
28									1215	76.74	1.09	120.1				
29									20	76.35	1.08	120.2				
30					189	82.78	1.17	120.9								
31					10	82.41	1.17	119.7								
32					10	81.87	1.16	118.8								
33	46	88.28	1.25	125.5	46	81.23	1.15	120.8								
34					124	83.42	1.18	119.4								
35					3	83.60	1.18	117.9								
36					144	82.98	1.17	119.3								
37	186	83.62	1.18	125.6	186	87.98	1.24	122.4								
38					136	83.32	1.18	120.3								
39					16	83.03	1.17	120.8								
40					49	83.43	1.18	120.1								
41	4	87.13	1.23	122.8	4	82.82	1.17	117.9					4	116.10	1.64	117.9
42	21	86.34	1.22	126.1	21	82.06	1.16	120.8					14	115.73	1.64	120.9
43	120	87.21	1.23	125.3	120	82.89	1.17	120.2								
44	15	86.48	1.22	126.2	15	82.20	1.16	120.8					15	109.25	1.55	120.8
45	51	87.30	1.23	126.0	51	82.98	1.17	120.5								
46	131	87.40	1.24	125.7	131	83.08	1.18	120.3								
47	47	88.32	1.25	125.9	47	81.26	1.15	119.8								
48	25	88.34	1.25	124.1	27	81.19	1.15	118.4								
49					126	82.93	1.17	120.3								
50					74	83.31	1.18	120.1								
51					193	82.93	1.17	120.6								
52					121	83.03	1.17	120.4								
53					819	82.97	1.17	120.3								
54					128	83.38	1.18	120.5								
55					52	83.35	1.18	120.4								
56					59	83.13	1.18	120.2								
57					4	83.26	1.18	116.5								
58					154	82.91	1.17	120.2								
59	11	87.10	1.23	126.5									11	116.06	1.64	120.1
60	70	87.36	1.24	127.1									70	116.41	1.65	120.7
61					204	84.72	1.20	121.0					204	116.87	1.65	120.4
62					202	84.75	1.20	120.2					202	116.74	1.65	119.6
63					160	84.83	1.20	119.8					160	116.82	1.65	119.6
64					243	84.90	1.20	120.3					243	116.82	1.65	120.1
65	102	89.70	1.27	126.2	102	85.63	1.21	120.9					102	116.51	1.65	120.1
66	19	89.58	1.27	125.7	22	85.14	1.20	121.9					22	116.28	1.64	121.9
67					125	85.29	1.21	121.1					125	115.80	1.64	121.0
68					7	85.39	1.21	121.0					7	115.80	1.64	120.9
69					73	85.22	1.21	120.9					73	115.82	1.64	120.8
70					22	84.95	1.20	120.9					22	115.56	1.63	120.8

Continuation of Table 41 – Summary of test cycles

Test cycle	CT01				CT02				CT03				CT04			
	Duration (hours)	U_meas (kV)	E_meas (p.u.)	θ_meas (°C)	Duração (horas)	U_med (kV)	E_meas (p.u.)	θ_med (°C)	Duração (horas)	U_med (kV)	E_meas (p.u.)	θ_med (°C)	Duração (horas)	U_med (kV)	E_meas (p.u.)	θ_med (°C)
71					404	85.32	1.21	120.3					404	115.91	1.64	120.2
72					5	85.67	1.21	119.4					5	116.33	1.65	119.3
73					300	85.85	1.21	120.2					300	116.49	1.65	120.1
74					114	85.45	1.21	120.2					114	116.00	1.64	120.1
75					248	85.88	1.21	120.1					248	116.40	1.65	120.0
76					75	85.85	1.21	120.2					75	116.27	1.64	120.1
77	115	88.77	1.26	125.3	115	83.53	1.18	120.2								
78	209	88.23	1.25	124.9	209	83.23	1.18	119.9								
79	898	88.32	1.25	125.1	898	83.38	1.18	120.0								
80	159	88.16	1.25	125.1	159	83.12	1.18	120.0								
81													16	116.33	1.65	120.0
82													302	116.95	1.65	120.0
83	80	89.29	1.26	125.2	80	83.32	1.18	120.1								
84	2	89.27	1.26	124.2	2	83.81	1.19	119.2								
85	122	89.40	1.26	125.1	122	83.64	1.18	120.1								
86	256	89.39	1.26	125.0	256	83.68	1.18	120.0								
87	79	89.27	1.26	125.1	79	83.40	1.18	120.0								
88	420	88.73	1.25	125.1	420	83.00	1.17	120.0								
89	672	88.45	1.25	125.2	672	82.72	1.17	120.1								
90	350	89.86	1.27	125.3	350	82.71	1.17	120.3								
91	277	89.61	1.27	125.7	277	82.45	1.17	120.7								
92	324	89.18	1.26	125.1	324	82.09	1.16	120.1								
93	426	88.81	1.26	125.1	426	82.42	1.17	120.1								
96					119	84.27	1.19	120.0					119	116.55	1.65	120.2
97					26	84.11	1.19	119.3					26	116.23	1.64	119.6
98					199	84.42	1.19	120.1					199	116.25	1.64	120.4
99					53	84.77	1.20	120.0					53	116.32	1.65	120.3
100					97	84.61	1.20	120.0					97	116.17	1.64	120.2
101					8	84.12	1.19	119.2					8	115.80	1.64	119.4
102					57	83.89	1.19	120.1					57	115.45	1.63	120.0
103					161	84.00	1.19	120.0								
104					77	84.04	1.19	119.9								
105					41	83.95	1.19	119.8								
106					204	83.89	1.19	120.0								
107					602	83.76	1.18	120.2								
108													126	116.17		120.2
109													66	116.08		119.9
110													398	115.87		120.3
111													80	116.29		120.1
112													296	116.19		120.2
113													146	115.83		120.1
114													218	115.99		120.0
115													99	116.10		120.3

APPENDIX B – Script in GNU Octave

```
% Initial value definitions
t1 = 7864; % t1 value in hours (CT01)
t2 = 13994; % t2 value in hours (CT02)
t3 = 5190; % t3 value in hours (CT04)
teta1 = 125.3; % temperature 1 in °C (CT01)
teta2 = 120.0; % temperature 2 in °C (CT02)
teta3 = 120.2; % temperature 3 in °C (CT04)

L_min = 422425; % Minimum L = 48.2 years (449177 hours) = 94% de 51.3 years based on L2 considering Montsinger only
L_max = 613200; % Maximum L = 54.35 years (476127 hours) = 106% de 51.3 based on Montsinger only

n_min = 1.00; % minimum n
n_max = 4.00; % maximum n
n_step = 0.001; % Increment for n

E0_min = 1.17; % E0 mimimum value
E0_max = 1.23; % E0 maximum value
E0_step = 0.001; % Increment for E0

found_solution = false; % Solution found indicator

n_values = []; % n values satisfying the conditions
E0_values = []; % E0 values satisfying the conditions

% Initialize vectors to store the values of LCT01, LCT02 and LCT04
LCT01_values = [];
LCT02_values = [];
LCT04_values = [];
```

```
% Calculate the values of LCT01, LCT02 and LCT04 and store them in the corresponding vectors
for n = n_min:n_step:n_max
   for E0 = E0_min:E0_step:E0_max
      LCT01 = (1.244/E0)^n * t1 * exp(0.0866 * (teta1 - 80));
      LCT02 = (1.181/E0)^n * t2 * exp(0.0866 * (teta2 - 80));
      LCT04 = (1.646/E0)^n * t3 * exp(0.0866 * (teta3 - 80));

      % Condition check – Maximum admissible difference 0.05 pu
      if (abs((LCT01-LCT02)/LCT01) <= 0.05) && (LCT04 <= LCT01) && (LCT04 <= LCT02) && (LCT01 >= L_min) && (LCT02 >= L_min) && (LCT01 <= L_max)
         LCT01_values = [LCT01_values, LCT01/365/24];
         LCT02_values = [LCT02_values, LCT02/365/24];
         LCT04_values = [LCT04_values, LCT04/365/24];
         E0_values = [E0_values, E0]; % Adding a valid E0 value to E0_values vector
         n_values = [n_values, n]; % Adding a valid n value to n_values vector
      end

   end
end

% Color line curve definitions
color_LCT01 = 'r';
color_LCT02 = 'b';
color_LCT04 = 'y';

% Marker color definitions
marker_color_LCT01 = [1 0 0]; % Red
marker_color_LCT02 = 'b'; % Blue
marker_color_LCT04 = [1 1 0]; % Yellow

% Plot 3D chart
figure;
```

```
scatter3(E0_values, n_values, LCT01_values, 30, marker_color_LCT01, 'filled', 'MarkerEdgeColor', color_LCT01);
hold on;
scatter3(E0_values, n_values, LCT02_values, 30, marker_color_LCT02, 'filled', 'MarkerEdgeColor', color_LCT02);
%scatter3(E0_values, n_values, LCT04_values, 30, marker_color_LCT04, 'filled', 'MarkerEdgeColor', color_LCT04);
xlabel('E0');
ylabel('n');
zlabel('L');
legend('LCT01', 'LCT02', 'LCT04');
title('L x E0 x n');
grid on;

% Plot E0 x n
figure;
scatter(E0_values, n_values, 30, 'g', 'filled');
xlabel('E0');
ylabel('n');
title('E0 x n');
grid on;
```